

*Sources and sinks of reactive Nitrogen  
in the German Bight*

Dissertation

zur Erlangung des Doktorgrades der Naturwissenschaften im Department  
Geowissenschaften der Universität Hamburg

vorgelegt von

Astrid Deek

aus Reinbek

Hamburg

2011

Als Dissertation angenommen  
vom Department für Geowissenschaften der Universität Hamburg  
auf Grund der Gutachten von

Prof. Dr. Kay-Christian Emeis  
und  
Dr. Justus van Beusekom

Hamburg, den 07.01.11

Prof. Dr. Jürgen Oßenbrüge

(Leiter des Departments für Geowissenschaften)

## Zusammenfassung

In die Deutsche Bucht werden erhebliche Mengen reaktiven Stickstoffs aus menschlichen Quellen über die Atmosphäre und Flüsse eingetragen. Der erhöhte Stickstoffeintrag führt zu einer gesteigerten Primärproduktion in der angrenzenden Küstenregion, welche in ein vermehrtes Wachstum von Algen, in eine Verschiebung der Artenzusammensetzung und teilweise auftretenden Sauerstoffmangel resultieren. Die technischen Maßnahmen zur Reduktion der N-Einträge und zur Zurückführung der Eutrophierung sind kostenintensiv, aber der Eutrophierung stehen auch natürliche Prozesse der Stickstoffzehrung – vorwiegend in Sedimenten der küstennahen Bereiche – entgegen. Um die Folgen und das Ausmaß der Eutrophierung abschätzen und um die natürlichen Senken reaktiven Stickstoffs quantifizieren zu können, sind Untersuchungen zu der Herkunft, der Variabilität in den Quellen und Senken, und zu internen Umsätzen von Stickstoff im Übergang vom Land zum Meer erforderlich.

In der vorliegenden Arbeit werden mit Hilfe der Isotopensignatur des Nitrats Quellen reaktiven Stickstoffs in Nordseezuflüssen bestimmt. Weiterhin werden Denitrifizierungsraten in Sedimenten des Elbeästuars und des Schleswig-Holsteinischen Wattenmeers bestimmt, so dass eine Abschätzung des natürlichen Nitratabbauvermögens der an die Elbe grenzende Küstenregion erfolgen kann.

In den Kapiteln 2 und 3 wird der isotopische Fingerabdruck des Nitrats in verschiedenen Flüssen bestimmt, die in die Deutsche Bucht münden. Diese Flüsse sind durch ein vorwiegend anthropogen genutztes Einzugsgebiet beeinflusst, was sich in einer charakteristischen Isotopensignatur widerspiegelt, die sich deutlich von der Isotopensignatur naturnaher Flüsse unterscheidet. Weiterhin zeigt sich eine starke saisonale Schwankung der Isotopensignatur, die durch Assimilationsprozesse von Mikroorganismen hervorgerufen wird. Die Quellen reaktiven Stickstoffs und die Effizienz des Nitratverbrauchs, beeinflusst von der jeweiligen Fließgeschwindigkeit, bestimmen wesentlich die Isotopensignatur flussbürtigen Nitrats.

In den Kapiteln 4 und 5 wird untersucht, inwiefern die erhöhten Nitratreinträge in Sedimenten der angrenzenden Küste und innerhalb des Elbeästuars auf natürliche Weise mikrobiell abgebaut, beziehungsweise denitrifiziert werden können. Hierzu werden in saisonaler Auflösung Denitrifizierungsraten in verschiedenen Sedimenttypen in unterschiedlicher Distanz zur Elbemündung erhoben. Weiterhin werden im Nährstoffgradienten des Elbeästuars Denitrifizierungsraten in unterschiedlichen Sedimenttypen bestimmt. Die Sedimente weisen generell ein relativ großes potentiell Nitratabbauvermögen auf. Es ist

abhängig von der Nitratkonzentration im überliegenden Wasserkörper, der Temperatur und dem organischen Kohlenstoffgehalt des Sedimentes. Sedimente des Schleswig-Holsteinischen Wattenmeers und des Elbeästuars neutralisieren etwa 17% der gesamten Nitratfracht der Elbe. Die Untersuchungen dieser Arbeit tragen also einerseits zur Identifizierung anthropogener Stickstoffquellen im Einzugsgebiet der Deutschen Bucht bei und zeigen zudem auf, dass küstennahe Sedimente der verbleibenden Flussästuare und der Wattengebiete der Deutschen Bucht eine begrenzte Kapazität besitzen, diese Quellen zu neutralisieren.

## Abstract

Anthropogenically influenced rivers discharge massive loads of reactive Nitrogen (rN) into the German Bight. Increasing rN inputs lead to increased primary production in adjacent coastal zones which causes enhanced algal growth, shift in species composition and occurring oxygen deficiency resulting in eutrophication of aquatic ecosystems. Reducing accompanied negative side-effects requires a detailed assessment of sources and sinks of rN.

In this thesis, nitrate sources in rivers discharging into the German Bight are determined by means of isotopic composition of nitrate. To estimate the amount of nitrate degraded in the adjacent coastal zone, denitrification rates in sediments of the north German Wadden Sea and the Elbe Estuary are determined.

In chapter 2 and 3, the isotopic signal of nitrate in several rivers discharging into the German Bight is investigated. In general, German rivers are influenced by anthropogenic land use in their catchment areas which is mirrored in the isotopic value of nitrate that differs from pristine riverine isotopic signals. Strong seasonal variations in isotopic values are caused by assimilation processes in biological active seasons. All together, sources of rN and the nitrate consumption efficiency interrelated with the current velocity determines the isotopic composition of riverine nitrate.

In chapter 4 and 5, the amount of nitrate degraded by denitrification within sediments of the adjacent coastal zone and within the Elbe Estuary is investigated. To do this, denitrification rates in various sediment types in seasonal resolution and varying distance to the Elbe River plume are determined. Furthermore denitrification rates along the nitrate gradient of the Elbe River are raised. It is seen that sediments under study have a generally high potential to degrade nitrate. The amount of denitrified nitrate depends mostly on nitrate concentration in the overlying water body, temperature and the organic matter content of the respective sediment. Even though relatively high denitrification rates in coastal German Bight sediments and in Elbe sediments are measured, respective sedimentary nitrate removal only buffers 17% of the total Elbe River nitrate load.

In sum, this study contributes to a better identification of anthropogenic rN sources within the German Bight catchment and demonstrates on the one hand a high potential of the German Bight to buffer increasing nitrate loads which is on the other hand a limited capacity due to environmental conditions.

## Table of Contents

1	Introduction .....	1
2	Isotopic composition of nitrate in five German rivers discharging into the North Sea.....	11
3	Seasonal variations in nitrate isotope composition of three rivers draining into the North Sea .....	33
4	Denitrification in coastal sediments of the German Wadden Sea .....	61
5	Denitrification in sediments of the Elbe Estuary and adjacent coastal zones..	87
6	Conclusions and Outlook .....	107
	Figure captions .....	110
	Table captions .....	112
	List of abbreviations.....	113
	References .....	115
	Acknowledgements .....	135
	Curriculum Vitae .....	136

# 1 Introduction

## 1.1 Eutrophication of coastal ecosystems

In aquatic environments N exists in a vast number of forms in both the dissolved and the particulate fractions which are linked within a cycle (Fig.1.1). The largest amount of N is in the form of atmospheric  $N_2$  which is simultaneously the least bioavailable form. The main forms of reduced or oxidized (=reactive) nitrogen in aquatic systems are nitrate ( $NO_3^-$ ), nitrite ( $NO_2^-$ ) and ammonium ( $NH_4^+$ ) (Canfield et al., 2005), summarized as dissolved inorganic nitrogen (DIN). DIN is utilisable, reactive N (rN) which is taken up and assimilated for algal and bacterial growth and incorporated into organic matter (Capone, 2000). Dissolved organic nitrogen (DON) is another major contributor to the total dissolved N (TDN) pool in coastal areas consisting of a heterogeneous mixture of biologically labile and refractory N-bearing molecules (Bronk, 2002).

Under natural conditions, rN is generated by nitrogen fixation of  $N_2$  (Galloway and Cowling, 2002); the ability to fix  $N_2$  is widespread in the marine environment with cyanobacteria as the dominant  $N_2$  fixing organisms (Stal et al., 1984). But within the last century, anthropogenic nitrogen loads to the global environment – including the coastal zones - have massively increased due to ever increasing industrial  $N_2$ -fixation via the Haber-Bosch process. The added anthropogenic reactive N presently supports an estimated 48% of the global population (Erisman and Sutton, 2008). Together with increased fossil combustion and cultivation of crops, the fertiliser production led to a doubling of the present day global release of rN, and locally even by more in some regions (Galloway et al., 1995). The benefits of artificially fixed  $N_2$  come at environmental and economic costs. The residues of unused rN discharged by rivers and atmospheric fluxes into oceans compromise ecosystem services of coastal environment. A number of undesirable effects such as increasing primary production leading to eutrophication, hypoxia, shifts in relative species abundance and a loss of biodiversity in coastal waters have been reported (Jickells, 1998; Laane et al., 2005; Galloway et al., 2008). Thus, excessive rN loading is globally considered to be one of the most severe pollution problems in coastal environments (Howarth et al., 2000; Rabalais, 2002).

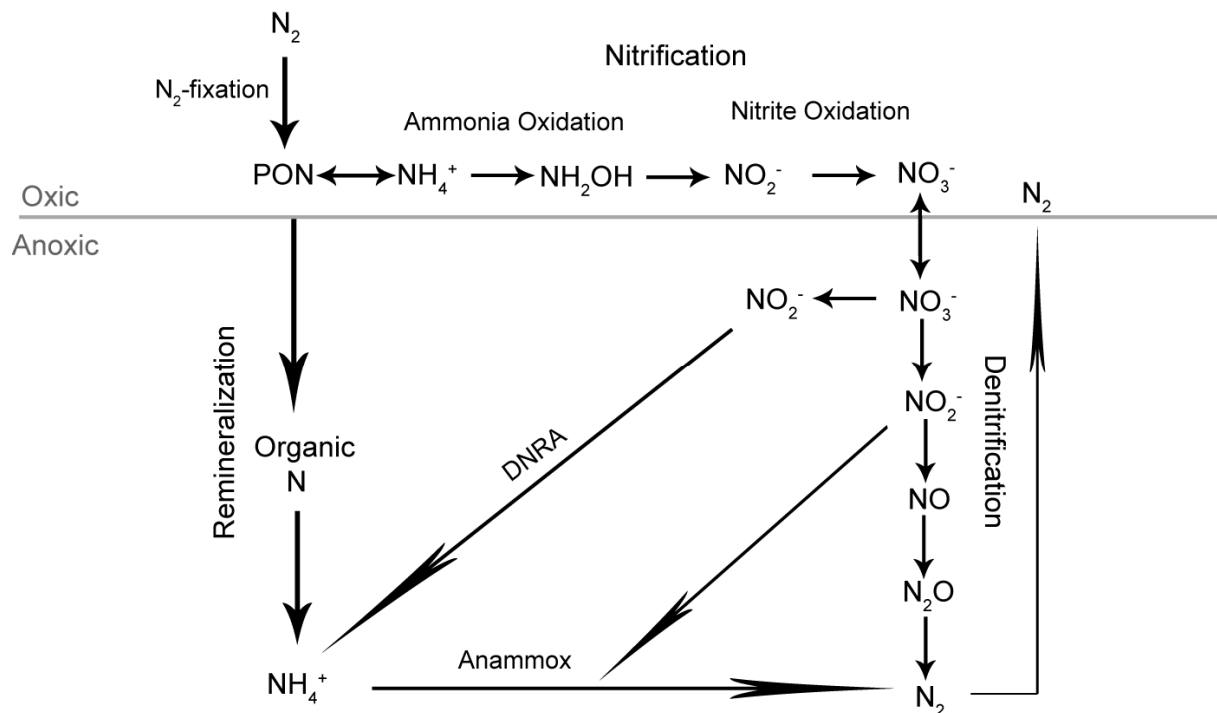


Fig. 1.1: The marine nitrogen cycle  
(modified after Francis et al., 2007).

## 1.2 Problem area: German Bight

According to the criteria of the OSPAR Commission for the Protection of the Marine Environment of the North-East Atlantic, the North Sea has been classified as a problem region in the North East Atlantic in terms of eutrophication (OSPAR Commission, 2008). The North Sea receives N inputs from the Atlantic to the north and via the English Channel to the south, in addition to massive inputs from discharging rivers. Due to its semi-enclosed nature resulting in long nutrient residence times (Weston et al., 2004) the North Sea is especially exposed to the effects of N surplus and resulting eutrophication.

As part of the Greater North Sea, the shallow German Bight in particular has been identified as a highly eutrophied area. Sources of rN in the German Bight are anthropogenic nitrogen loads, which derive from densely populated adjacent land and reach the German Bight mostly via atmospheric depositions or riverine input (Beddig et al., 1997; Brion et al., 2004).

The nutrient pollution of the inner German Bight and the north German Wadden Sea is dominated by the discharges of the rivers Elbe and Weser, whereas the southern German Wadden Sea is under influence of the rivers Rhine, Ems and Maas and the IJsselmeer (Weigelt-Krenz et al., 2010).

After the observation of oxygen deficiency in large areas of the German Bight in the 1980's (Rachor and Albrecht, 1983), a number of policies (i.e. the 2<sup>nd</sup> International North Sea Conference and the OSPAR) were introduced along with associated monitoring programs to reduce nutrient inputs (Laane et al., 2005). As result, phosphorus loads have been reduced (by 3%  $y^{-1}$ ) successfully due to replacement of phosphates in detergents, whereas N loads decreased by around 2%  $y^{-1}$  since the mid-1980's (van Beusekom et al., 2008). According van Beusekom (2005) and Radach and Pätsch (2007) DIN concentrations in the German Bight show a decreasing trend since 1985 due to gradually declining riverine DIN discharges. Legally binding specifications in the European Water Framework Directive (WFD) demand re-establishment of a good ecological and chemical status of surface water bodies including the German Bight (WFD, 2000). The legal guidelines pose a scientific challenge, namely to define a pristine or ecologically healthy status for the German Bight. To do this requires an inventory of the modern situation, including a survey of actual rN inputs by rivers and internal riverine rN sources. Another important detail is the assessment of natural rN attenuation capacities. In this context, the amount of sedimentary denitrification within the rN cycle of the German Bight has not been quantified yet.

### **1.3 Stable Isotopes**

To assess biological turnover processes and sources of rN, the two stable isotopes of nitrogen,  $^{14}\text{N}$  and  $^{15}\text{N}$ , have been used both in experiments with artificial labelling and isotope tracking, and in studies on their natural abundances in different compartments of global, regional, or local N cycles. Isotopes are different types of atoms of the same chemical element having a different number of neutrons. Correspondingly, the stable isotopes of an element differ in mass number (or number of nucleons), whereas the number of protons and the electron configuration are the same.

In this study, we used the nitrogen and oxygen natural abundance to characterize sources and rN turnover processes in rivers discharging into the German Bight. As  $\text{NO}_3^-$  is by far the predominant form of rN in the systems under study, we focussed on the stable isotope composition of nitrate.

The two stable isotope ratios  $^{15}\text{N}/^{14}\text{N}$  and  $^{18}\text{O}/^{16}\text{O}$  have been assessed in riverine water column nitrate. Isotope ratios are expressed in the delta notation ( $\delta^{15}\text{N}$  relative to atmospheric  $\text{N}_2$  and  $\delta^{18}\text{O}$  relative to Vienna Standard Mean Ocean Water, both defined as 0‰):

$$\delta \text{ sample [‰]} = (R_{\text{sample}}/R_{\text{standard}} - 1) \times 1000 \quad [1.1]$$

where R is  $^{15}\text{N}/^{14}\text{N}$  or  $^{18}\text{O}/^{16}\text{O}$  ratio of sample and standard, respectively.

Due to mass differences between isotopes, they exhibit slightly different chemical and physical behaviour resulting in isotope fractionation during conversion processes (Faure and Mensing, 2005; Kendall, 1998). Two main processes cause isotope fractionation: equilibrium isotope exchange reactions and kinetic reactions such as biologically mediated processes (Hoefs, 2004; Kendall, 1998). The magnitude of the fractionation depends on mass differences of the isotopes, on reaction rates and the relative bond energies being broken or formed during the course of the reaction (Hoefs, 2004; Kendall, 1998). Within aquatic environments, nitrogen transformation processes, many of which are microbially mediated, cause N isotopic variations in the diverse pools of reactive N (Sigman and Casciotti, 2001). The isotope fractionation factor ( $\epsilon$ ) of a given reaction is approximated by the difference in  $\delta^{15}\text{N}$  between the substrate and the initial product:

$$\epsilon \text{ (‰)} = (R_{\text{product}}/R_{\text{substrate}} - 1) \times 1000 \quad [1.2]$$

where R is  $^{15}\text{N}/^{14}\text{N}$  or  $^{18}\text{O}/^{16}\text{O}$  ratio of substrate and product, respectively.

As bonds of lighter isotopes ( $^{14}\text{N}$  and  $^{16}\text{O}$ ) are slightly more easily ruptured than the bonds of heavier isotopes ( $^{15}\text{N}$  and  $^{18}\text{O}$ ), the reaction products are generally enriched in light isotopes and the residual substrate is progressively enriched in the heavy isotopes (Kendall, 1998). The isotopic effect is highly variable depending on factors such as reaction pathway, substrate availability and the organisms involved.

Different kinetic isotope effects can be attributed to different processes, i.e. assimilation, denitrification, nitrification and N-fixation. These N isotope effects for microbial processes in pure culture are listed in Table 1.1 (Casciotti, 2009 and the references therein).

Tab. 1.1: Fractionation factors for microbial processes in pure culture.

<sup>14</sup>N preference is expressed by negative values.

Process	Reaction	$\epsilon$ (‰)
Nitrate reduction (denitrification)	$\text{NO}_3^- \rightarrow \text{NO}_2^-$	-13‰ to -30‰
Nitrite reduction (denitrification)	$\text{NO}_2^- \rightarrow \text{NO}$	-5‰ to -25‰
Nitrous oxide reduction (denitrification)	$\text{N}_2\text{O} \rightarrow \text{N}_2$	-4‰ to -13‰
Nitrate reduction (nitrate assimilation)	$\text{NO}_3^- \rightarrow \text{NO}_2^-$	-5‰ to -10‰
Nitrogen fixation	$\text{N}_2 \rightarrow \text{N}_{\text{org}}$	+2‰ to -2‰
Ammonium assimilation	$\text{NH}_4^+ \rightarrow \text{N}_{\text{org}}$	-14‰ to -27‰
Ammonia oxidation (nitrification)	$\text{NH}_4^+ \rightarrow \text{NO}_2^-$	-14‰ to -38‰
Nitrite oxidation (nitrification)	$\text{NO}_2^- \rightarrow \text{NO}_3^-$	+12.8‰

The  $\text{NO}_3^-$  dual isotope approach (simultaneous analysis of N and O isotopes) offers an additional tool to identify  $\text{NO}_3^-$  sources and N cycling. As for N isotopes,  $\text{NO}_3^-$  assimilation (net sink of O atoms) discriminates between <sup>18</sup>O and <sup>16</sup>O isotopes and preferentially incorporates light isotopes. The additional measurement of O isotopes in  $\text{NO}_3^-$  allows distinguishing processes that overprint each other when looking at  $\delta^{15}\text{N}$  alone. In freshwater studies, combined analysis of  $\delta^{15}\text{N}$  and  $\delta^{18}\text{O}$  allows a better separation of  $\text{NO}_3^-$  sources, i. e. fertiliser origin and atmospheric origin (Kendall, 1998). Thus, a powerful tool used within this study to construct riverine N cycling.

## 1.4 Denitrification in sediments

Remineralisation of organic matter dominated by bacterial dissimilatory metabolism plays a key role in geochemical transformations that occur in marine sediments. The acquisition of energy involves either respiration or fermentation. During fermentation (an anaerobic process) organic compounds are partially oxidized and reduced with no external electron acceptor involved; it is a relatively inefficient process in terms of ATP (adenosine triphosphate) production (2–4 mol ATP per mol glucose). On the other hand, respiration involves the oxidation of organic carbon substrate coupled to the reduction of an external electron acceptor which is compared to fermentation a more efficient process (~32 mol ATP per mol glucose) (Burdige, 2006).

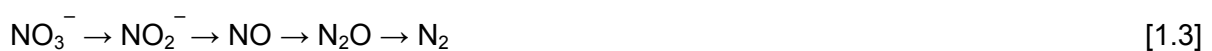
The occurrence of specific respiratory processes and associated microorganism is controlled by the free energy yield per mole of organic carbon oxidized by each of these electron acceptors (Froelich et al., 1979). Thus, the electron acceptor that provides the greatest amount of free energy will be utilized first, and when this oxidant is consumed the next efficient electron acceptor will be utilized. Hence, in oxic zones of the sediment, the diagenesis occurs via aerobic metabolisms, whereas in oxygen-free environments, alternate electron acceptors are utilized. Fig. 1.2 depicts the classical sedimentary vertical zonation of sequentially utilized electron acceptors and the respective standard-state free energy changes.

From a chemical perspective, the biogeochemical zonation is comparable with a redox cascade.

Water			
Sediment	<u>Electron Acceptor</u>	<u>Process</u>	$\Delta G^\circ$ (kJ mol Glucose <sup>-1</sup> )
	O <sub>2</sub>	Aerobic respiration	-2.82
	NO <sub>3</sub> <sup>-</sup>	Denitrification	-2.66
	Mn <sup>4+</sup>	Manganese Reduction	-2.38
	Fe <sup>3+</sup>	Iron Reduction	-0.79
	SO <sub>4</sub> <sup>2-</sup>	Sulfate Reduction	-0.45
		Methanogenesis (e.g. glucose)	-0.30

Fig. 1.2: Biogeochemical zonation in marine sediments and respective free energy changes (modified after Froelich et al., 1979; Burdige, 1993).

With sediment depth, oxygen concentration decreases, nitrate becomes the next preferred electron acceptor and denitrification occurs. The reduction pathway for nitrate is (see also Fig. 1.1):



Nitrate used in denitrification derives either directly from the overlying water column or from nitrate produced within the oxic zones of the sediment by ammonification of particulate N, ammonia oxidation, and nitrification. Often, there is a tight spatial coupling between denitrification and nitrification in redox boundaries within sediments (Middelburg et al., 1996).

Controlling factors for denitrification rates in sediments are amount and quality of sedimentary organic matter, concentrations of nitrate in water overlying the sediment, permeability of the sediment, and secondary factors, such as bioturbation/bio-irrigation, macrophytes and availability of manganese and iron (Cornwell et al., 1999). The influence of controlling factors on denitrification also depends on the amount of direct denitrification and coupled nitrification-denitrification (Cornwell et al., 1999). Whereas coupled nitrification-denitrification is limited by bottom-water oxygen concentration and oxygen diffusion/advection into the sediment, direct denitrification is enhanced by a low oxygen environment (Rysgaard et al., 1994).

Denitrification converts rN to gaseous products, mainly  $N_2$ , that escape from the sediment to the overlying water or atmosphere by diffusion (Nixon et al., 1996) and is lost from the system (Fig. 1.1). Together with the process of anaerobic ammonia oxidation (anammox), denitrification in sediments is the most important sink for nitrate on a global scale and a first order regulation mechanism for the nitrogen cycle of coastal ecosystems (Middelburg et al., 1996).

## 1.5 Thesis outline

The overall objective of this study was to quantify and identify sources and sinks of the rN pool in the German Bight. Because riverine discharges are known to be the main source of rN, the study focussed primarily on nitrate sources deriving from rivers draining into the North Sea (chapters 2 and 3). Secondly, denitrification rates were determined to estimate an annual nitrate removal rate in sediments of the northern Wadden Sea and Elbe Estuary. As these sediments have been previously suspected to eliminate a high amount of nitrate delivered to the German Bight and available data have been sparse, a first data set of seasonal denitrification rates in different sediment types has been raised (chapters 4 and 5).

The following chapters of this thesis constitute the basis of four articles that are published, submitted or in preparation for peer-reviewed scientific journals.

### *Chapter 2*

#### ***Isotopic composition of nitrate in five German rivers discharging into the North Sea***

*Astrid Johannsen, Kirstin Dähnke, Kay Emeis*

*Organic Geochemistry (2008) 39: 1678–1689*

Nitrate isotopic signatures and nitrate concentration of five German rivers were determined on a bimonthly basis. The ranges of isotope values for the rivers under study (Rhine, Elbe, Weser, Ems and Eider) suggest that nitrate in these rivers derives from soil nitrification, sewage, and/or manure.  $\delta^{15}N-NO_3^-$  and  $\delta^{18}O-NO_3^-$  values varied considerably with season indicating that assimilation of nitrate is the main fractionation process of riverine nitrate. These data represent the first seasonal measurement of nitrate isotopes in rivers of the German Bight catchment. The obtained isotopic fingerprint of riverine nitrate can be used to estimate respective nitrate isotopic composition based on land use patterns in river catchments and to model nitrogen transport and isotopic mixtures from land to the North Sea in the past.

### Chapter 3

#### **Seasonal variations in nitrate isotope composition of three rivers draining into the North Sea**

*Astrid Deek, Kay Emeis, Ulrich Struck*

*Biogeosciences Discussions (2010) 7: 6051–6088*

To identify nitrate sources, sinks, and turnover,  $\delta^{15}\text{N-NO}_3^-$  and  $\delta^{18}\text{O-NO}_3^-$  in nitrate and  $\delta^{15}\text{N}$  of particulate nitrogen for the period 2006 – 2009 were determined in three German rivers (Rhine, Weser and Ems) that discharge into the German Bight.  $\delta^{18}\text{O-H}_2\text{O}$  of river water was determined to examine nitrification as major nitrate source which has been previously indicated by relatively low  $\delta^{18}\text{O-NO}_3^-$  values. Diffuse nitrate inputs from organic fertilizers and nitrification in soils were identified as major contributors to the riverine nitrogen pools of the rivers under study. Strong interdependencies between stream sizes, consumption efficiency and fractionation range were found comparing the three rivers of different sizes, with highest nitrate consumption rates associated with highest nitrate isotopic variation in the small river Ems. This study suggests that sources of rN and the nitrate consumption efficiency interrelated with the current velocity determines mostly the isotopic composition of riverine nitrate.

### Chapter 4

#### **Denitrification in coastal sediments of the German Wadden Sea**

*Astrid Deek, Kay Emeis, Justus van Beusekom*

resubmitted to *Biogeochemistry*

To estimate the amount of nitrate denitrified in German Wadden Sea sediments, denitrification rates were determined over seasonal cycles at two locations with two sediments types each, the first site (Meldorf Bight) receiving nitrate during all seasons from the Elbe river plume, and a second site on the island of Sylt, where nitrate is depleted during summer months. Major factors controlling denitrification rates have been the nitrate concentrations in the overlying water, the ambient temperature, and the organic matter content of the sediment. By extrapolation of seasonal mean denitrification rates classified into different sediment types and nitrate availability, an annual nitrogen removal rate around 10 kt N  $\text{y}^{-1}$  for the entire northern sector of the German Wadden Sea area has been estimated. This corresponds to 12% of the annual Elbe river nitrate load. The results of this

study show that Wadden Sea sediments have a high potential to remove nitrate if available, thus providing an internal mechanism counteracting eutrophication.

*Chapter 5*

***Denitrification in sediments of the Elbe Estuary and adjacent coastal zones***

*Astrid Deek, Kay Emeis, Justus van Beusekom, Sven Mayer, Maren Voss*

in preparation

Denitrification rates in sediments in riparian zones along the nitrate gradient of the Elbe Estuary and in shallow areas in the adjacent coastal zone of the North Frisian Wadden Sea were determined for two sampling campaigns in March and September 2009. Sediments of shallow water areas in the inner Elbe Estuary are still effective sinks for nitrate but the capacity of the Elbe Estuary to retain nutrients has been ruined by morphological changes of the Elbe River such as the reduction of shallow water areas accompanied by higher current velocities and lower water residence time. Extrapolating average denitrification rates for sediments in the Elbe River results nitrate removal rates between 1.6 kt and 3.3 kt N during spring and summer months reducing the nitrate load of the Elbe River ( $79 \text{ kt y}^{-1}$ ) by around 5%. Thus, most rN is transported channel like to the open North Sea. Coastal sediments partly buffer nitrate in the overlying water delivered by the Elbe River plume but we observe that in summer months, nitrate availability limits sediment denitrification indicating an additional capacity to remove  $\text{NO}_3^-$  from the water column.

## 2 Isotopic composition of nitrate in five German rivers discharging into the North Sea

Astrid Johannsen, Kirstin Dähnke, Kay Emeis

*Organic Geochemistry* (2008) 39: 1678–1689

### Abstract

We determined concentrations and isotopic composition of nitrate in five German rivers (Rhine, Elbe, Weser, Ems, and Eider) that discharge into the North Sea. Samples were obtained on a biweekly to monthly basis and chemical and isotopic analyses were conducted for the period January 2006 to March 2007 at sampling stations situated before estuarine mixing with North Sea water. We observed maximum nitrate loads in winter and fall, when both discharge and concentration of nitrate are highest. Mean annual isotope values in nitrate ranged from 8.2‰ to 11.3‰ for  $\delta^{15}\text{N-NO}_3^-$  and 0.4‰ to 2.2‰ for  $\delta^{18}\text{O-NO}_3^-$ . The ranges of isotope values suggest that nitrate in these rivers derives from soil nitrification, sewage, and/or manure. These and published data on other rivers in northern Europe and northern America reveal a correlation between agricultural land use (>60% in the catchment areas of rivers examined) and  $\delta^{15}\text{N-NO}_3^-$  values. The rivers Rhine, Elbe, Weser and Ems show similar seasonal patterns of the isotopic fractionation of nitrate with increasing  $\delta^{15}\text{N-NO}_3^-$  values and simultaneously decreasing  $\text{NO}_3^-$  concentrations during summer months, indicating that assimilation of nitrate is the main fractionation process of riverine nitrate. Isotopic signals in winter are more depleted than the mean summer isotope values, attributed to less microbial activity and assimilative processes. Load weighted nitrate  $\delta^{15}\text{N}$  of the riverine input to the German Bight Coastal Water mass before estuarine mixing and processing is between 8 and 12‰. The high  $\delta^{15}\text{N}$  value of river nitrate is matched by high  $\delta^{15}\text{N}$  of nitrate in surface sediments in the German Bight.

## 2.1 Introduction

According to the OSPAR Commission for the Protection of the Marine Environment of the northeast Atlantic, nutrient pollution is one of the main environmental problems of the North Sea (OSPAR, 2003). The south eastern North Sea, including the German Bight (Fig. 2.1), in particular is facing considerable environmental problems due to high nutrient concentrations and subsequent eutrophication (van Beusekom et al., 2001; OSPAR, 2003). Because reactive nitrogen (rN) is a limiting factor for primary production in the North Sea (Owens et al., 1990; van Beusekom et al., 2001; Skogen et al., 2004), increase of rN inputs drastically influences primary production rates. Over the past decades rN inputs into the North Sea increased remarkably (Howarth and Marino, 2006), the biomass production tripled in many regions (Cloern, 2001), with a two- to threefold increase in the Wadden Sea region (van Beusekom, 2005). In the German Bight, oxygen depletion and phytoplankton blooms in the summer (Brockmann et al., 2003), shifts in the abundance of species (Lancelot et al., 1987; OSPAR, 2003), a decline of seagrass beds (Reise et al., 2005), and a massive development of green algal mats (Reise and Siebert, 1997) have been attributed to eutrophication. In an ongoing research project we aim to detect the modern contribution of riverine and atmospheric sources to the reactive nitrogen pool of the North Sea, and to reconstruct the pristine status of the North Sea by means of combined analysis of stable nitrogen isotope records in sediments and N-isotope distribution in an ecosystem model with explicit treatment of nitrogen isotopes under modern and assumed pristine loading conditions (Emeis et al., 2006). In the case of nitrate, which contains the stable isotope pairs  $^{15}\text{N}/^{14}\text{N}$  and  $^{18}\text{O}/^{16}\text{O}$ , the stable isotope composition offers a tool for source identification, because the dual isotopic signature of  $\delta^{15}\text{N}-\text{NO}_3^-$  and  $\delta^{18}\text{O}-\text{NO}_3^-$  of different sources is specific, and is therefore regarded as characteristic of origin (Kendall, 1998). However, the isotopic composition of nitrate does not reflect exactly the isotope values of its source, but is altered due to transformation processes (Kendall, 1998) like volatile loss of ammonia (Wassenaar, 1995), denitrification (Mariotti et al., 1981; Böttcher et al., 1990) and nitrification (Mayer et al., 2001) or uptake by organisms (Wada and Hattori, 1978). These biological turnover processes may be reconstructed by the measurement of  $\delta^{15}\text{N}-\text{NO}_3^-$  and  $\delta^{18}\text{O}-\text{NO}_3^-$  (Wankel et al., 2006). The main goal here is to identify the isotopic signal of riverborne nitrate inputs into the south eastern North Sea, its seasonal variability, and relationships to land use in the catchment and nitrate loads. To do this, we gathered data on riverine nitrogen loads and stable nitrogen and oxygen isotope composition of nitrate in the rivers Rhine, Elbe, Weser, Ems, and Eider discharging into the North Sea covering an annual cycle. We thus establish annual and seasonal loads of nitrate and load weighted averages of its isotopic signature for later use in coupled mass and isotope balance models of N cycling in the German Bight.

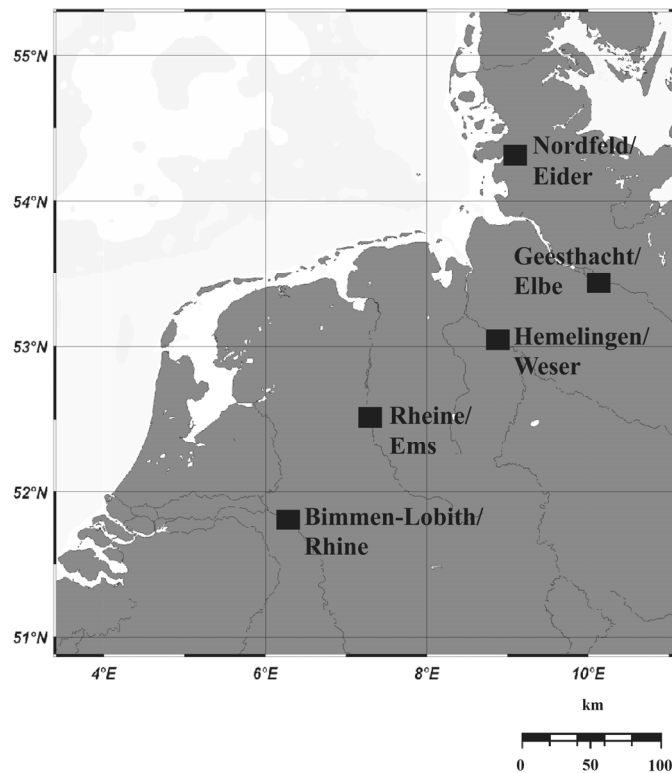


Fig. 2.1: Locations of sampling stations at rivers in the north western part of Germany.

## 2.2 Material and methods

### 2.2.1 Study area

The North Sea has considerable spatial gradients in biogeochemical characteristics (Thomas, 2004) and is subject to different influences on the nutrient budgets of sub-basins (Smith et al., 1997). While the northern part of the North Sea has oceanic characteristics due to water depths of up to 200 m and free water exchange with the Atlantic Ocean, water circulation in the south eastern part of the North Sea (the German Bight that has a maximum water depth of only 35 m) is strongly influenced by freshwater inputs from several large rivers and is hydrographically more isolated, causing an average flushing time of 33 days (Lenhart and Pohlmann, 1997). In a numerical simulation of river nitrate fluxes, Radach and Paetsch (2007) found that mean export of total nitrogen (TN) per area for the continental rivers draining into the North Sea was  $1685 \text{ kg N km}^{-2} \text{ yr}^{-1}$ , comprising approximately 25% of the mean anthropogenic N input of  $7044 \text{ kg N km}^{-2} \text{ yr}^{-1}$  into the watersheds of the North Sea. Among the rivers analysed by Radach and Paetsch (2007) are several that were investigated in the course of this study; together, the five rivers analysed here drain approximately 48% of

the 841,500 km<sup>2</sup> and are populated by approximately 53% of the entire population of 184 million persons in the North Sea watershed.

### 2.2.1.1 Rhine

With a length of 1320 km and an annual discharge of 69.4 km<sup>3</sup> (Frankignoulle and Middelburg, 2002), the Rhine is one of the most important water routes in Europe (Lòzan and Kausch, 1996) connecting the port of Rotterdam with a highly industrialized hinterland. The catchment area is 185,000 km<sup>2</sup> (22% of the entire North Sea catchment area), of which 50% is situated in Germany. The Rhine is highly impacted by human activities; approximately 58 million inhabitants live in its catchment area. Average annual nutrient loads of the Rhine are the highest of all German rivers discharging into the North Sea (Behrendt et al., 2002).

### 2.2.1.2 Elbe

The Elbe River, one of the main transport waterways of central Europe, runs from the Czech Republic through Germany to the North Sea. The total length of the Elbe is 1165 km and the annual freshwater discharge is about 23 km<sup>3</sup>. Its total drainage area is 148,000 km<sup>2</sup> (17.6% of the entire North Sea catchment area), about 25 million inhabitants live in its catchment area (Lòzan and Kausch, 1996).

### 2.2.1.3 Weser

The Weser is a stream of 452 km length that drains 46,000 km<sup>2</sup> (5.5% of the entire North Sea catchment area and including the basins of the headwaters Fulda and Werra; NLÖ, 1995). The river Weser has an annual freshwater discharge of 10.3 km<sup>3</sup> and the catchment area is inhabited by 9.3 million people (FGG-Weser, 2005).

### 2.2.1.4 Ems

With a length of 331 km (Lòzan and Kausch, 1996), the annual water discharge of the Ems is about 2.5 km<sup>3</sup> (Frankignoulle and Middelburg, 2002). The catchment of the Ems covers an area of 18,000 km<sup>2</sup> (2.1% of the entire North Sea catchment area) which is inhabited by 3.8 million people (UBA, 2006).

### 2.2.1.5 Eider

The smallest river examined in this study is the river Eider with a length of 108 km (Lòzan and Kausch, 1996) and an annual discharge of 0.8 km<sup>3</sup> (Bakker et al., 1999). The catchment area of 9350 km<sup>2</sup> (1.1% of the entire North Sea catchment area) is sparsely populated by 0.57 million people. Of the four rivers examined in this study, the Eider is least influenced by industrial waste water (Huntenburg et al., 1995).

### 2.2.2 Sampling

The water sampling was done at official LAWA (Länderarbeitsgemeinschaft Wasser) monitoring sites located upstream of the transition zone between fresh water and salt water so that alteration of nitrate concentration and isotope values by mixing with marine water can be precluded. Between March 2006 and March 2007 the rivers were sampled monthly (river Eider at the sampling station in Nordfeld) to biweekly (river Rhine in Bimmen-Lobith, river Weser in Bremen-Hemelingen and river Ems in Rheine) by staff of the authorities responsible for the monitoring sites. The river Elbe (Geesthacht) was sampled between January 2006 and December 2006. Sampling sites are indicated in Fig. 2.1. Water volumes of 50–200 ml were taken from the surface (1–2 m water depth), filtered through PVDF (polyvinylidene fluoride) filters (0.45 µm), then frozen and sent to the GKSS Institute for Coastal Research for further analysis.

### 2.2.3 Analyses

Nitrate concentrations were measured using a continuous flow analyzer (Bran & Luebbe, Auto Analyzer 3). The nitrate analysis described in Bran & Luebbe Auto Analyzer Method No. G-067-92 Rev.2 (2000) is a modification of the Armstrong et al. (1967) procedure which reduces nitrate to nitrite in a column of copperized cadmium. The nitrite ion is then reacted with sulfanilamide and N-1-naphthylethylenediamine to form a red azo dye. The method has been validated according to DIN 32645 resulting in a detection limit of 5.9 µmol NO<sub>3</sub><sup>-</sup> within the expected range of 50–450 µmol NO<sub>3</sub><sup>-</sup> for anthropogenically influenced rivers. Isotopic analyses of nitrogen and oxygen of NO<sub>3</sub><sup>-</sup> were carried out using the denitrifier method (Sigman et al., 2001; Casciotti et al., 2002) which is based on the isotopic analysis of nitrous oxide (N<sub>2</sub>O) produced by denitrifying *Pseudomonas* strains. The N<sub>2</sub>O is concentrated and purified on a Gas Bench (Thermo Finnigan Gas Bench II) and the isotopic composition was determined using an isotope ratio mass spectrometer (Delta Plus XP) calibrated with ultra high purity N<sub>2</sub> gas against air nitrogen. Nitrogen and oxygen isotope ratios are expressed in

the delta notation ( $\delta^{15}\text{N}$  and  $\delta^{18}\text{O}$ ) relative to atmospheric nitrogen and Vienna Standard Mean Ocean Water (VSMOW) in the conventional isotope terminology:

$$\delta \text{ sample } [\text{‰}] = (R_{\text{sample}}/R_{\text{standard}} - 1) \times 1000 \quad [2.1]$$

where R is  $^{15}\text{N}/^{14}\text{N}$  or  $^{18}\text{O}/^{16}\text{O}$  ratio of sample and standard, respectively. Results are given in per mil (‰). Analyses of  $\delta^{15}\text{N-NO}_3^-$  and  $\delta^{18}\text{O-NO}_3^-$  were standardized using the internationally distributed  $\text{KNO}_3$  reference material IAEA-N3 with an assigned  $\delta^{15}\text{N}$  value of 4.7‰ versus air  $\text{N}_2$  (Böhlke and Coplen, 1995) and a reported  $\delta^{18}\text{O}$  value of 22.7‰ versus SMOW (Revesz et al., 1997). For further quality assurance of the results, we used an internal potassium nitrate standard that was measured with each batch of samples. Analytical precision (one standard deviation) was better than 0.2‰ for  $\delta^{15}\text{N}$  and better than 0.4‰ for  $\delta^{18}\text{O}$ . The denitrifier method measures the isotopic composition of both nitrate and nitrite, but nitrite in the examined rivers represents only a negligible portion of reactive nitrogen and has therefore been disregarded in this study.

#### 2.2.4 Annual $\text{NO}_3^-$ loads and load weighted isotopic value

We used our concentration data and discharge rates for the sampling intervals to roughly calculate mass and isotope loads for the rivers examined here. The data of the flow rates used in this study were provided by the authorities responsible for monitoring at the respective sampling dates (Figs. 2.2–2.5). The annual  $\text{NO}_3^-$ -N loads were calculated by:

$$L(\text{NO}_3^- - \text{N}) = \sum_{i=1}^n |J_i| \times C_i \times \text{flow}_i \quad [2.2]$$

where the whole time interval J of 12 months was divided in n sampling intervals with the duration  $|J_i|$  the concentration  $C_i$  and discharge  $\text{flow}_i$ . The annual  $\text{NO}_3^-$ -N load L ( $\text{NO}_3^-$ -N) is the sum of the single loads in the sampling intervals  $J_i$  (Hebbel and Steuer, 2006). To calculate the load weighted annual isotope values, the isotope values for a certain month were multiplied with the respective concentration and weighted with the loads according to the following formula:

$$\delta^{15}\text{N}_{\text{wml}} = \frac{\sum_i \delta^{15}\text{N}_i \times C_i \times \text{flow}_i}{\sum_i C_i \times \text{flow}_i} \quad [2.3]$$

$$\delta^{18}O_{wml} = \frac{\sum_i \delta^{18}O_i \times C_i \times flow_i}{\sum_i C_i \times flow_i} \quad [2.4]$$

where  $\delta^{15}N_{wml}$  and  $\delta^{18}O_{wml}$  are the load weighted annual isotope values,  $\delta^{15}N_i$  and  $\delta^{18}O_i$  are the isotope values for a certain month,  $C_i$  is the concentration in  $\mu\text{mol/L}$  and  $flow_i$  the flow in  $\text{m}^3/\text{month}$ .

## 2.3 Results

### 2.3.1 Seasonal variation in concentration of nitrate and its isotopic composition

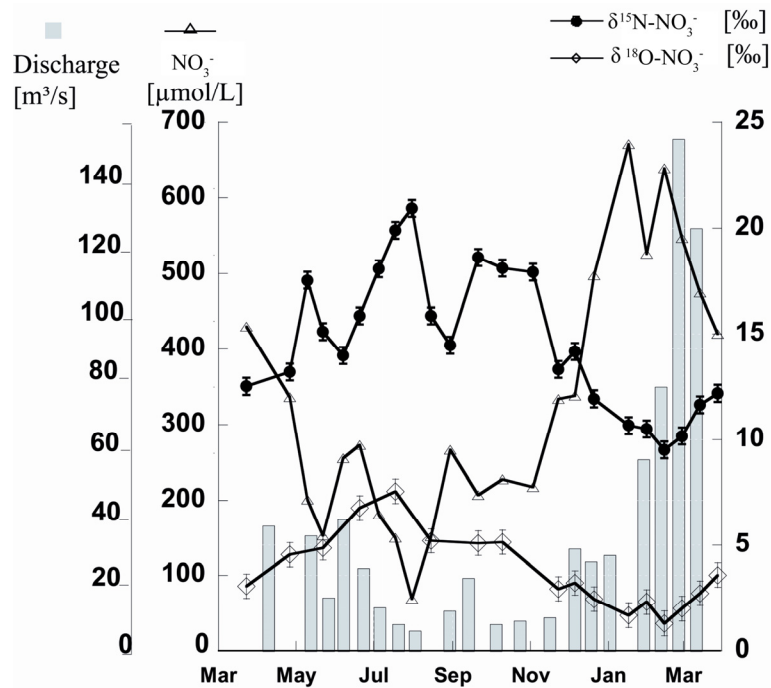


Fig. 2.2: The annual cycle of discharge, nitrate concentrations and  $\delta^{15}\text{N}/\delta^{18}\text{O}$  of nitrate for the river Ems, March 2006–March 2007.

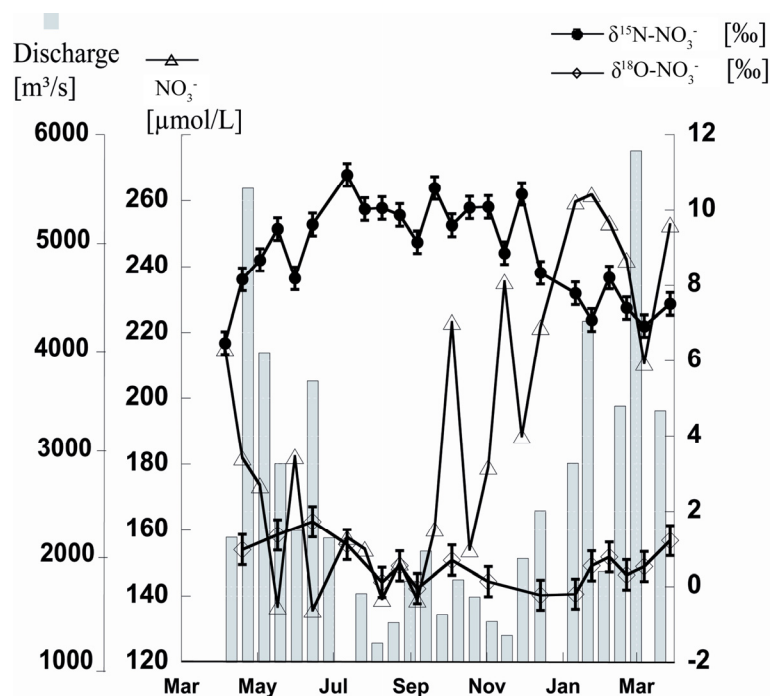


Fig. 2.3: The annual cycle of discharge, nitrate concentrations and  $\delta^{15}\text{N}/\delta^{18}\text{O}$  of nitrate for the river Rhine, March 2006–March 2007.

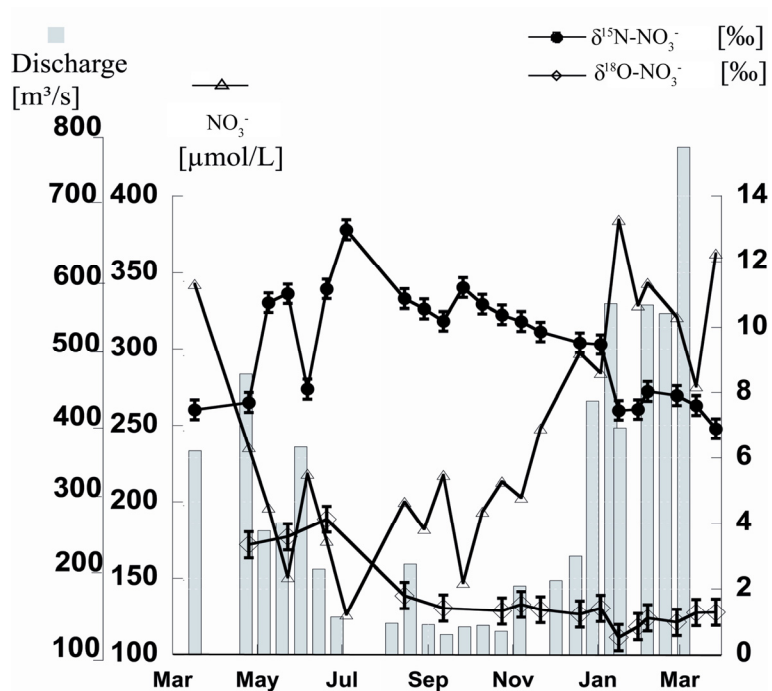


Fig. 2.4: The annual cycle of discharge, nitrate concentrations and  $\delta^{15}\text{N}/\delta^{18}\text{O}$  of nitrate for the river Weser, March 2006–March 2007.

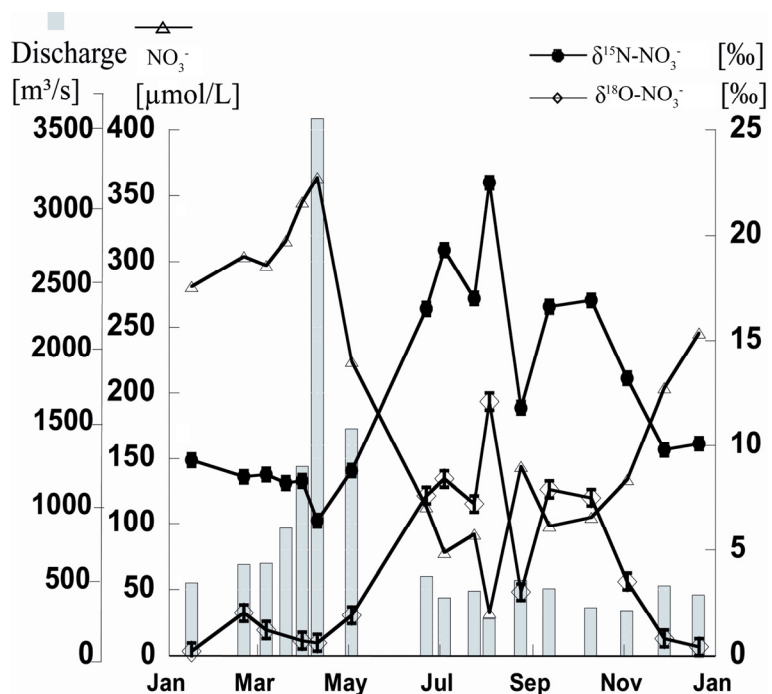


Fig. 2.5: The annual cycle of discharge, nitrate concentrations and  $\delta^{15}\text{N}/\delta^{18}\text{O}$  of nitrate for the river Elbe, January 2006–December 2006.

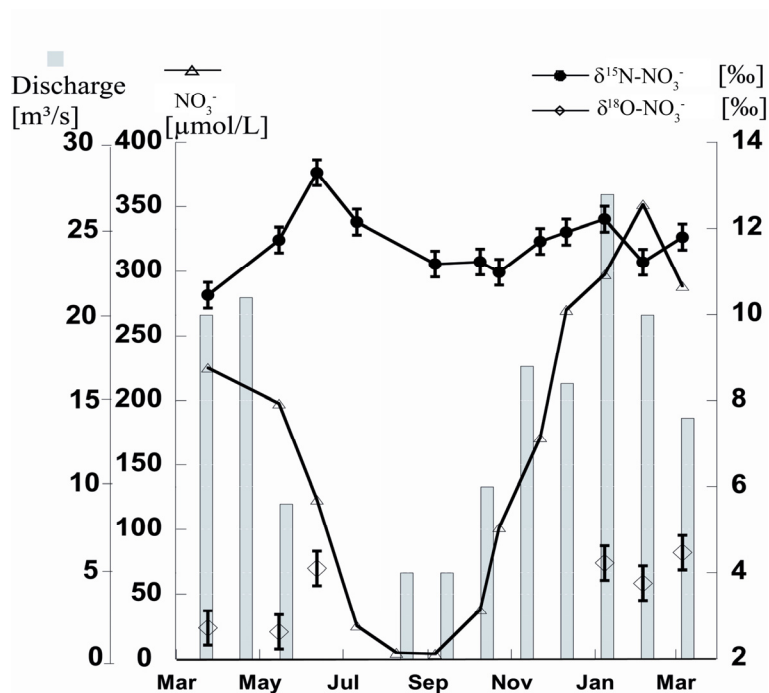


Fig. 2.6: The annual cycle of discharge, nitrate concentrations and  $\delta^{15}\text{N}/\delta^{18}\text{O}$  of nitrate for the river Eider, March 2006–March 2007.

Both nitrate concentrations and isotopic composition of  $\text{NO}_3^-$  (Figs. 2.2–2.6) showed seasonal variations that were similar in all investigated rivers. In all rivers, nitrate concentrations were highest in the winter season with maxima during the months January and April. Highest nitrate concentrations were measured in the river Ems (Fig. 2.2) with a peak concentration of almost 700  $\mu\text{mol/l}$  nitrate in January 2007. In the river Rhine (Fig. 2.3), the maximum concentration of 260  $\mu\text{mol/l}$  was measured between January and March 2007. The river Weser (Fig. 2.4) had a maximum value of 380  $\mu\text{mol/l}$  in January 2007, the river Elbe (Fig. 2.5) reached up to 350  $\mu\text{mol/l}$  in April 2006, as did the river Eider in February 2006 (Fig. 2.6). Generally, nitrate concentrations were lowest between May and September. During these months, nitrate had minimum concentrations below 150  $\mu\text{mol/l}$  in the rivers Rhine, Weser and Ems; less than 100  $\mu\text{mol/l}$  for the river Elbe and below 10  $\mu\text{mol/l}$  for the river Eider in August and September 2006. In general, the  $\delta^{15}\text{N-NO}_3^-$  values varied inversely with nitrate concentrations and the  $\delta^{15}\text{N-NO}_3^-$  values were higher in summer than in winter (Figs. 2.2–2.5). Maximum values of  $\delta^{15}\text{N-NO}_3^-$  were measured in the river Elbe with 22‰ in August 2006, in the Ems with almost 20‰ in July 2006, and in the river Weser with 13‰ in the same month. Also, the river Rhine had a maximum  $\delta^{15}\text{N-NO}_3^-$  value of 11‰ in July 2006, when the nitrate concentrations were at their minimum. The river Eider had its maximum  $\delta^{15}\text{N-NO}_3^-$  value of 13‰ in June 2006. The  $\delta^{18}\text{O-NO}_3^-$  patterns of the river borne nitrate were

also similar in the course of the year 2006. In the river Ems, highest  $\delta^{18}\text{O-NO}_3^-$  values were 7.6‰ in June and July 2006; in the Weser and the Rhine, maximum values of 4.1‰ and 1.7‰, respectively, were measured in June 2006. The  $\delta^{18}\text{O-NO}_3^-$  minimum values were all measured between December 2006 and February 2007: 1.3‰ in the Ems, 0.5‰ in the river Weser, 0.4‰ and -0.2‰ in the rivers Elbe and Rhine, respectively.

### 2.3.2 Nitrate load and annual isotopic value

#### 2.3.2.1 Nitrate load

At the sampling site Bimmen-Lobith, the river Rhine had a mean annual flow rate of 2500 m<sup>3</sup>/s for the period March 2006 to March 2007, the highest discharge among the examined rivers, followed by the Elbe with 765 m<sup>3</sup>/s (sampled from January until December 2006), the Weser with 300 m<sup>3</sup>/s in Bremen-Hemelingen and the river Ems with 30 m<sup>3</sup>/s at the sampling site Rheine. The mean flow rates at the sampling site of the River Eider are based on the mean monthly flow rates; accordingly, the Eider has a mean annual flow rate of 13 m<sup>3</sup>/s in Nordfeld, the lowest among the examined rivers. The discharges in all rivers are highest between January and April, lowest discharges occur during the summer months (Figs. 2.2–2.6). The rivers transport maximum nitrate loads during winter and spring. In annual average, the river Rhine transports the highest loads of nitrate with a mean value of 500 mol/s, compared with mean values of 200, 85, 15 and 3 mol/s for the Elbe, Weser, Ems and Eider, respectively. The estimated annual NO<sub>3</sub><sup>-</sup>-N load at the respective sampling sites are 220 kt (kilotons) for the Rhine, 82 kt for the Elbe, 40 kt for the Weser, 6 kt, for the Ems, and 1 kt for the Eider.

#### 2.3.2.2 Annual load weighted isotopic value

Results of the load weighted annual isotope values of the five rivers are given in Table 2.1. Eider and Ems have the highest mean annual isotope values ( $\delta^{15}\text{N-NO}_3^-/\delta^{18}\text{O-NO}_3^-$ ) of 11.2‰/2.2‰ for the river Ems, and a mean annual  $\delta^{15}\text{N-NO}_3^-$  value of 11.3‰ for the river Eider (for which the mean annual  $\delta^{18}\text{O-NO}_3^-$  was not determined). The mean annual isotope values ( $\delta^{15}\text{N-NO}_3^-/\delta^{18}\text{O-NO}_3^-$ ) for the rivers Rhine, Elbe and Weser are similar at 8.2‰/0.4‰, 8.5‰/1.3‰, and 8.3‰/0.9‰, respectively. We also estimated the load weighted isotope values separately for the summer season (April–September) and the winter season (October–March) (Table 2.1). The data illustrate that load weighted isotope values are generally lower in the winter season. The mean  $\delta^{15}\text{N-NO}_3^-$  values in summer are 0.5–3.9‰

higher than in winter, whereas the mean  $\delta^{18}\text{O-NO}_3^-$  values in summer are 0.3–3.1‰ higher than in winter.

Tab. 2.1: Load weighted annual isotope values in reference to the mean summer and winter isotope values.

River	Mean annual isotope value		Mean summer isotope value		Mean winter isotope value	
	$\delta^{15}\text{N-NO}_3^-$ [‰]	$\delta^{18}\text{O-NO}_3^-$ [‰]	$\delta^{15}\text{N-NO}_3^-$ [‰]	$\delta^{18}\text{O-NO}_3^-$ [‰]	$\delta^{15}\text{N-NO}_3^-$ [‰]	$\delta^{18}\text{O-NO}_3^-$ [‰]
Rhine	8.2	0.4	8.4	0.6	7.9	0.3
Elbe	8.5	1.3	11.7	3.9	7.8	0.8
Weser	8.3	0.9	9.3	1.3	8.1	1.0
Ems	11.2	2.2	14.3	3.2	10.6	1.9
Eider	11.3	n.a.	11.6	n.a.	10.8	n.a.

## 2.4 Discussion

In the discussion, we examine our new and published data in relation to land use in the river watersheds, discuss processes responsible for the seasonal variations observed, and finally address the riverine contribution to the nitrate pool of the German Bight.

### 2.4.1 Influence of watershed land use on isotopic character

To a first approximation, mixtures of nitrate in the rivers under study reflect land use patterns in river basins, an observation in line with previous studies (Harrington et al., 1998; Mayer et al., 2002; Voss et al., 2006). When plotting the annual load weighted  $\delta^{15}\text{N-NO}_3^-$  values of the rivers Rhine, Elbe, Weser, Ems and Eider (Table 2.1) versus the respective land use data (Table 2.2), and including data presented by Voss et al. (2006) for rivers discharging into the Baltic Sea, and of Mayer et al., 2002, for rivers draining watersheds in the north eastern US, we find a robust positive correlation ( $R^2 = 0.71$ ,  $n = 33$ ) between  $\delta^{15}\text{N-NO}_3^-$  values and the proportion of arable and urban land in the catchments (Fig. 2.7). Nitrate nitrogen (e.g. organic fertilizers) leaching from agricultural soils and nitrate deriving from municipal waste water (sewage) is characterized by high  $\delta^{15}\text{N-NO}_3^-$  values (4–9‰ and more than 10‰, respectively, Grischek et al., 1997), so that the  $\delta^{15}\text{N-NO}_3^-$  values rise with increasing proportion of agricultural and urban land use. The  $\delta^{15}\text{N-NO}_3^-$  values for the river catchments with more than 60% of agricultural and urban land use are all above 7‰. We suggest, therefore, that elevated  $\delta^{15}\text{N-NO}_3^-$  values in rivers draining catchments with significant urban and agricultural land use are caused by nitrate from sewage and/or manure.

Tab. 2.2: Land use of the sub-basins according to CORINE landcover (Statistisches Bundesamt, 1990)

River	Catchment Area	Subbasin	Area; Subbasin	Agriculture	Urban	Forest	Others
	[km <sup>2</sup> ]		[km <sup>2</sup> ]	[%]	[%]	[%]	[%]
Rhine	185,000	Lower Rhine	18,900	52.6	17.6	29.1	0.8
Elbe	148,300	Middle Elbe/Elde	16,600	69.5	4.2	23.5	2.8
Weser	46,300	Middle Weser	8,400	69.3	7.5	21.4	1.8
Ems	17,800	Upper Ems	4,800	77	8.9	9.9	4.2
Eider	9,400	Eider/Treene	2,200	87	4	6	3

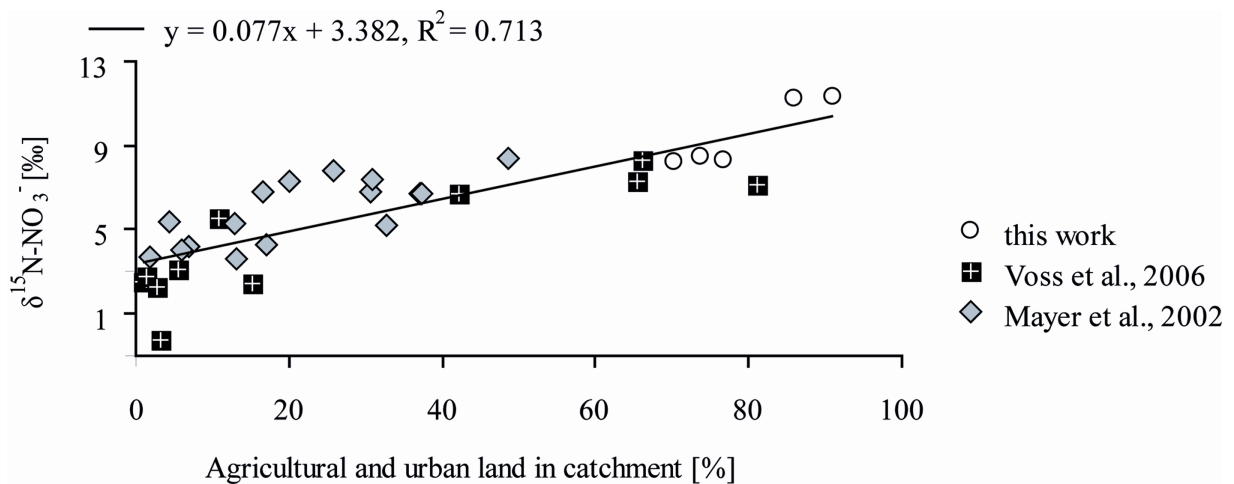


Fig. 2.7:  $\delta^{15}\text{N-NO}_3^-$  plotted against agricultural and urban land use values for rivers in North America and Europe.

Land use data for the rivers Rhine, Elbe, Weser, Ems and Eider are based on CORINE data (Table 2.2). Rivers in the Baltic Sea catchment were analysed by Voss et al. (2006). Data for 16 rivers in NE America are from Mayer et al. (2002). Note that, in contrast to the two other data sets, the data presented in Mayer et al. (2002) are not load weighted data.

## 2.4.2 Identification of nitrate sources and sinks based on the isotopic composition

The isotopic value of riverine  $\text{NO}_3^-$  is a collective signal of various sources contributing to the nitrate pool in the river. Biogeochemical processes in soils and aquifers affect the isotopic composition of reactive nitrogen inputs before they enter the rivers, so that the direct attribution to the  $\text{NO}_3^-$  sources is complex (Komor and Anderson, 1993). In the rivers under study, isotopically high  $\delta^{15}\text{N-NO}_3^-$  values between 8‰ and 12‰, and  $\delta^{18}\text{O-NO}_3^-$  values between 0‰ and 3‰ characterize the overall annual signal. The  $\delta^{15}\text{N-NO}_3^-$  values are in agreement with data from other rivers of Northern Europe under anthropogenic influence, such as the Oder or the Vistula rivers (Voss et al., 2006), and identify  $\text{NO}_3^-$  as deriving from sewage, manure and/ or soil nitrification (Kendall, 1998) (Fig. 2.8).

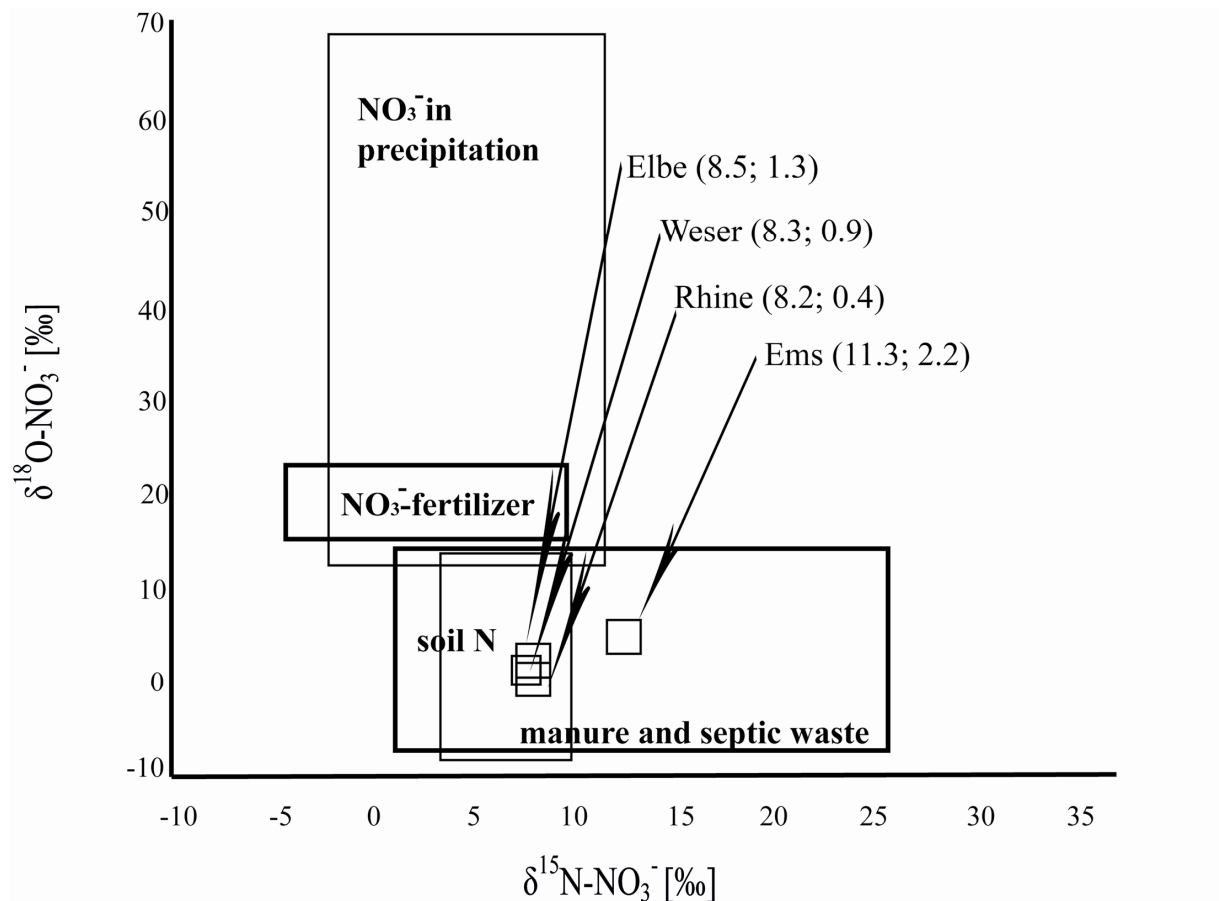


Fig. 2.8: General fingerprints of  $\text{NO}_3^-$  sources in a diagram of  $\delta^{15}\text{N}$  and  $\delta^{18}\text{O}$  (modified from Kendall, 1998) and character of nitrate isotopic composition in the rivers examined here.

When binning the mean annual isotopic values into mean winter (October–March) and mean summer (April–September) isotopic values, the load weighted  $\delta^{15}\text{N-NO}_3^-$  are approximately 0.5–3.9‰, and the  $\delta^{18}\text{O-NO}_3^-$  are 0.3–3.1‰ more depleted in the winter than in the summer season. This is due to seasonal changes in biological activity that causes variations in nitrate concentrations, and is associated with different isotopic fractionation processes. In general, biological processes cause an increase in heavy isotopes ( $^{15}\text{N}$  and  $^{18}\text{O}$ ) in the residual  $\text{NO}_3^-$  pool because organisms preferentially incorporate the light isotopes over the heavy isotopes (Kendall, 1998). Since biological activity increases at higher temperatures, enrichment of  $^{15}\text{N}$  and  $^{18}\text{O}$  in the residual  $\text{NO}_3^-$  pool is to be expected in the summer season. In regions with excess anthropogenic N input, a dominant source of river nitrate is nitrate leaching from soils (van Breemen et al., 2002; Brion et al., 2004), influencing both the nitrate concentration and its isotopic composition in the rivers. This source is isotopically elevated, because it is a residue of rN that has undergone kinetic fractionation in several processes and locations. After application of organic fertilizers (like manure with a  $\delta^{15}\text{N}$  of 10–20‰; Heaton, 1986; Aravena et al., 1993) and mineral fertilizers (with a  $\delta^{15}\text{N}$  of  $0 \pm 4$ ‰; Kendall, 1998) to agricultural soils,  $^{14}\text{N}$  is preferentially removed by ammonia volatilization (Wassenaar, 1995), by harvesting  $^{15}\text{N}$  depleted crops, or by denitrification in suboxic aquifers (Amberger and Schmidt, 1987) and soils (Grischek et al., 1997). The residual,  $^{15}\text{N}$  enriched rN pool is in part nitrified in water unsaturated soils (Wassenaar, 1995), making nitrification an important source of nitrate. Because nitrification leaves an imprint on  $\delta^{18}\text{O}$  in nitrate, the data on  $\delta^{18}\text{O-NO}_3^-$  for the rivers under study (between 0.4‰ and 2.2‰) may serve to identify nitrate derived from soil nitrification. Based on the assumption that nitrification acquires three oxygen atoms, two of which are assumed to be derived from ambient water, whereas the third atom comes from dissolved (atmospheric) oxygen (Anderson and Hooper, 1983; Yoshinari and Wahlen, 1985), the expected range of  $\delta^{18}\text{O}$  values of nitrate produced by nitrification can thus be calculated from known  $\delta^{18}\text{O-NO}_3^-$  values for atmospheric oxygen ( $\delta^{18}\text{O-O}_2$ ) and ambient water ( $\delta^{18}\text{O-H}_2\text{O}$ ):

$$\delta^{18}\text{O-NO}_3^- = \frac{2}{3} (\delta^{18}\text{O-H}_2\text{O}) + \frac{1}{3} (\delta^{18}\text{O-O}_2) \quad [2.5]$$

(Mayer et al., 2001).

The atmospheric oxygen is known to have a  $\delta^{18}\text{O}$  value of 23.5‰ (Kroopnick and Craig, 1972), and the ambient water, which is expected to be similar to the isotopic value in the river water and in the precipitation, can be derived from previous studies. In the Rhine basin, Buhl et al. (1991) measured  $\delta^{18}\text{O-H}_2\text{O}$  values of -8‰ in the precipitation, other estimations for  $\delta^{18}\text{O-H}_2\text{O}$  values in precipitation for the river catchments of the rivers Rhine, Elbe, Weser and Ems range from -8.1‰ to -8.6‰ (Bowen and Wilkinson, 2002; Bowen and Revenaugh,

2003; Bowen et al., 2005; OIPC, 2007). For the period 2002–2007 measured  $\delta^{18}\text{O}\text{-H}_2\text{O}$  of river water for the rivers Rhine, Elbe, Ems and Weser ranged between  $-7\text{‰}$  and  $-9.1\text{‰}$  (Stichler, pers. comm., 2008). Inserting these values into Eq. (2.5) results in an expected value for nitrate from nitrification around  $2\text{‰}$  which is close to the mean  $\delta^{18}\text{O}\text{-NO}_3^-$  values for the river under study between  $0.4\text{‰}$  and  $2.3\text{‰}$ . Thus, the  $\delta^{18}\text{O}$  values in nitrate imply nitrification as a dominant source, and soil leaching as an important transport mechanism of nitrate into river water. That soil leaching does indeed influence the isotopic composition of nitrate is suggested by data from a massive spring flood event in April 2006 in the Elbe catchment, when a significant input of soil nitrate is indicated by increased concentrations paired with decreased  $\delta^{18}\text{O}$  in nitrate (Fig. 2.5). At this time of year biological activity was inhibited by low temperatures, so any changes in the isotopic composition must be a consequence of input from soils. Our results are in line with a study by Deutsch et al. (2006), who investigated drainage waters from soils in a small river catchment in northern Germany. These waters had concentration weighted  $\delta^{15}\text{N}$  and  $\delta^{18}\text{O}$  in nitrate of  $10.4\text{‰}$  and  $4.7\text{‰}$ , respectively, and the low  $\delta^{18}\text{O}$  was attributed to nitrification. In a mixing model, these authors calculated that 86% of the nitrate in that particular river derived from soil drainage. From the relatively low  $\delta^{18}\text{O}$  values in nitrate of the rivers under study, we also derive that atmospheric deposition with high  $\delta^{18}\text{O}$  values in nitrate between  $25\text{‰}$  and  $70\text{‰}$  (e.g. Durka et al., 1994; Kendall, 1998) does not contribute a high share of nitrate. This is in line with a study of Mayer et al. (2002) who revealed that the influence of atmospheric deposition on the isotopic composition of riverine nitrate in watersheds with significant agricultural and urban land use is low due to the comparatively low nitrate concentrations in rainwater. In any case the elevated isotopic signature of nitrate inputs from the apparent main sources (soil water, sewage and manure) is further modified by biological activity in the river itself, as inferred from different  $\delta^{15}\text{N}$  values in the biologically active and inactive seasons (Kendall, 1998). We measured relatively depleted  $\delta^{15}\text{N}$  of riverine  $\text{NO}_3^-$  in fall and winter, when biological activity in the river itself was inhibited by low temperatures. Because phytoplankton activity is highest in the spring and summer months, significant decreases in river nitrate concentrations and increases in  $\delta^{15}\text{N}\text{-NO}_3^-$  characterize the time series from June until September (Figs. 2.2–2.5). The characteristic seasonal variation with minimum nitrate concentrations during summer and increase to a late fall or winter maximum is a result of biological uptake, consumption of nitrate and nitrite (Berounsky and Nixon, 1985), and reflects the annual phytoplankton production cycle with high nitrate assimilation rates in summer (van Beusekom and de Jonge, 1998). Nitrate concentrations and its isotope composition are correlated in most rivers (except Rhine and Eider), but the slope varies among the five rivers (Fig. 2. 9).

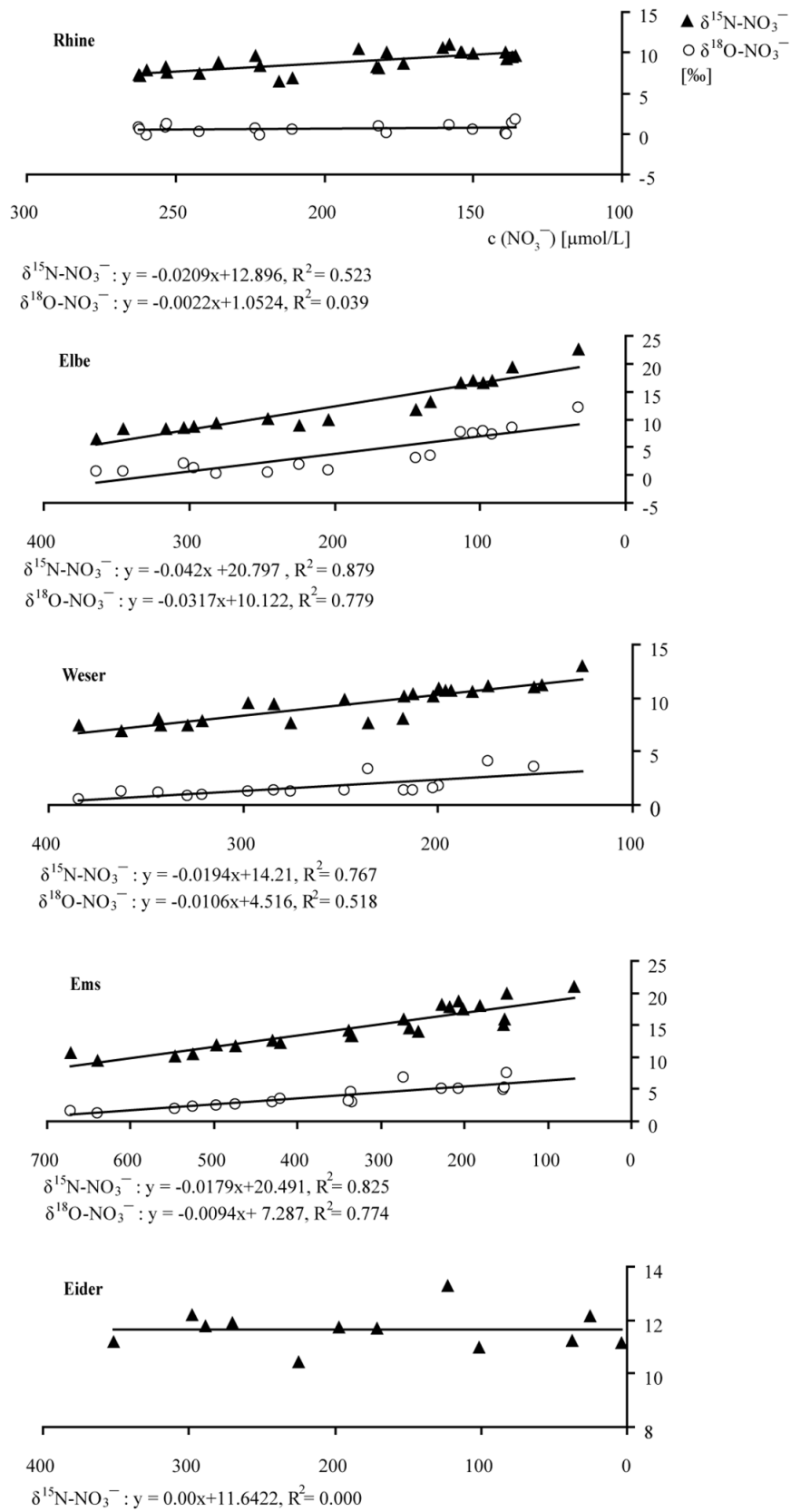


Fig. 2.9: Plot of isotopic values against nitrate concentrations.

See text for discussion.

The strong correlation of  $R^2 \geq 0.77$  for the plot of nitrate against  $\delta^{15}\text{N-NO}_3^-$  and the correlation of  $R^2 \geq 0.52$  for the plot of nitrate against  $\delta^{18}\text{O-NO}_3^-$  in the rivers Elbe, Weser and Ems indicates an important influence of changing nitrate concentrations on the isotopic value, suggesting fractionation during nitrate consumption. The expected fractionation of  $^{18}\text{O}/^{16}\text{O}$  and  $^{15}\text{N}/^{14}\text{N}$  with a ratio of 1:1 for assimilation (Granger et al., 2004) is not given for the rivers examined here. We assume that additional transformation processes or additional nitrate sources contribute nitrate with low  $\delta^{18}\text{O}$  values (e.g. nitrate from soil nitrification) and mask the fractionation caused by assimilation.

In the river Rhine, the correlation between  $\delta^{15}\text{N-NO}_3^-$  values and nitrate concentration is weak ( $R^2 = 0.52$ ) (Fig. 2.9). The  $\text{NO}_3^-$  concentrations show seasonal variations with low nitrate concentrations in summer and high concentrations in winter, whereas the variation of  $\delta^{15}\text{N-NO}_3^-$  values is low comparing to the rivers Elbe, Weser and Ems.  $\delta^{18}\text{O-NO}_3^-$  values do not vary at all, and show no apparent fractionation (Figs. 2.3 and 2.9). We hypothesize that the hydrodynamic regime of the Rhine influences nitrate concentrations in dependence on season. The discharge of the river Rhine is dominated by two different hydrological regimes: from May to November the greater part of the discharge is derived from the Swiss part of the drainage basin, whereas from December to May the discharge consists largely of water from the German and French parts of the drainage basin because the precipitation in the Swiss Alps is largely retained as snow. Water components from higher catchment areas are still dominant at lowlands of the river Rhine (Stichler et al., 2005). Hence, the summer flow is supported by a base flow of snowmelt and precipitation in the Alps, the winter flow consists of surface runoff from the German/French part of the drainage basin (Davis and Keller, 1983). The seasonal behaviour of  $\text{NO}_3^-$  concentration in the river Rhine can be attributed to the fact that the  $\text{NO}_3^-$  concentration in the summer snowmelt is lower than the  $\text{NO}_3^-$  concentration in the winter flow (Dijkzeul, 1982), largely derived from surface runoff influenced by leaching of fertilizers from arable land in the drainage basin (Probst, 1985; Kattan et al., 1986). Because of the different hydrological regimes, it remains difficult to evaluate the transformation processes influencing the isotopic composition of nitrate. Any kind of fractionation signal is likely to be masked by the varying source signature. Furthermore, we speculate that the high discharge in the river Rhine (Fig. 2.3) associated with a short water residence time is responsible for comparatively low fractionation of  $\text{NO}_3^-$  in the river Rhine. Water residence time is an important factor in nutrient processing efficiency (Kadlec, 1994; James et al., 2006) and the development of plankton communities (Lack, 1971; Winner, 1975). Generally, phytoplankton abundance increases with higher residence time and reduced velocity (Lack, 1971; Jones, 1984; Descy et al., 1987). The lower the concentrations of nitrate and the shorter the residence time of micro-organisms in river water, the smaller is the fractionation (Kendall, 1998).

Considering the river Eider, the seasonal variations of nitrate concentrations are largest among all rivers examined. Nitrate concentrations in summer decrease below 10  $\mu\text{mol/l}$  from 350  $\mu\text{mol/l}$  in winter months. It is remarkable that the  $\delta^{15}\text{N-NO}_3^-$  values vary only in the narrow range between 10‰ and 13‰ and do not show the characteristic pattern of maximum isotopic values in summer and minimum isotopic values in winter (Fig. 2.6), suggesting no fractionation and no increase of  $\delta^{15}\text{N-NO}_3^-$  over the course of the year. Because the nitrate concentrations from July until early fall are below 10  $\mu\text{mol/l}$ , we assume that the nitrate pool is almost completely assimilated in the summer months.

In small rivers such as the river Eider, nitrate in river water is generally in close and frequent contact with benthic detritus, biofilms and sediments (Hamilton et al., 2001). Under these conditions, nitrate is presumably rapidly and completely turned over several times. A complete conversion leads to a lack of apparent fractionation (Kendall, 1998), which is consistent with our data.

Nitrate, regardless of its source, is subject to denitrification within the riverine ecosystem (Howarth et al., 1996; Kellman and Hillaire-Marcel, 1998) in suboxic zones of water and sediments. Bacterial denitrification converts  $\text{NO}_3^-$  to  $\text{N}_2\text{O}$  and  $\text{N}_2$ , the fractionation resulting in the progressive enrichment of  $^{15}\text{N}$  and  $^{18}\text{O}$  in the residual nitrate (Kendall, 1998). The process is linked to environments which are oxygen limited with a readily oxidizable carbon source. Because the oxygen concentrations in all rivers examined here significantly exceed the threshold of 0.2 mg/l (Painter, 1970) at all seasons, denitrification in the water column is unlikely to contribute to the seasonal variability. However, denitrification may consume nitrate from the overlying water column (Kaushik et al., 1981) in anaerobic sediments. Benthic denitrification acts as a significant sink since nitrate diffusing across the water-sediment interface is completely consumed irrespective of its isotopic composition (Reinhardt et al., 2006). Sebilo et al. (2003) assessed the feasibility of using  $\delta^{15}\text{N-NO}_3^-$  as an indicator of denitrification at the scale of large river systems and hypothesized that benthic denitrification does not affect the isotopic composition of riverine nitrate significantly when the rate limiting step is the diffusive migration of nitrate through the water-sediment interface ( $^{15}\text{N}$  isotopic enrichment factor about -2%). We derive from this study and from other studies carried out in different kind of water bodies that denitrification in sediments does not result in apparent fractionation of  $^{15}\text{N}/^{14}\text{N}$  and  $^{18}\text{O}/^{16}\text{O}$  (Brandes and Devol, 1997; Lehmann et al., 2003; Sebilo et al., 2003; Reinhardt et al., 2006). Hence, sedimentary denitrification cannot be traced by isotope techniques, and our data are not suited to evaluate this process for the rivers under study.

According to Howarth et al. (1996) and Schroeder et al. (1996), benthic denitrification eliminates between 20% and 80% of nitrate input to rivers, whereas recent studies suggest that this rate has significantly decreased (Fulweiler et al., 2007; Savage, 2005). Further

investigations of processes in sediments are required to give a complete picture of N cycling in riverine ecosystems.

### 2.4.3 The riverine contribution of nitrate to the German Bight

Eutrophication of the seas and estuaries in Europe is mainly attributed to nutrient inputs from the land, with rivers as the main carriers (Behrendt et al., 2002). Nitrogen budgets and models of nitrogen in- and output of river systems include different pathways, e.g. point discharges, paved urban areas, atmospheric deposition, tile drainage and groundwater (Behrendt, 1996; Bach et al., 1998; Kunkel, 2006; Luc and Bernhard, 2006). A discrepancy between nutrient loading of river systems and the actual nutrient load is a general feature of all budgets, and most of the anthropogenic N loading of the watersheds is lost in transit through the hydrological system before reaching oceans by riverine transport (Howarth et al., 1996; Alexander et al., 2000; Radach and Pätsch, 2007). In this study, we only considered the isotopic signals of nitrate in rivers before entering the estuarine transition zones between fresh water and salt water. The turnover of nitrogen is expected to be most intense in this transition zone, because the tidal circulation generally causes a long residence time of water (de Wilde and De Bie, 2000). However, the data from this study suggest that river discharge delivers nitrate with high  $\delta^{15}\text{N-NO}_3^-$  between 8‰ and 12‰, and with low  $\delta^{18}\text{O-NO}_3^-$  between 0‰ and 3‰ to the German Bight. We do not expect considerable change in the isotopic composition of  $\text{NO}_3^-$  in the main course of the river before reaching the German Bight, because denitrification in the water column, accompanied with fractionation of nitrate, can be excluded. Since denitrification in the sediment does not cause a significant enrichment of  $\delta^{15}\text{N-NO}_3^-$  and  $\delta^{18}\text{O-NO}_3^-$  (Lehmann et al., 2003; Sebiló et al., 2003), the isotopic signal measured at the sampling stations before estuarine mixing might be stable along the course of the river. Recent studies in the estuary of the river Elbe do not suggest alteration of  $\delta^{15}\text{N}$  and  $\delta^{18}\text{O}$  in nitrate, because the measured range along the estuary and in the German Bight Coastal Water mass (salinities between 31 and 33) is between 7‰ and 10‰ for  $\delta^{15}\text{N-NO}_3^-$  and around 0‰ for  $\delta^{18}\text{O-NO}_3^-$  (K. Dähnke, pers. comm., 2007), a clear imprint of riverine nitrate.

## 2.5 Conclusions

The primary goal of this study was to assess the riverine background signature of rivers discharging into the southern North Sea. We examined the rivers Rhine, Elbe, Weser, Ems and Eider for the period of one year during January 2006–March 2007. The data give evidence that riverine nitrate of the rivers examined in this study originally derives from anthropogenic input, e.g. sewage and/or manure which is consistent with high agricultural and urban land use in the catchment areas. In the rivers Rhine, Elbe, Weser and Ems we observed seasonal variations of increasing  $\delta^{15}\text{N-NO}_3^-$  values with decreasing  $\text{NO}_3^-$  concentrations during summer, whereas such a variation of the isotopic composition of  $\text{NO}_3^-$  was not observed in the river Eider. We attribute this concentration dependent effect to bacterial or phytoplankton nitrate assimilation, which is the dominant nitrate removal process in the rivers during biologically active seasons that coincide with smaller discharges.

The isotopic signal is more depleted in  $^{15}\text{N}$  and  $^{18}\text{O}$  during winter, when riverine nitrate fluxes are maximal, and bears an imprint of nitrate leaching from soils at times of high precipitation. Generally low  $\delta^{18}\text{O-NO}_3^-$  values point towards significant nitrate inputs from nitrification in soils, where oxygen derives partly from ambient water and accordingly has a low  $\delta^{18}\text{O}$  signature.

Future investigations have to verify that seasonal variations of nitrate concentrations and isotopic composition measured during this study are representative and typical for each river. If the data turn out to be robust, we will on the one hand be able to estimate nitrate isotopic composition in river discharges based on land use patterns in river catchments, which are available. On the other hand, the isotopic mixture of each river may possibly be extrapolated from individual  $\delta^{15}\text{N}$ -nitrate relationships for each river. In light of available data on land use changes and river loads in past decades, both steps will greatly advance our ability to numerically model nitrogen transport and isotopic mixtures from land to the North Sea in the past. In an inverse modelling approach with a numerical ecosystem model, we then expect to be able to reconcile combined mass and isotope balances with data from suitable archives of pristine conditions.

## **Acknowledgements**

We would like to thank all the institutions and many helpful people that have supported the project by collecting samples at the respective river sites. In particular we acknowledge the efforts of T. Gerke (IMBL Bimmen-Lobith), of Dr. H. Schimmer and H. Petry (Bezirksregierung Münster), Dr. Schulz (LANU, Schleswig-Holstein), and B. Freiheit (Senator für Bau, Umwelt und Verkehr in Bremen) for coordination and help with sampling at the river sites. The authors thank Maren Voss for improving a first draft of the manuscript. Funding by the Deutsche Forschungsgemeinschaft under Grant DFG Em/26 is gratefully acknowledged.

### 3 Seasonal variations in nitrate isotope composition of three rivers draining into the North Sea

Astrid Deek, Kay Emeis, Ulrich Struck

*Biogeosciences Discussions* (2010) 7: 6051–6088

#### Abstract

Nitrate loading of coastal ecosystems by rivers that drain industrialised catchments continues to be a problem in the south eastern North Sea, in spite of significant mitigation efforts over the last 2 decades. To identify nitrate sources, sinks, and turnover in three German rivers that discharge into the German Bight, we determined  $\delta^{15}\text{N-NO}_3^-$  and  $\delta^{18}\text{O-NO}_3^-$  and  $\delta^{15}\text{N}$  of particulate nitrogen for the period 2006 – 2009 (biweekly samples). The nitrate loads of Rhine, Weser and Ems varied seasonally in magnitude and  $\delta^{15}\text{N-NO}_3^-$  (6.5–21‰), whereas the  $\delta^{18}\text{O-NO}_3^-$  (-0.3–5.9‰) and  $\delta^{15}\text{N-PN}$  (4–14‰) were less variable. Overall temporal patterns in nitrate mass fluxes and isotopic composition suggest that a combination of nitrate delivery from nitrification of soil ammonium in the catchment and assimilation of nitrate in the rivers control the isotopic composition of nitrate. Nitrification in soils as a source is indicated by low  $\delta^{18}\text{O-NO}_3^-$  in winter, which traces the  $\delta^{18}\text{O}$  of river water. Mean values of  $\delta^{18}\text{O-H}_2\text{O}$  were between -9.4‰ and -7.3‰; combined in a ratio of 2:1 with the atmospheric oxygen  $\delta^{18}\text{O}$  of 23.5‰ agrees with the found  $\delta^{18}\text{O}$  of nitrate in the rivers.

Parallel variations of  $\delta^{15}\text{N-NO}_3^-$  and  $\delta^{18}\text{O-NO}_3^-$  within each individual river are caused by isotope effects associated with nitrate assimilation in the water column, the extent of which is determined by residence time in the river. Assimilation is furthermore to some extent mirrored both by the  $\delta^{15}\text{N}$  of nitrate and particulate N. Although  $\delta^{15}\text{N-NO}_3^-$  observed in Rhine, Weser and Ems are reflected in high average  $\delta^{15}\text{N-PN}$  (between 6‰ and 9‰), both are uncorrelated in the time series due to lateral and temporal mixing of PN. That a larger enrichment was consistently seen in  $\delta^{15}\text{N-NO}_3^-$  relative to  $\delta^{18}\text{O-NO}_3^-$  is attributed to constant additional diffuse nitrate inputs deriving from soil nitrification in the catchment area. A statistically significant inverse correlation exists between increasing  $\delta^{15}\text{N-NO}_3^-$  values and

decreasing  $\text{NO}_3^-$  concentrations. This inverse relationship - observed in each seasonal cycle - together with a robust relationship between human dominated land use and  $\delta^{15}\text{N-NO}_3^-$  values demonstrates a strong influence of human activities and riverine nitrate consumption efficiency on the isotopic composition of riverine nitrate.

### 3.1 Introduction

On a global scale, human activity has resulted in a doubling of the reactive nitrogen pool since pre-industrial times (Galloway, 2003) with more localised hot spots at the land-sea interface (Gruber and Galloway, 2008). In the North Sea area, the reactive nitrogen discharge by rivers has increased remarkably since the 1960's over assumed pristine conditions (Howarth and Marino, 2006). Today, the German Bight in the south eastern North Sea receives approximately 350 kt of reactive N (mainly in the form of nitrate) per year from rivers draining densely populated and industrialised areas of NW Europe (Johannsen et al., 2008). The increased reactive nitrogen loads and ensuing eutrophication continue to be an environmental pressure on many coastal seas (Howarth and Marino, 2006). The long average water residence time (Weston et al., 2004) permits severe eutrophication to unfold in the German Bight (Hickel et al., 1993). Most nutrients deriving from Germany enter the southern North Sea via the Rhine and the Elbe rivers and also from medium-sized rivers, such as the Weser River and Ems River (UBA, 2009). Nitrate inputs from point sources have decreased from their peak in the 1980's in response to environmental legislation (Pätsch and Radach, 1997), but the annual average nitrate loads of these rivers are slow in responding to pollution reduction measures, and thus are not solely determined by inputs from manageable sources. There is a continuing need to understand the nature of this apparent buffering. At present, total nitrogen loads in German rivers are thought to derive mainly from diffuse sources, dominated by a reactive nitrogen surplus stemming from agriculture (fertiliser and manure) (Hamm, 1996; Behrendt et al., 2002; Gömann et al., 2005). Previous studies of nitrate isotope properties (Johannsen et al., 2008; Dähnke et al., 2008) and microbial communities (Herfort et al., 2009) in rivers draining into the North Sea suggested that sources and sinks of nitrate within rivers may have been overlooked. Additionally, hydrological characteristics of the rivers highly influence transformation processes of riverborne nitrate, and are controlled by stream size and discharge regime.

The natural abundance of  $\delta^{15}\text{N-NO}_3^-$  and  $\delta^{18}\text{O-NO}_3^-$  has been used to identify sources and to trace transformation processes of riverborne nitrate (Deutsch et al., 2006; Mayer et al., 2002; Sebiló et al., 2006; Wankel et al., 2009; Schlarbaum et al., 2010). Different sources of stream water nitrate (direct fertiliser input, atmospheric deposition, sewage and wastewater inputs, or leaching of nitrate produced by nitrification of ammonia from agricultural soils; Behrendt et al., 2002) are specific in their dual isotopic composition. In precipitation, the  $\delta^{15}\text{N-NO}_3^-$  varies depending on location and season between -4‰ and +9‰ and is similar to the  $\delta^{15}\text{N-NO}_3^-$  of nitrate produced by nitrification (Kendall, 1998). Added attributes of these two sources are distinct ranges of  $\delta^{18}\text{O-NO}_3^-$  in nitrate, with atmospheric  $\text{NO}_x$  in precipitation having a  $\delta^{18}\text{O}$  value between 20‰ and 60‰ (Kendall, 1998), and nitrate originating from

nitrification falling in a range between -10‰ and +16‰ (Kendall, 1998; Mayer et al., 2001; Burns and Kendall, 2002).  $\delta^{15}\text{N-NO}_3^-$  of nitrate from organic fertilizers and from municipal waste water is characterized by high  $\delta^{15}\text{N}$  values between 4‰ and 9‰, sometimes even higher (Grischek et al., 1998).

The isotopic mixture of nitrate sources is processed within rivers by different biological processes that in turn are associated with specific isotopic fractionation. Isotopic fractionation arises from biological processes, such as assimilation and denitrification, and each process is associated with characteristic fractionation factors  $\epsilon$  (the isotopic enrichment/depletion of the product relative to the substrate in ‰) that determine the isotopic composition of residual nitrate and of any products. A useful indicator of nitrate assimilation in rivers is  $\delta^{15}\text{N}$  in suspended particulate organic matter ( $\delta^{15}\text{N-PN}$ ). Although particulate nitrogen originates from either external sources or from production within the river, analysis of paired  $\delta^{15}\text{N-NO}_3^-$  and  $\delta^{15}\text{N-PN}$  may shed light on the contribution of assimilation.

This study expands on a previous investigation (Johannsen et al., 2008) of river nitrate in five rivers that contribute substantially to eutrophication in the German Bight of the SW North Sea. That study was performed over the course of only one year and did not include particulate matter and  $\delta^{18}\text{O-H}_2\text{O}$ . By expanding our time series, we wished to answer the following questions: (1) Can we characterize major nitrate sources by means of specific isotopic fingerprints? (2) How does river discharge and water residence time influence nitrate concentration and its isotopic composition? (3) Do we find evidence for biological processes within the rivers that influence nitrate loads and nitrate isotopic variability?

### **3.2 Material and methods**

#### **3.2.1 Rivers studied**

This study was conducted at monitoring sites of three rivers (Rhine, Weser, Ems) that differ substantially in annual loads. The load of Rhine is approximately 220 kt N/year, whereas the rivers Weser and Ems discharge 40 kt and 6 kt N per year, respectively. All three rivers are highly impacted by human activities, the populations in their watersheds are dense, and agricultural land-use is comparatively high (70 – 90% of urban and arable land-use). More details are given in Johannsen et al. (2008).

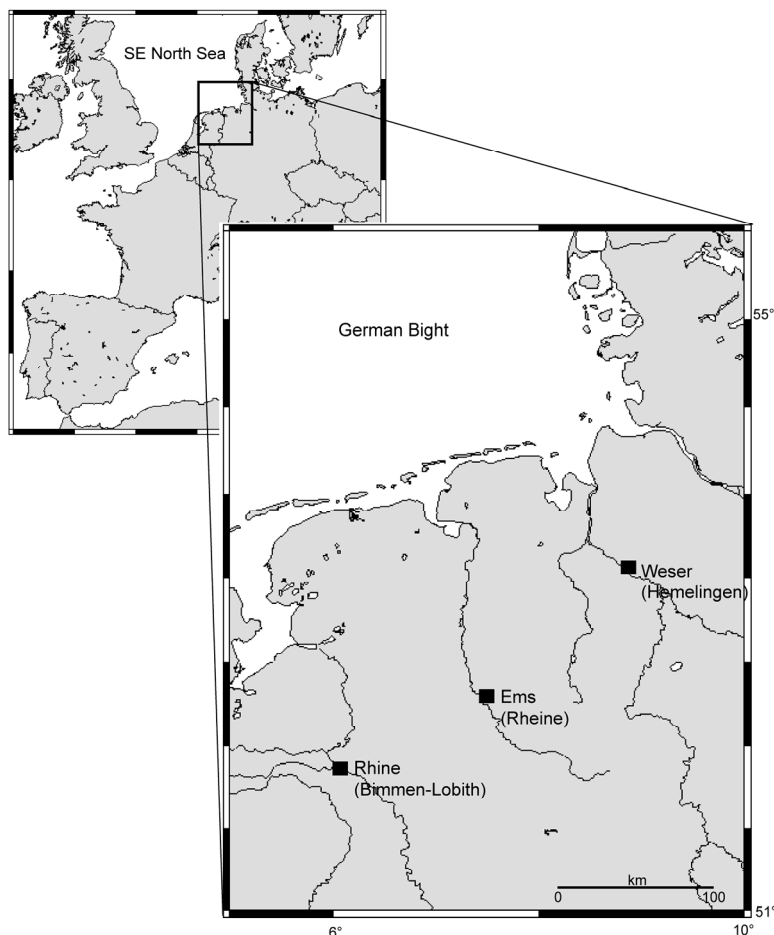


Fig. 3.1: Sampling locations at the river Rhine, Weser and Ems.

### 3.2.2 Sampling

Water was sampled by staff of official LAWA (Länderarbeitsgemeinschaft Wasser) monitoring sites located upstream of the estuaries at salinities around 0 (PSU) (Fig. 3.1). During the first sampling period (2006/2007), surface water samples were filtered through a PVDF filter (0.45  $\mu\text{m}$ ). After 2007, water samples were filtered through a pre-combusted (400°C, 6hrs) GFF filter. These were used to determine the concentration and  $\delta^{15}\text{N}$  of particulate N. Filtrate was frozen in acid rinsed PE bottles for analyses of nitrate concentrations and isotopic composition. Aliquots of selected samples were carefully defrosted in February 2010 and sent to the laboratory of the Museum für Naturkunde in Berlin for the analysis of  $\delta^{18}\text{O}\text{-H}_2\text{O}$ .

### 3.3 Laboratory analyses

#### 3.3.1 Nitrate concentrations

Nitrate concentrations were measured using a continuous flow analyzer (Bran & Luebbe, Auto Analyzer 3) according a modified method of Armstrong et al. (1967). The method has a detection limit of 6  $\mu\text{mol NO}_3^-/\text{L}$  within the expected range of 50–450  $\mu\text{mol NO}_3^-/\text{L}$  for anthropogenically influenced rivers.

#### 3.3.2 Isotopic analyses of nitrate

Isotopic analyses of nitrogen and oxygen of  $\text{NO}_3^-$  were carried out using the denitrifier method (Casciotti et al., 2002; Sigman et al., 2001) which is based on the isotopic analysis of nitrous oxide ( $\text{N}_2\text{O}$ ) produced by denitrifying *Pseudomonas aureofaciens* (ATCC#13985) strains. Isotope ratios are expressed in the delta notation ( $\delta^{15}\text{N}$  relative to atmospheric  $\text{N}_2$  and  $\delta^{18}\text{O}$  relative to Vienna Standard Mean Ocean Water, both defined as 0‰):

$$\delta \text{ sample } [\text{‰}] = (R_{\text{sample}}/R_{\text{standard}} - 1) \times 1000 \quad [3.1]$$

where R is  $^{15}\text{N}/^{14}\text{N}$  or  $^{18}\text{O}/^{16}\text{O}$  ratio of sample and standard, respectively. Analyses of  $\delta^{15}\text{N}-\text{NO}_3^-$  were corrected using the international nitrate isotope standard IAEA-N3 ( $\delta^{15}\text{N}=4.7\text{‰}$ ). Analyses of  $\delta^{18}\text{O}-\text{NO}_3^-$  were corrected for exchange, fractionation, and blank against IAEA-N3 with an assigned  $\delta^{18}\text{O}-\text{NO}_3^-$  of 22.7‰. We applied this value (which is now accepted to be 25.6‰; Böhlke et al., 2003), because we compare results with those of a previous study of river nitrate (Johannsen et al., 2008) that was based on a  $\delta^{18}\text{O}-\text{NO}_3^-$  for IAEA-N3 of 22.7‰ (Silva et al., 2000; Révész et al., 2002). Analytical precision ( $\pm 1\sigma$ ) based on replicate measurements of samples and standard was generally 0.2‰ for  $\delta^{15}\text{N}-\text{NO}_3^-$  and 0.4‰ for  $\delta^{18}\text{O}-\text{NO}_3^-$ . It should be noted that the denitrifier method measures the isotopic composition of nitrate + nitrite, but the contribution of nitrite to reactive nitrogen is negligible (<0.3%) in our sample set and has therefore been ignored.

#### 3.3.3 Oxygen isotope measurements of water

Stable isotope ratios of oxygen ( $^{18}\text{O}/^{16}\text{O}$ ) in  $\text{H}_2\text{O}$  in water samples were measured with a PICARRO L1102-i isotope analyzer. The L1102-i is based on the WS-CRDS (wavelength-scanned cavity ring down spectroscopy) technique (Gupta et al., 2009). Measurements were calibrated by the application of linear regression of the analyses of IAEA calibration material

VSMOW, SLAP and GISP. The stable isotope ratios of oxygen in H<sub>2</sub>O ( $\delta^{18}\text{O}\text{-H}_2\text{O}$ ) are reported in ‰ versus VSMOW. For each sample, 6 replicate injections were performed and arithmetic means and standard deviations ( $\pm 1\sigma$ ) were used. The reproducibility of replicate measurements is generally better than 0.1 ‰ for  $\delta^{18}\text{O}\text{-H}_2\text{O}$ .

### 3.3.4 Particulate nitrogen

The  $\delta^{15}\text{N}$  of particulate nitrogen on filters ( $\delta^{15}\text{N}\text{-PN}$ , expressed in ‰ versus air N<sub>2</sub>) was determined in duplicate on subsamples of individual GFF-filters with an EA interfaced via a Con-Flo III to an Isotope Mass Spectrometer (Finnigan Delta Plus XP), calibrated using IAEA-N-1 ( $\delta^{15}\text{N} = 0.4\text{‰}$ ) and IAEA-N-2 ( $\delta^{15}\text{N} = 20.3\text{‰}$ ). The reproducibility for  $\delta^{15}\text{N}\text{-PN}$  was 0.3‰, but the variability in  $\delta^{15}\text{N}\text{-PN}$  for sub-samples of the same filter was higher than 0.3‰ (see error bars in Fig. 3.2), and was caused by heterogeneities of the material on the filters.

### 3.3 Results

The time series of  $\text{NO}_3^-$  concentrations,  $\delta^{15}\text{N-NO}_3^-$ ,  $\delta^{18}\text{O-NO}_3^-$ ,  $\delta^{15}\text{N-PN}$ , and  $\delta^{18}\text{O-H}_2\text{O}$  of individual rivers are displayed in Fig. 3.2a–3.2c.

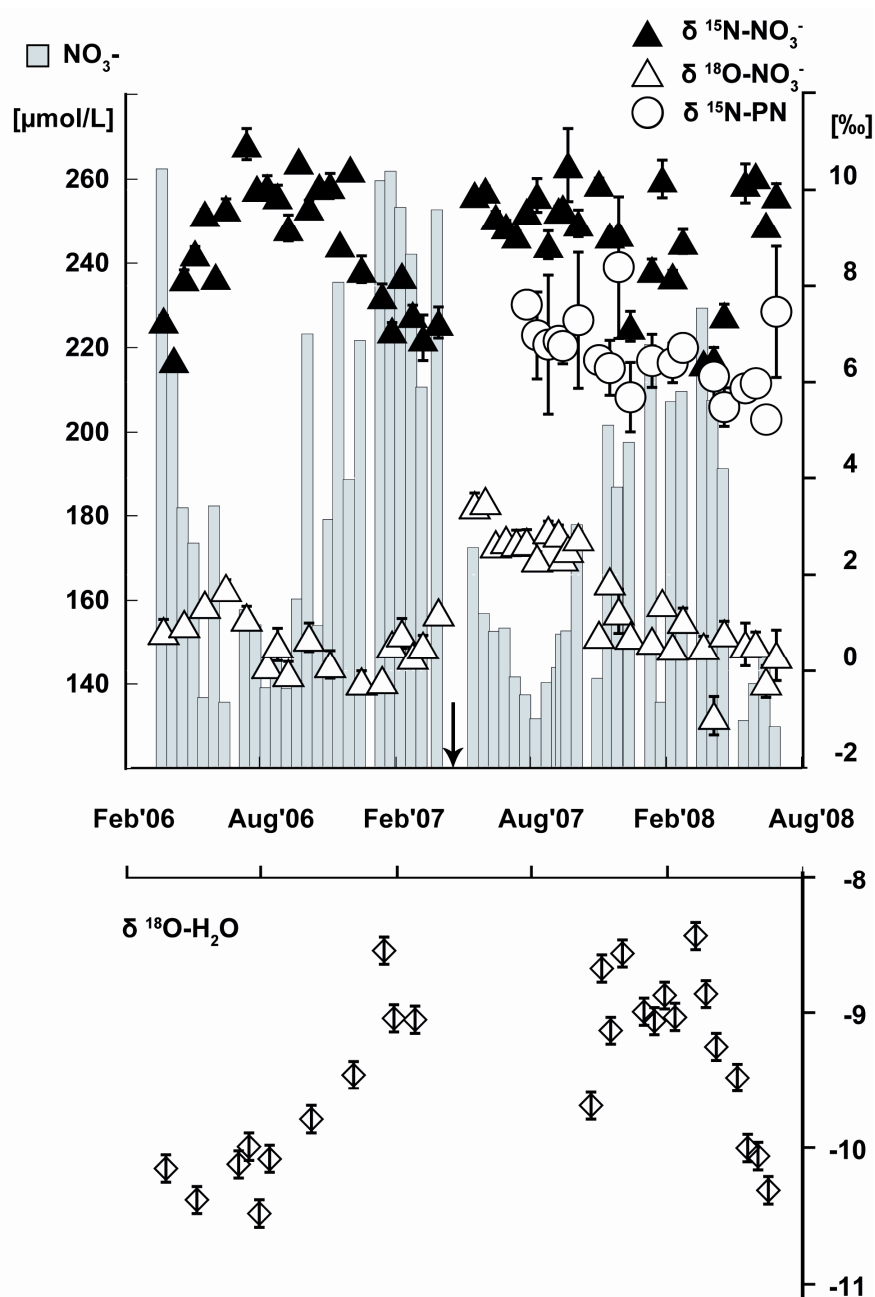


Fig. 3.2a: Seasonal cycles of  $\text{NO}_3^-$  concentrations,  $\delta^{15}\text{N-NO}_3^-$ ,  $\delta^{18}\text{O-NO}_3^-$ ,  $\delta^{15}\text{N-PN}$  and  $\delta^{18}\text{O-H}_2\text{O}$  of the Rhine River.

The arrow indicates the beginning of the 2nd sampling campaign.

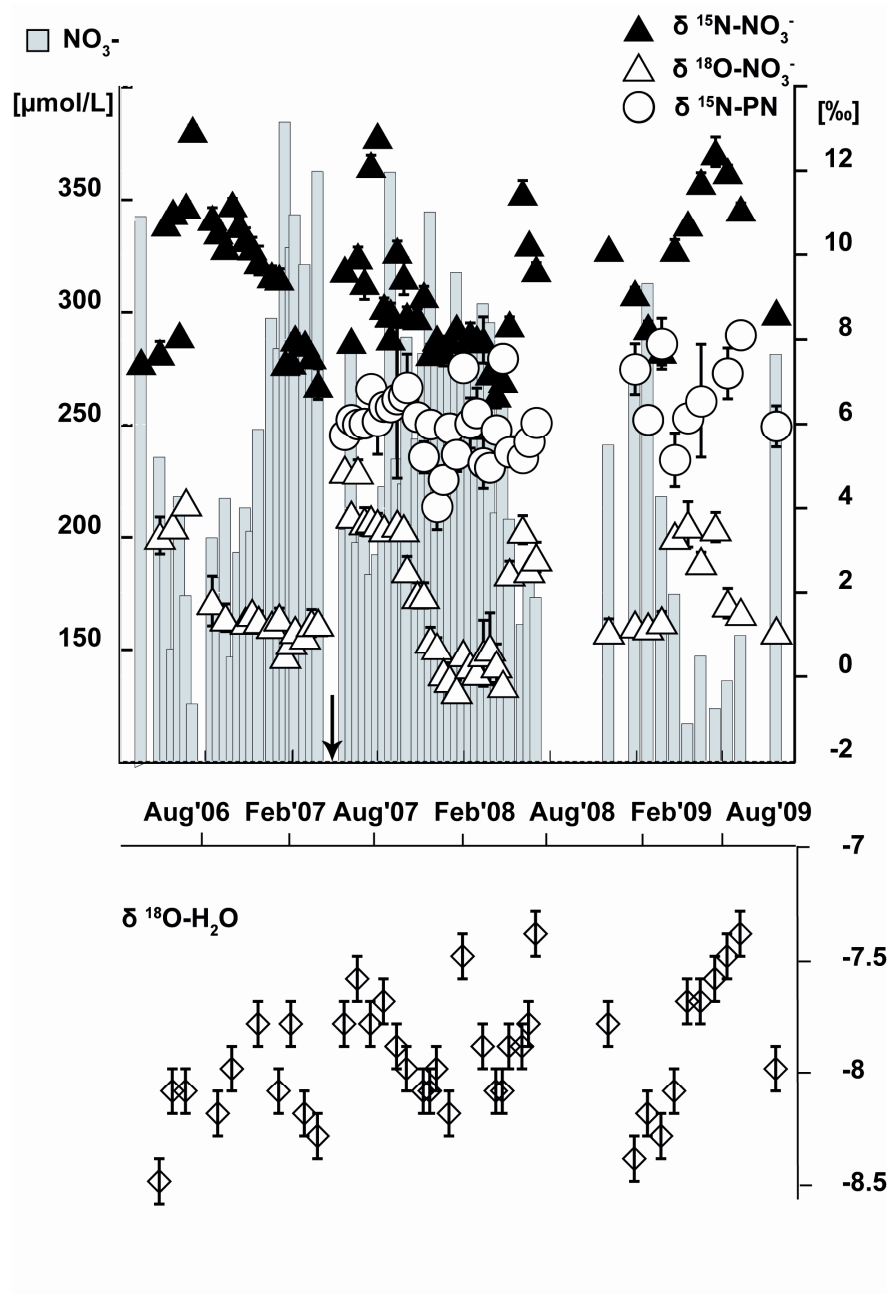


Fig. 3.2b: Seasonal cycles of  $\text{NO}_3^-$  concentrations,  $\delta^{15}\text{N-NO}_3^-$ ,  $\delta^{18}\text{O-NO}_3^-$ ,  $\delta^{15}\text{N-PN}$  and  $\delta^{18}\text{O-H}_2\text{O}$  of the river Weser.

The arrow indicates the beginning of the 2nd sampling campaign.

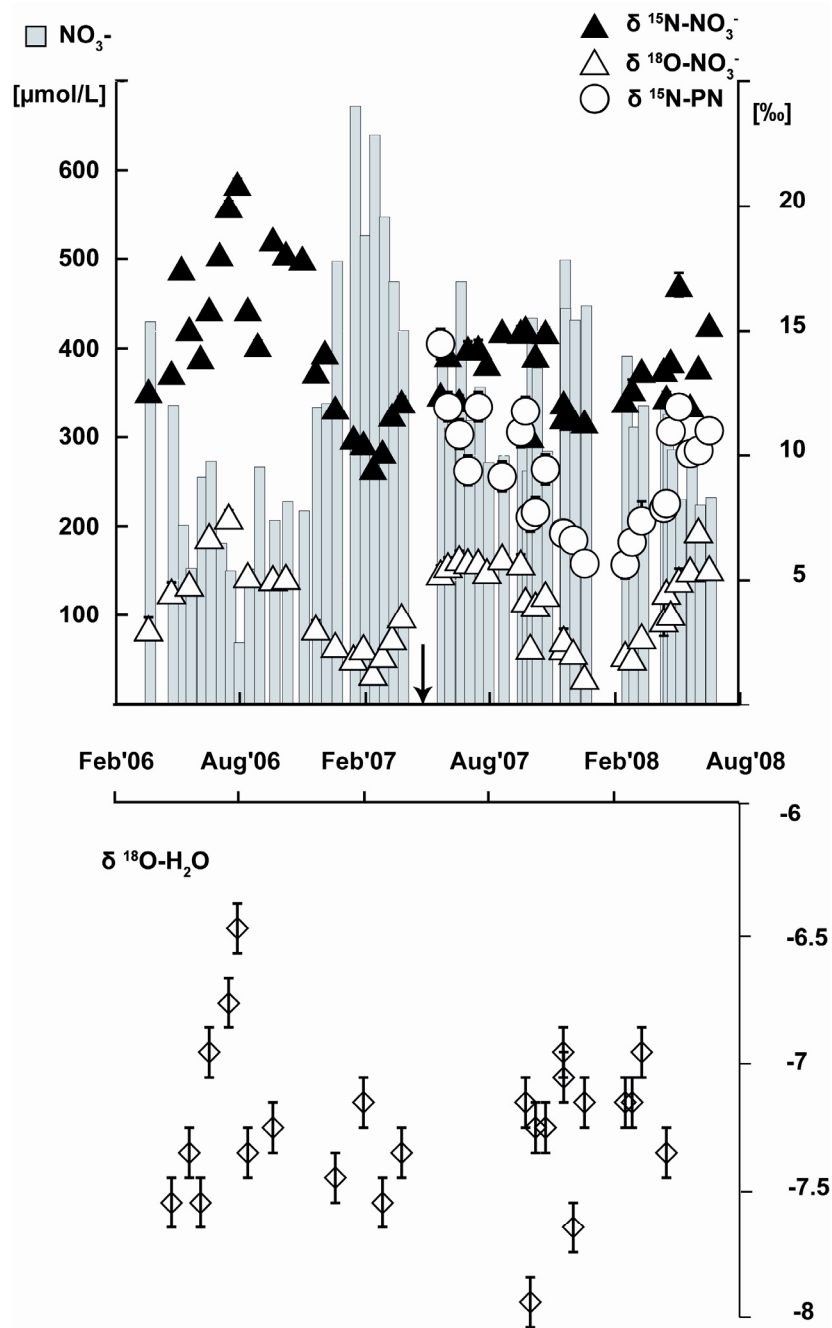


Fig. 3.2c: Seasonal cycles of  $\text{NO}_3^-$  concentrations,  $\delta^{15}\text{N-NO}_3^-$ ,  $\delta^{18}\text{O-NO}_3^-$ ,  $\delta^{15}\text{N-PN}$  and  $\delta^{18}\text{O-H}_2\text{O}$  of the river Ems.

The arrow indicates the beginning of the 2nd sampling campaign.

Highest nitrate concentrations were measured in January and February of 2007 in all three rivers (Ems > 600  $\mu\text{mol/L}$ , Weser 380  $\mu\text{mol/L}$ , Rhine 260  $\mu\text{mol/L}$ ), which all displayed a similar seasonal pattern with highest  $\text{NO}_3^-$  concentrations in the winter seasons (October – March) and lowest in the summer seasons (April – September) over the two years. Mean annual  $\text{N-NO}_3^-$  discharges and isotopic compositions are listed in Tab. 3.1. Rhine River discharged 228 kt  $\text{N-NO}_3^-$  in 2006/2007 and 195 kt  $\text{N-NO}_3^-$  in 2007/2008. Weser delivered 28 kt and 58 kt  $\text{N-NO}_3^-$  to the estuary, respectively, and Ems only 6 and 8 kt  $\text{N-NO}_3^-$  (Tab. 3.1).

Tab. 3.1:  $\text{N-NO}_3^-$  discharge and load weighted isotope values for the respective sampling periods subdivided into seasons.

River	Period	$\delta^{15}\text{N-NO}_3^-$	$\delta^{18}\text{O-NO}_3^-$	$\text{N-NO}_3^-$	$\delta^{15}\text{N-NO}_3^-$	$\delta^{18}\text{O-NO}_3^-$	$\text{N-NO}_3^-$	$\delta^{15}\text{N-NO}_3^-$	$\delta^{18}\text{O-NO}_3^-$	$\text{N-NO}_3^-$
		annual	annual	Load [kt]	summer	summer	Load [kt]	winter	winter	Load [kt]
Rhine	2006/2007	8.1	0.4	228	8.5	0.4	94	7.9	0.4	135
	2007/2008	8.6	1.5	195	8.9	1.9	81	8.2	1.0	114
Weser	2006/2007	8.4	1.2	37	9.7	1.9	10	8.0	1.0	27
	2007/2008	8.2	1.1	58	8.7	2.2	17	8.0	0.7	41
	2008/2009	9.2	1.7	28	11.0	2.9	8	8.5	1.2	20
Ems	2006/2007	11.6	2.3	6	15.3	3.3	1	11.1	2.2	5
	2007/2008	12.8	3.3	8	13.8	5.1	2	12.2	2.3	5

The hydrological annual course differed and influenced the loads: Whereas water discharge of Ems and Weser peaked in spring (between February and April), Rhine has peak discharges during summer months (Fig. 3.3).  $\text{N-NO}_3^-$  loads in all rivers co-vary with discharge (Fig. 3.3), illustrated by the significant positive correlation (>0.9 in all three rivers) of  $\text{N-NO}_3^-$  loads and discharge (Tab. 3.2).

Mean annual (years 2006 – 2009)  $\delta^{15}\text{N-NO}_3^-$  ranged from 8.1‰ to 8.6‰ in Rhine, from 8.2‰ to 9.2‰ in Weser, and from 11.6‰ to 12.8‰ in Ems with a maximum in the sampling interval 2007/2008. The  $\delta^{15}\text{N-NO}_3^-$  are generally lower in winter than in summer months, and vary inversely with  $\text{NO}_3^-$  concentrations, reflected in a negative correlation between  $\text{NO}_3^-$  concentrations and  $\delta^{15}\text{N-NO}_3^-$  (<-0.7; Tab. 3.2). Maximum  $\delta^{15}\text{N-NO}_3^-$  was 21‰ in Ems, 13‰ in Weser, and 10.9‰ in Rhine, all in July 2006, and summer maxima were consistently seen in all summers.

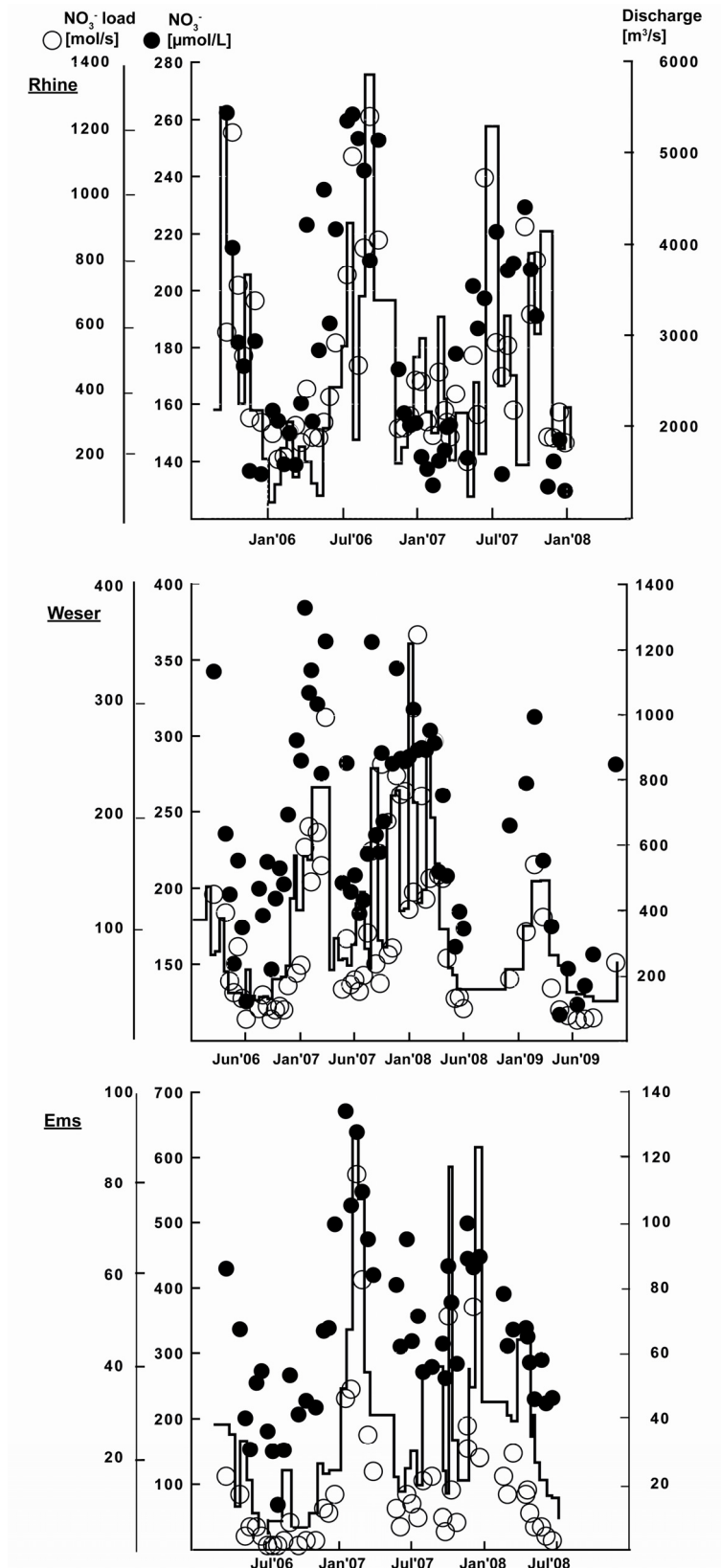


Fig. 3.3: Temporal variation in discharge in relation to nitrate concentrations and nitrate load.

The difference in isotopic composition between mean summer and winter varied among the three rivers. Mean load-weighted  $\delta^{15}\text{N-NO}_3^-$  in Rhine and Weser for summer are 0.6‰ – 1.7‰ higher than mean-load weighted winter  $\delta^{15}\text{N-NO}_3^-$ , whereas mean  $\delta^{15}\text{N-NO}_3^-$  in Ems are up to 4.2‰ higher in summer than in winter. A similar (but subdued) seasonality is seen in  $\delta^{18}\text{O-NO}_3^-$  that is usually also higher in summer than in winter. Again, Ems had highest  $\delta^{18}\text{O-NO}_3^-$  of 7.6‰ in July 2006 (Fig. 3.2a–3.2c), followed by Weser (4.9‰ in May 2007) and Rhine (2.9‰ in August 2007). The pattern of  $\delta^{18}\text{O-NO}_3^-$  in the Rhine River differs from that observed in the Weser and Ems, and both  $\delta^{18}\text{O-NO}_3^-$  and  $\delta^{15}\text{N-NO}_3^-$  had smaller seasonal amplitude through the course of the year in this river.

The highest  $\delta^{15}\text{N-PN}$  in the Ems was 14.5‰, compared to 8‰ in the Weser and Rhine (Fig. 3.2a–3.2c).  $\delta^{15}\text{N-PN}$  increased systematically towards summer in Ems, whereas a consistent seasonal pattern is not obvious in the Weser and Rhine River.  $\delta^{18}\text{O-H}_2\text{O}$  ranged between -10.3‰ and -8.5‰ in Rhine, -8.5‰ and -7.6‰ in Weser, and -8.0‰ and -6.5‰ in Ems (Fig. 3.2a–3.2c).

Tab. 3.2: Correlation matrix (Pearson's) of biogeochemical parameters of the rivers Rhine, Weser and Ems.

\*Correlation is significant ( $p < 0.05$ ); \*\* Correlation is significant ( $p < 0.01$ ).

<b>Rhine</b>	$T^{\circ}$	$c(\text{NO}_3^-)$	$\text{NO}_3^-$ - load	$\delta^{15}\text{N}-\text{NO}_3^-$	$\delta^{18}\text{O}-\text{NO}_3^-$	$\delta^{15}\text{N}-\text{PN}$	
	-0.453**	0.373**	0.935**	-0.788**	-0.166	-0.422	Discharge
		-0.754**	-0.616**	0.658**	-0.384*	0.138	$T^{\circ}$
			0.660**	-0.731**	-0.392*	-0.180	$c(\text{NO}_3^-)$
				-0.887**	-0.308*	-0.436	$\text{NO}_3^-$ - load
					0.396*	0.324	$\delta^{15}\text{N}-\text{NO}_3^-$
						0.554*	$\delta^{18}\text{O}-\text{NO}_3^-$
<b>Weser</b>	$T^{\circ}$	$c(\text{NO}_3^-)$	$\text{NO}_3^-$ - load	$\delta^{15}\text{N}-\text{NO}_3^-$	$\delta^{18}\text{O}-\text{NO}_3^-$	$\delta^{15}\text{N}-\text{PN}$	
	-0.574**	0.609**	0.970**	-0.726**	-0.378**	0.050	Discharge
		-0.773**	-0.642**	0.738**	0.732**	0.250	$T^{\circ}$
			0.754**	-0.803**	-0.387**	0.098	$c(\text{NO}_3^-)$
				-0.764**	-0.401**	0.023	$\text{NO}_3^-$ - load
					0.446**	0.103	$\delta^{15}\text{N}-\text{NO}_3^-$
						0.199	$\delta^{18}\text{O}-\text{NO}_3^-$
<b>Ems</b>	$T^{\circ}$	$c(\text{NO}_3^-)$	$\text{NO}_3^-$ - load	$\delta^{15}\text{N}-\text{NO}_3^-$	$\delta^{18}\text{O}-\text{NO}_3^-$	$\delta^{15}\text{N}-\text{PN}$	
	-0.538**	0.671**	0.959**	-0.694**	-0.660**	-0.595**	Discharge
		-0.632**	-0.537**	0.653**	0.929**	0.830**	$T^{\circ}$
			0.765**	-0.864**	-0.721**	-0.450*	$c(\text{NO}_3^-)$
				-0.699**	-0.681**	-0.589**	$\text{NO}_3^-$ - load
					0.723**	0.557**	$\delta^{15}\text{N}-\text{NO}_3^-$
						0.782**	$\delta^{18}\text{O}-\text{NO}_3^-$

### 3.4 Discussion

All three rivers under study are impacted by human activity, but the degree of agricultural land use and specializations differ in the catchment areas. The Ems drainage basin is dominated by intensive animal husbandry, because it is more competitive on the prevailing sandy soils, and the livestock production in the Ems catchment is high compared to the German average. Similarly, Weser drains grassland with intensive cattle farming and milk production (Osterkamp et al., 2001; Statistisches Bundesamt, 1990). The Rhine drains forested and urban areas with higher population density (Gömann et al., 2005; Wendland et al., 1993) than the two other rivers; land use is dominated by grassland, cattle production and intensive cash cropping. In a previous study (Johannsen et al., 2008), we found a robust positive correlation ( $R^2=0.7$ ) between the percentage of urban and agricultural land use in catchment areas and  $\delta^{15}\text{N-NO}_3^-$  values for a range of several rivers. Furthermore, we observed a significant negative correlation between  $\delta^{15}\text{N-NO}_3^-$  values and the nitrate load ( $R^2<-0.7$ ) for each seasonal cycle. This suggested that mean annual  $\delta^{15}\text{N-NO}_3^-$  over river borne nitrate should generally increase with decreasing annual nitrate loads, as a result of a relatively higher proportion of in-river nitrate consumption. We felt that longer term data sets would substantiate this assumption, and that additional information on the in-river consumption of nitrate should be gleaned from analysis of particulate N. In other studies, significant positive correlations have been observed between  $\delta^{15}\text{N-PN}$  and human population density catchment areas (e.g., Nishikawa et al., 2009), which is directly related to the percentage of residential and agricultural area. We observed the highest average  $\delta^{15}\text{N-PN}$  of 9.2‰ in the river Ems, which is most impacted in terms of agricultural and urban land use. Average  $\delta^{15}\text{N-PN}$  of 6.1‰ in Weser and 6.6‰ in Rhine River are also relatively high and in the same range reported for  $\delta^{15}\text{N-PN}$  in non-pristine rivers (Middelburg and Nieuwenhuize, 1998; Sigleo and Macko, 2002; Voss et al., 2006).  $\delta^{15}\text{N-PN}$  thus appears to be a good indicator for the degree of human impact on watersheds, and together with mean winter  $\delta^{15}\text{N-NO}_3^-$  characterise dominant anthropogenic sources of reactive nitrogen in rivers.

#### 3.4.1 Nitrate sources

##### 3.4.1.1 Nitrate from organic and synthetic fertilizers

The high mean annual  $\delta^{15}\text{N-NO}_3^-$  (between 8.1‰ and 12.8‰) in Ems, Rhine and Weser mark them as anthropogenically influenced rivers (Mayer et al., 2002; Johannsen et al., 2008; Deutsch et al., 2006; Voss et al., 2006). In contrast,  $\delta^{18}\text{O-NO}_3^-$  in the range between 0.4‰ and 3.3‰ are low compared to potential direct sources, but compare well with  $\delta^{18}\text{O-}$

$\text{NO}_3^-$  determined in non-pristine rivers in northern Europe (Dähnke et al., 2008; Deutsch et al., 2006; Bristow, 2009).

As stated above, agriculture prevails in all three watersheds, and agricultural soils are known to host large amounts of reactive nitrogen. Nitrate in rivers draining these soils may originate from different sources and processes, such as direct elution of atmospheric deposition, inorganic fertiliser and manure, or recycled nitrate from mineralization of soil organic nitrogen or nitrification of ammonia. All these sources are known to contribute to nitrate stocks in surface and groundwater, and each has more or less specific isotopic compositions (Kendall, 1998). Synthetically produced nitrate in fertilizer has a  $\delta^{18}\text{O}-\text{NO}_3^-$  between 18‰ and 22‰, which is close to the atmospheric  $\delta^{18}\text{O}$  value (Kroopnick and Craig, 1972; Amberger and Schmidt, 1987; Wassenaar, 1995). Typical mineral fertiliser applied in Germany is between 19.4‰ and 25.7‰ (Deutsch et al., 2005). Ranges of  $\delta^{15}\text{N}-\text{NO}_3^-$  are typically between -5‰ and 8‰ (Kendall, 1998; Macko and Ostrom, 1994);  $\delta^{15}\text{N}-\text{NO}_3^-$  between 0.8‰ and 4.4‰ were measured for mineral fertiliser in Germany (Deutsch et al., 2005). The  $\delta^{15}\text{N}$  value of fertilized soils is usually higher (between 0‰ and 14‰; Fogg et al., 1998; Kendall, 1998) than that of fertilizers applied (Kendall, 1998; Macko and Ostrom, 1994), because  $^{15}\text{N}$  is enriched by an array of fractionation processes acting on the original isotopic mixture during N-assimilation, harvesting of crops, and denitrification in soils. The relatively low  $\delta^{18}\text{O}-\text{NO}_3^-$  in Rhine, Weser and Ems compared to synthetic fertilizers (between 18‰ and 22‰) suggest that direct leaching of mineral fertilizer from soils into rivers is only of minor relevance. This reflects increasing popularity of good (and cheaper) farming practise of targeted synthetic fertilisation immediately near the individual crop plants.

But it is known that agricultural soils in Germany are over-saturated with reactive N from decades of poor fertilising practise (UBA, 2009), and the legacy of excessive fertilisation has undergone massive fractionation when finally reaching stream waters, resulting in high  $\delta^{15}\text{N}$  of this contribution. In contrast to synthetic fertilizers, organic fertilizers are by-products of animal breeding and discharged directly by free range husbandry or are generously applied as organic fertilizer to field crops to remove waste (Renger, 2002). Nitrate originating from this practise (after nitrification of ammonia) has high  $\delta^{15}\text{N}$  values between 8‰ to 25‰ (Kendall, 1998; Macko and Ostrom, 1994) caused by fractionation during ammonium volatilization, which enriches the residual ammonium pool in  $^{15}\text{N}$  (Frank et al., 2004). According to Blume (2004), up to 80% of the ammonium in organic fertilizers is volatilized during the first days after application, if not worked into the soil properly. Similar to the residual of mineral fertilizer, subsequent nitrification of the residual ammonia produces  $\text{NO}_3^-$  enriched in  $^{15}\text{N}$ . Together with other processes, such as partial denitrification, selective

assimilation by and harvesting of crops, this leads to a progressive enrichment of  $\delta^{15}\text{N-NO}_3^-$  and  $\delta^{18}\text{O-NO}_3^-$  that is then collected by rivers draining intensively farmed watersheds (Ahad et al., 2006; Ostrom et al., 1997; Horrigan et al., 1990).

### 3.4.1.2 Nitrate from nitrification

A key process in nitrate generation in soils and a significant source of riverine nitrate pools is nitrification of reduced N species (Hales, 2007). Nitrification is the bacterial oxidation of ammonia to nitrate via nitrite, mediated in two steps by aerobic chemolithoautotrophic bacteria and archaea. The first step, oxidation of ammonia into nitrite, is performed by two groups of organisms, ammonia-oxidizing bacteria (AOB) and ammonia-oxidizing archaea (AOA) dominating both marine and terrestrial environments (Francis et al., 2007). The second step, oxidation of nitrite into nitrate, is known to be performed by four genera of bacteria: Nitrococcus, Nitrospina, Nitrospira and Nitrobacter (Casciotti, 2009). Nitrobacter was generally considered the dominant or even the sole nitrifier in soils, but evidence has been lately given that Nitrospira is as well a common soil bacterium (Bartosch et al., 2002, Attard et al., 2010). Nitrate deriving from nitrification has a  $\delta^{15}\text{N}$  that is a legacy of the ammonia substrate (with reported fractionation factors  $\epsilon_{\text{AMO}}$  for the ammonium oxidation process that range from 14 to 38‰; Casciotti, 2009 and the references therein). The  $\delta^{18}\text{O}$  of this nitrate is apparently determined by the combined isotope ratios of ambient water and atmospheric (soil) molecular oxygen. Studies in fresh water environments suggest that two of the oxygen atoms originate from ambient water and another one from dissolved oxygen (Hollocher, 1984; Anderson and Hooper, 1983; Kumar et al., 1983), resulting in a  $\delta^{18}\text{O-NO}_3^-$  equal to:

$$\delta^{18}\text{O-NO}_3^- = 2/3 \delta^{18}\text{O-H}_2\text{O} + 1/3 \delta^{18}\text{O-O}_2 \quad [3.2].$$

Atmospheric oxygen has a known  $\delta^{18}\text{O}$  value of 23.5‰ (Kroopnick and Craig, 1972).  $\delta^{18}\text{O-H}_2\text{O}$  ranged between -10.3‰ and -8.5‰ in Rhine, -8.5‰ and -7.6‰ in Weser and -8.0‰ and -6.5‰ in Ems (Fig. 3.2a–3.2c). Assuming that the  $\delta^{18}\text{O-H}_2\text{O}$  of river water is close to the value of ambient soil water used for nitrification, and that  $\delta^{18}\text{O}$  of soil  $\text{O}_2$  is approximately equivalent to atmospheric  $\text{O}_2$  yields expected  $\delta^{18}\text{O-NO}_3^-$  of 1.6‰, 2.6‰ and 3‰ for nitrate derived from nitrification in Rhine, Weser and Ems, respectively. We note that these are all close to the mean annual  $\delta^{18}\text{O-NO}_3^-$  values measured in the rivers (Tab. 3.1). River nitrate in our data set has a slightly lower but similar  $\delta^{18}\text{O-NO}_3^-$  compared with nitrate in tile drain water sampled in winter months from two fields in northern Germany (2.9–5.1‰) reported in Deutsch et al. (2005) and obtained with a different method. The correspondence of

theoretical and found  $\delta^{18}\text{O}-\text{NO}_3^-$  in our data set is somewhat surprising, because Eq. (3.2) makes the assumptions that no isotopic fractionation operates during incorporation of water oxygen or dissolved  $\text{O}_2$  into nitrate formed, that the original atmospheric isotopic composition of  $\text{O}_2$  used for nitrification is maintained in soils, and that no significant oxygen exchange occurs between  $\text{H}_2\text{O}$  and intermediate compounds involved in  $\text{NO}_3^-$  formation (Spoelstra et al., 2007; Pardo et al., 2004; Aravena et al., 1993; Kendall et al., 1995; Kendall, 1998; Wassenaar, 1995; Mayer et al., 2001; Kool et al., 2007). Furthermore, recent studies (Wankel et al., 2006; Sigman et al., 2005; Sigman et al. 2009, Buchwald and Casciotti, 2010) in marine environments and culture studies have raised uncertainties about the exact source of  $\delta^{18}\text{O}$  in nitrate produced by nitrification and have questioned the premises assumed in Eq. (3.2). Casciotti et al. (2002) found that the  $\delta^{18}\text{O}$  of recycled nitrate in marine environments is apparently closer to the  $\delta^{18}\text{O}-\text{H}_2\text{O}$  of ambient water and proposed that  $\delta^{18}\text{O}-\text{NO}_3^-$  is set by:

$$\delta^{18}\text{O}-\text{NO}_3^- = 5/6 \delta^{18}\text{O}-\text{H}_2\text{O} + 1/6 \delta^{18}\text{O}-\text{O}_2 \quad [3.3].$$

We note that our data fit the relationships in equation (3.2) for soil nitrification (Hollocher, 1984; Anderson and Hooper, 1983; Kumar et al., 1983), but that average  $\delta^{18}\text{O}-\text{NO}_3^-$  in each river is slightly below the theoretical value. The range of  $\delta^{18}\text{O}-\text{NO}_3^-$  found suggests that chemolithoautotrophic nitrification is the dominant source, a process that is used to gain energy and assimilates  $\text{CO}_2$ . Mayer et al. (2001) and Spoelstra et al. (2007) suggested that the contribution to  $\delta^{18}\text{O}-\text{NO}_3^-$  soil water and dissolved oxygen depends on ammonia concentration and the type of nitrifying organisms present in soils. Heterotrophic nitrifiers (no energy yield) apparently appear in soils with low ammonium concentrations and perform at characteristically low nitrification rates, possibly in a series of oxidation steps of organic-bound amino-groups. In this reaction sequence, two oxygen atoms may originate from the organic nitrogen compound, and only one from water (Mayer et al., 2001). The nitrate thus produced appears to be relatively higher in  $\delta^{18}\text{O}-\text{NO}_3^-$  than that produced from the second pathway, nitrification by chemolithoautotrophic consortia (Spoelstra et al., 2007) dominating environments with relatively high nitrification rates (Focht and Verstraete, 1977). As mentioned before, AOB and AOA are the prevailing chemolithoautotrophic ammonia oxidizers. Nitrification by AOA is operative over a wide range of environmental conditions (pH, temperature) in soils, where archaeotal cells far outweigh bacterial cells (Leininger et al., 2006), being potentially important actors within the nitrogen cycle in several ecosystems (Erguder et al., 2009). For the archaea, the isotopic systematics of nitrification is unknown, because they are as yet not cultivated for this experimental purpose. Considering the bacterial ammonia oxidizers, at least the genera *Nitrobacter* is assumed to produce nitrate with a  $\delta^{18}\text{O}-\text{NO}_3^-$  according to Eq. (3.2) (Mayer et al., 2001; Spoelstra et al., 2007).

Under favourable conditions (e.g., availability of ammonia), nitrification in the water column of the river is likely to be an additional source of stream nitrate. During winter months, when ammonium, nitrate and nitrite concentrations were measurable, Herfort et al. (2009) detected genes of *Crenarchaeota* Group 1.1a, the major ammonia oxidizer in marine environments, in Rhine samples and reported that they accounted for 0.3% of the total microbial community in surface waters. Crenarchaeotal nitrification potential in the Rhine River in summer was lower, attributed to higher competition from bacteria and phytoplankton. To our knowledge, nothing is known about the oxygen isotopic composition of nitrate deriving exclusively from archeal nitrification, but it is safe to assume that it constitutes an internal nitrate source for the studied rivers during winter, albeit of unknown magnitude and isotopic fingerprint. In any event, based on the ammonia availability in agricultural soils and in river water, the contribution to nitrate in rivers from internal nitrification should be smaller than the contribution from soil nitrification, although Dähnke et al. (2008) reported significant (>50%) additions to estuarine nitrate pools of the Elbe river from nitrification in the estuarine turbidity maximum .

#### 3.4.1.3 Atmospheric deposition

The isotopic signature of nitrate deriving from atmospheric deposition is distinct from any other nitrate source. The range of  $\delta^{18}\text{O-NO}_3^-$  in precipitation in Europe is between 55‰ and 75‰ (Durka et al., 1994), whereas the  $\delta^{15}\text{N-NO}_3^-$  of precipitation varies widely due to various sources of oxidized nitrogen and numerous fractionation processes preceding deposition (Heaton, 1986; Freyer, 1991). The  $\delta^{18}\text{O-NO}_3^-$  in river nitrate here are much lower than in atmospheric  $\text{NO}_3^-$ , so that precipitation cannot be a significant contribution to the nitrate pools of rivers Rhine, Weser and Ems. This agrees with a study by Burns and Kendall (2002), who investigated different nitrate sources in two American watersheds.

#### 3.4.2 Influence of river discharge

Besides their discharge (Rhine has a seven times higher discharge yield than the Weser and a seventy higher discharge than the Ems; 2500 m<sup>3</sup>/s, 370 m<sup>3</sup>/s and 36 m<sup>3</sup>/s respectively), the rivers differ in their respective discharge regimes. Whereas the discharge regimes of the rivers Weser and Ems is pluvial, the discharge regime of the Rhine River is glacial-nival upstream (the Alpine Rhine) and pluvial in the lower Rhine region. The Alpine Rhine discharge is controlled by the alpine snow- and glacier melt, which depends on temperature, having a minimum in winter and a maximum in summer. The influence of the pluvial regime increases downstream and the discharge becomes compensated by winter precipitation, but

high discharges are maintained during summer (Hirschfeld, 2003; Kempe and Krahe, 2005). This mix of water sources buffers the Rhine hydrograph with regard to discharge minima, so that discharge varies by a factor of three whereas the discharge in Weser and Ems is six times higher during winter than during summer months (Fig. 3.3). The variability in  $\delta^{18}\text{O}\text{-H}_2\text{O}$  in Rhine water is a consequence of these different hydrological regimes. As the  $\delta^{18}\text{O}\text{-H}_2\text{O}$  of precipitation in central Europe decreases southwards (Buhl et al. 1991), the  $\delta^{18}\text{O}\text{-H}_2\text{O}$  of surface waters in the Rhine catchment is spatially and temporally quite variable. Variations in  $\delta^{18}\text{O}\text{-H}_2\text{O}$  values reflect the alpine influence in isotopically lighter  $\delta^{18}\text{O}\text{-H}_2\text{O}$  compared to the precipitation in the lower Rhine area. According to Buhl et al. (1991) and Hirschfeld (2003), discharge of the Alpine Rhine has a  $\delta^{18}\text{O}\text{-H}_2\text{O}$  between -12‰ and -13.5‰, whereas  $\delta^{18}\text{O}\text{-H}_2\text{O}$  of lowland precipitation is around -8‰ (Yurtsever, 1975; Bowen and Revenaugh, 2005). We measured lowest  $\delta^{18}\text{O}\text{-H}_2\text{O}$  (<-10‰) in Rhine at Bimmen-Lobith between April and August when snow melt takes place (Fig. 3.2a). During winter season (October – March),  $\delta^{18}\text{O}\text{-H}_2\text{O}$  values are higher (>-9‰) due to higher influence of the pluvial regime. Rivers Weser and Ems are solely rain-fed (de Jonge, 1995), and such seasonal variations in  $\delta^{18}\text{O}\text{-H}_2\text{O}$  were not observed (Fig. 3.2b–3.2c).

Nitrate concentrations in rivers depend substantially on the time course of precipitation and its influence on discharge amounts. In seasons of high precipitation and during flood events in winter, when biological activity is low, high amounts of rN are leached and transported into rivers (Hamm, 1996). This is reflected in significant positive correlations ( $R^2 > 0.9$ ) between  $\text{NO}_3^-$  loads and water discharge in all 3 rivers (Tab. 3.2). It also underscores that diffuse sources dominate the nitrate pools: If more or less constant point sources (waste water inlets, tributaries) were the dominant source, the  $\text{NO}_3^-$  loads would decrease at times of higher discharges due to dilution (Hamm, 1996). Assuming an ideal dilution, the nitrate concentration of a point source would behave according to:

$$c [\text{NO}_3^-] = c_0 + A/Q \quad [3.4],$$

where  $c_0$  is the constant background concentration of  $\text{NO}_3^-$ ,  $A$  is the load of a point source and  $Q$  the discharge (Hebbel and Steuer, 2006). In Fig. 3.4 we display a theoretical dilution curve against mean nitrate loads of the river Rhine, Weser and Ems. The actual nitrate discharge clearly differs from the theoretical dilution curve and indicates massive diffuse nitrate inputs instead. Moreover, nitrate concentrations increase with increasing discharge: Low nitrate concentrations in summer months (Fig. 3.2a–3.2c) increase towards winter accompanied by higher discharges fed by precipitation events by that season. The correlation between  $\text{NO}_3^-$  concentrations and riverine discharge is best in the river Ems,

where precipitation in the catchment is immediately funnelled into the river through permeable sandy soils. The high infiltration rates of the sandy soils favour nitrogen leaching to the groundwater and their discharge into the river (Liersch and Volk, 2009).

But the nitrate concentrations and isotopic mixtures are not solely determined by diffuse groundwater seepage. Seasonally varying biological productivity and nitrate assimilation in the rivers is clearly a major process. Because assimilation is low in winter (as indicated by the indirect, but significant, negative correlation between  $\text{NO}_3^-$  concentration and water temperature; Tab. 3.2), the more intense soil source and low consumption rates result in higher nitrate loads in winter.

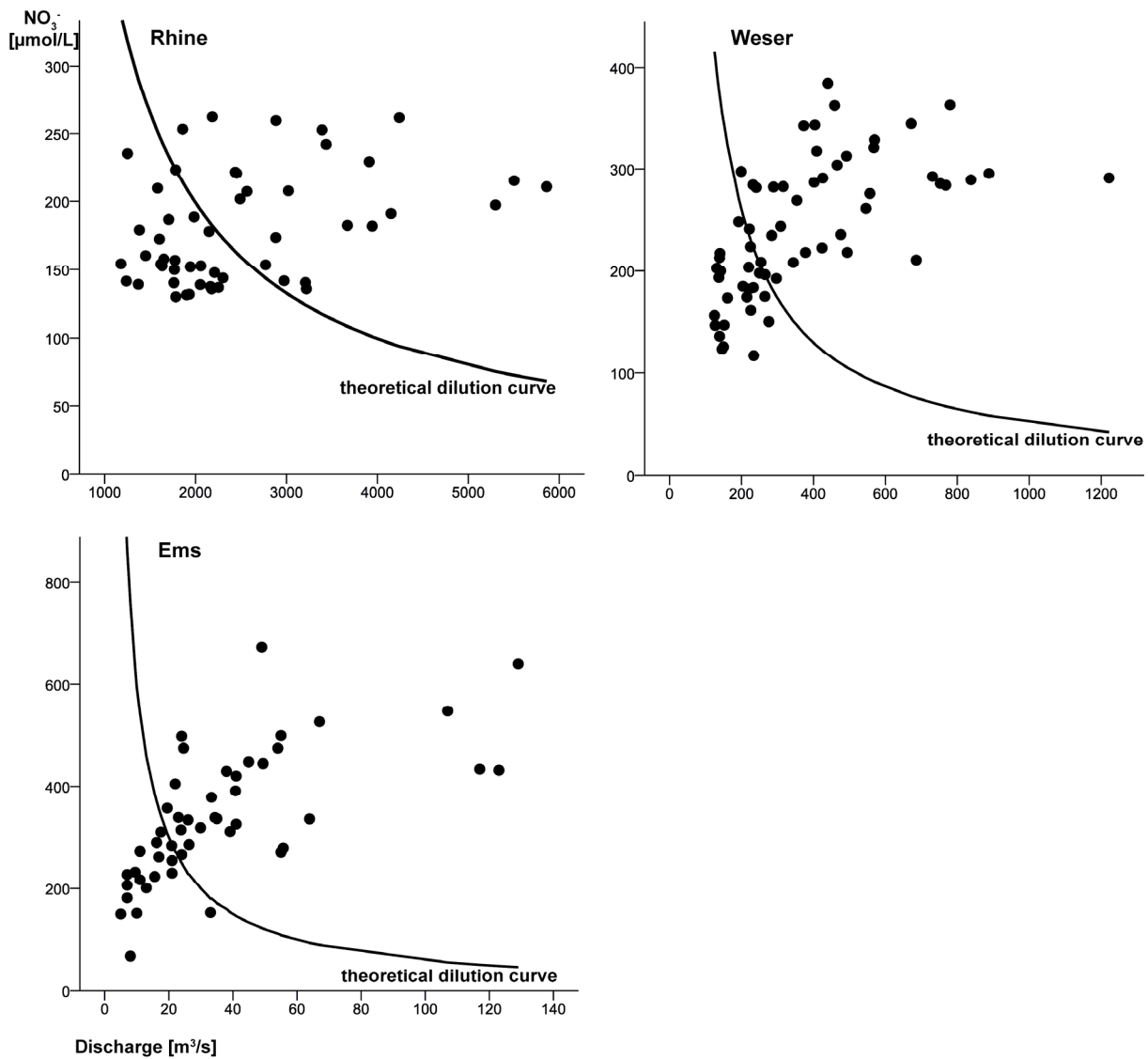


Fig. 3.4: Nitrate discharge relationship in comparison with the theoretical dilution curve.

### 3.4.3 Biological processes in the rivers

Anthropogenic sources of rN external to the rivers determine the base level isotopic composition of  $\text{NO}_3^-$  in winter, but biological activity alters the initial  $\delta^{15}\text{N}-\text{NO}_3^-$  and  $\delta^{18}\text{O}-\text{NO}_3^-$  in the course of the year. Two processes that remove nitrate are associated with preferential removal of  $\delta^{14}\text{N}-\text{NO}_3^-$ : denitrification and assimilation of nitrate (Mariotti et al., 1981; Kendall, 1998). Denitrification, a microbial process which is obligate anaerobic supposedly begins below oxygen levels of around 2 mg/L (Painter, 1970) and is unlikely to occur to any significant extent in the well oxygenated water columns of Rhine, Weser or Ems. Denitrification in sediments, according to present knowledge, causes only small fractionation because the rate limiting step is the non-discriminating process of nitrate diffusion (Sebilo et al., 2003; Reinhardt et al., 2006; Lehmann et al., 2007). Although sedimentary denitrification is likely to occur in the river beds and in riparian mud flats, where organic matter substrate is available in high amounts, this nitrate sink would go unnoticed in the isotopic mixture of river nitrate. Assimilation of nitrate, on the other hand, is likely to occur when temperature and light conditions are favourable. During assimilation, microorganisms preferentially incorporate  $\delta^{14}\text{N}-\text{NO}_3^-$ . As for N isotopes,  $\delta^{16}\text{O}-\text{NO}_3^-$  is favoured relative to  $\delta^{18}\text{O}-\text{NO}_3^-$  causing an enrichment of the heavy isotopes  $\delta^{15}\text{N}$  and  $\delta^{18}\text{O}$  in the residual  $\text{NO}_3^-$  pool. Seasonal variation in both  $\delta^{15}\text{N}$  and  $\delta^{18}\text{O}$  combined with decreasing  $\text{NO}_3^-$  concentrations in Rhine, Weser and Ems have similar trends with maxima in summer and minima in winter for all sampling periods (Fig. 3.2a–3.2c), suggesting that  $\text{NO}_3^-$  is consumed during summer months when biological activity increases. Isotope effects  $^{15}\epsilon$  and  $^{18}\epsilon$  during nitrate assimilation are similar, because the slope of  $\delta^{18}\text{O}$  to  $\delta^{15}\text{N}$  in residual nitrate has been observed to follow a 1:1 line in culture studies (Granger et al., 2004). A plot of  $\delta^{18}\text{O}-\text{NO}_3^-$  against  $\delta^{15}\text{N}-\text{NO}_3^-$  (Fig. 3.5) for individual rivers in our study yielded slopes of 0.37, 0.53 and 0.54 for the rivers Rhine, Weser and Ems respectively. The deviation means that the increases in  $\delta^{18}\text{O}$  and  $\delta^{15}\text{N}$  in nitrate are not solely due to assimilation, and that other processes and nitrate sources interfere with a single phytoplankton sink for nitrate. This is not surprising, because the enrichment slope of 1:1 during assimilation is typically observed in closed systems, where nitrate is consumed without external replenishment. The dominant external input from soil water nitrate seepage obviously represents an open system, where drainage- and ground water supply continuously and diffusely adds nitrate with a more or less invariant isotopic composition over the entire year. In this case, a less steep slope due to incidentally added nitrate is to be expected. Plotting  $\delta^{18}\text{O}-\text{NO}_3^-$  versus  $\delta^{15}\text{N}-\text{NO}_3^-$  and evaluation of differences in slopes during winter and summer helps to identify a fractionation effect (Fig. 3.5).

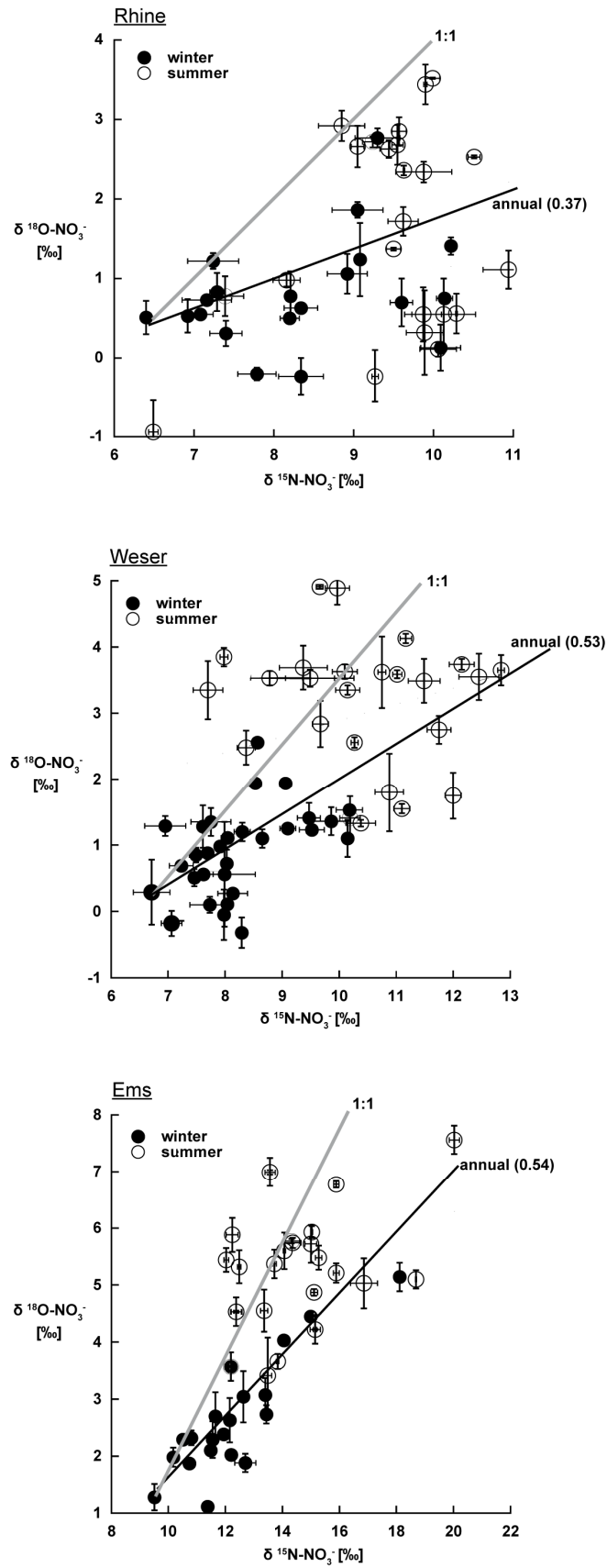


Fig. 3.5: Variation in  $\delta^{18}\text{O-NO}_3^-$  in relation to  $\delta^{15}\text{N-NO}_3^-$  for the Rhine, Weser and Ems.

Winter  $\delta^{18}\text{O}-\text{NO}_3^-$  and  $\delta^{15}\text{N}-\text{NO}_3^-$  increase with increasing temperature towards summer in all three rivers (seen also in significant positive correlations in Tab. 3.2), but differences emerge for Rhine compared to the patterns observed in the Weser and Ems. The complete lack of correlation between  $\delta^{18}\text{O}-\text{NO}_3^-$  and  $\delta^{15}\text{N}-\text{NO}_3^-$  in the Rhine and no systematic differences between winter and summer suggest that assimilation is not causing strong fractionation. Rhine River has by far highest discharges of the three rivers (Fig. 3.3) and we assume that the prevailing high current velocity and low water residence time impede phytoplankton growth (Peterson et al., 2001; Wollheim et al., 2001). Conversely, a decrease in current velocity enhances the removal rate of nitrate from the water column via assimilation and results in  $\delta^{15}\text{N}$  enrichment in the residual nitrate (Trudeau and Rasmussen, 2003). Because of their high surface to volume ratios, smaller streams are more efficient in processing nutrients relative to transport (Alexander et al., 2000). In Ems, the range of  $\text{NO}_3^-$  concentrations and its isotopic composition is wider than in the rivers Weser and Rhine. Its initial  $\text{NO}_3^-$  concentration, assumed to be the maximum concentration measured in winter and normalized to 1, declines to 0.1 in the river Ems, whereas the initial  $\text{NO}_3^-$  concentration declines only to 0.5 in Rhine. Comparing the three rivers, we find a strong relationship between 1) stream size, 2) consumption efficiency and 3) fluctuation of  $\delta^{15}\text{N}$  and  $\delta^{18}\text{O}$ : With higher discharge amounts, the consumption efficiency is lower and summer increase in  $\delta^{15}\text{N}$  and  $\delta^{18}\text{O}$  of nitrate smaller.

Consumption of nitrate produces particulate nitrogen that is locked to the  $\delta^{15}\text{N}$  of nitrate by the fractionation factor  $\epsilon$  associated with assimilation. In previous studies, the isotopic fractionation factor ( $\epsilon$ ) associated with nitrate assimilation was in the range of 4 to 9‰ for field observations (Altabet et al., 1991; Horrigan et al., 1990; Sigman et al., 1999; Wu et al., 1997) and is often assumed as 5‰. Under nitrate-replete conditions, the  $\delta^{15}\text{N}$ -PN produced at any time during assimilation should be  $\delta^{15}\text{N}-\text{NO}_3^- - 5\%$  (Mariotti et al., 1981). In theory, we should thus expect a negative correlation of  $\delta^{15}\text{N}$ -PN with  $\text{NO}_3^-$  concentrations, and is observed in the river Ems ( $R^2=-0.45$ ;  $p < 0.05$ ), but is neither observed in the Rhine River ( $R^2=-0.18$ ), nor in the Weser ( $R^2=0.098$ ). The increase of  $\delta^{15}\text{N}$ -PN in the river Ems in April corresponds to the onset of primary productivity and to the decrease of nitrate concentration in river water. Higher rates of N recycling, microbial decomposition of PN and utilization of DIN favour the enrichment of  $\delta^{15}\text{N}$ -PN and higher variability of  $\delta^{15}\text{N}$ -PN in the smaller river Ems. The associated apparent N-isotope effect can be estimated from the difference between the source,  $\delta^{15}\text{N}-\text{NO}_3^-$  and the product,  $\delta^{15}\text{N}$ -PN ( $\Delta\delta^{15}\text{N}$ ). Using the annual  $\delta^{15}\text{N}-\text{NO}_3^-$  and  $\delta^{15}\text{N}$ -PN values for the three rivers, we estimate an apparent fractionation factor of around 2‰ for the Rhine River, between 2‰ and 3‰ for the Weser and around 3‰ for the Ems. Why only a subdued seasonal amplitude of  $\delta^{15}\text{N}$ -PN has been observed in Rhine River and Weser remains speculation. A possible explanation might be a varying species

composition among the rivers and between seasons. Several culture studies (e.g. Montoya and McCarthy, 1995) have shown that fractionation factors are different depending on organisms, e.g. nitrate assimilation by diatoms were associated with higher fractionation than nitrate assimilation by green algae. On the other hand, the Rhine and Weser apparent isotope effects may be lower than expected because external PN-loading masks the effects of autochthonous assimilation.

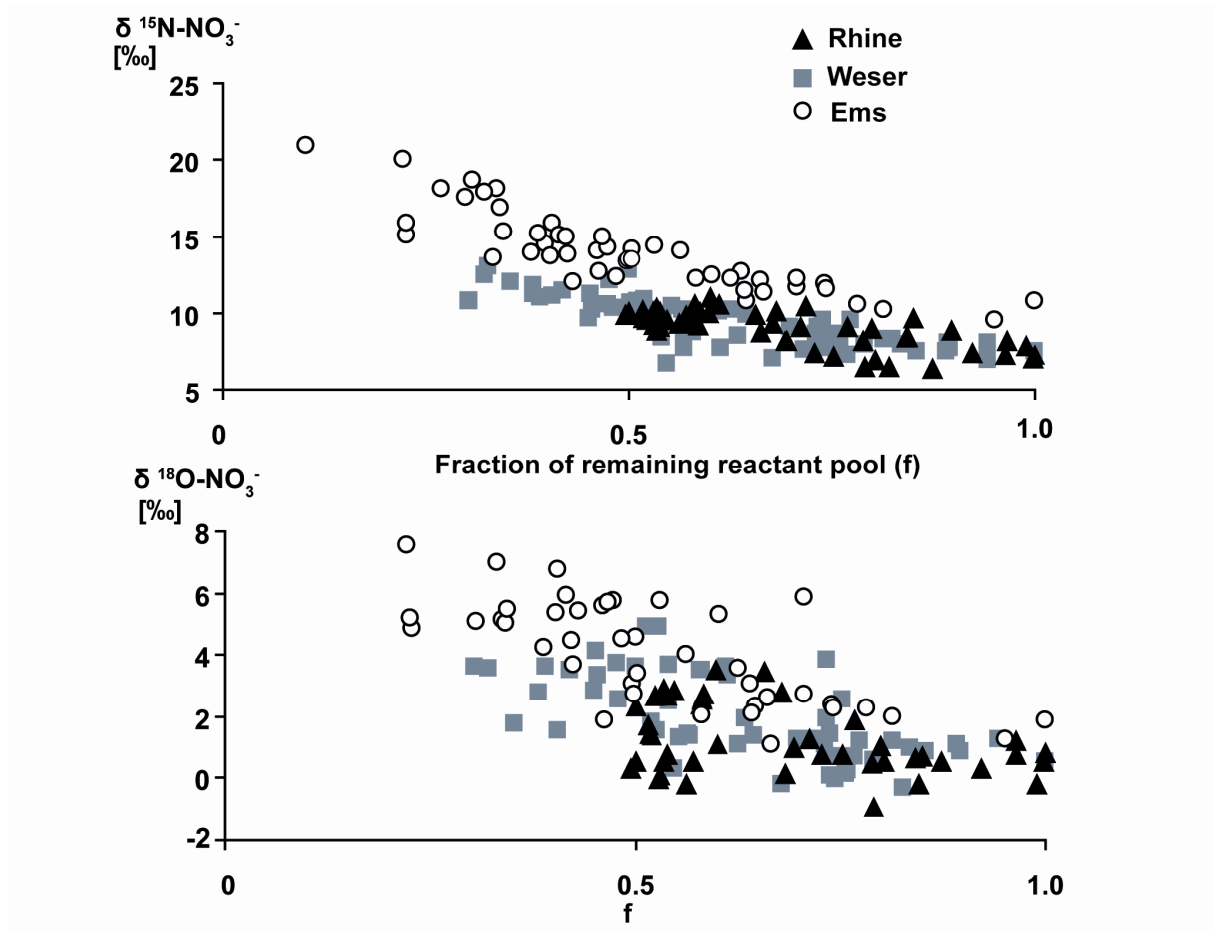


Fig. 3.6: Change in  $\delta^{15}\text{N-NO}_3^-$  and  $\delta^{18}\text{O-NO}_3^-$  relative to the fraction of the remaining reactant ( $\text{NO}_3^-$ ) pool.

### 3.5 Conclusions

The results presented in this paper demonstrate that the determination of  $\delta^{15}\text{N-NO}_3^-$  and  $\delta^{18}\text{O-NO}_3^-$  values in combination with  $\delta^{18}\text{O-H}_2\text{O}$  and  $\delta^{15}\text{N-PN}$  helps to understand the nitrogen cycle in riverine systems. We identified diffuse nitrate inputs from organic fertilizers as major contributors to the riverine nitrogen pools of the rivers Rhine, Ems and Weser. Comparatively high annual mean  $\delta^{15}\text{N-NO}_3^-$  values between 8‰ and 13‰ are indicative for a significant animal waste and manure contribution which is in accordance with the high urban and agricultural land use in the respective catchment areas. A second major diffuse nitrate source is assumed to be nitrate from nitrification in soils. Evidence is given by the combined analysis of  $\delta^{18}\text{O-NO}_3^-$  and  $\delta^{18}\text{O-H}_2\text{O}$ . Comparatively low  $\delta^{18}\text{O-NO}_3^-$  between 0.4‰ and 3.3‰ measured in the Rhine, Weser and Ems bear the  $\delta^{18}\text{O}$  signature of ambient water. Measured  $\delta^{18}\text{O-H}_2\text{O}$  of riverine water was between -9.4‰ and -7.3‰ which accounts for 2/3 to the  $\delta^{18}\text{O}$ -signal of  $\text{NO}_3^-$  from nitrification in soils. Besides external nitrate inputs, a potential internal nitrate source during winter when ammonium is abundant was vaguely attributed to water column nitrification. Furthermore, we revealed that assimilative processes are responsible for fractionation of  $\delta^{15}\text{N-NO}_3^-$  and  $\delta^{18}\text{O-NO}_3^-$  values in summer months when biological activity takes place. In all rivers, a decrease in  $\text{NO}_3^-$  concentrations was inversely correlated with an increase in  $\delta^{15}\text{N-NO}_3^-$  values as consequence of an enrichment of heavy isotopes in the residual  $\text{NO}_3^-$  pool during assimilation. Variations of isotopic values and fractionation range were attributed to the hydrological characteristics of the respective rivers. The Rhine River is an exception in terms of discharge yield; the nitrate consumption efficiency is lower than in the rivers Weser and Ems due to the fact that a higher current velocity decreases the rate of biogeochemical transformation processes. Strong interdependencies between stream sizes, consumption efficiency and fractionation range were found comparing the three rivers of different sizes. Highest  $\text{NO}_3^-$  values and highest nitrate consumption rates associated with a high variation of  $\delta^{15}\text{N-NO}_3^-$  values and  $\delta^{18}\text{O-NO}_3^-$  values were observed in the smaller river Ems. We conclude from this that sources of rN and the nitrate consumption efficiency interrelated with the current velocity determines mostly the isotopic composition of riverine nitrate.

## **Acknowledgements**

We thank the GKSS Research Center, Institute for Coastal Research and DFG (Em 37-29) for support. The authors would like to acknowledge N. Lahajnar and F. Langenberg (IfBM, University of Hamburg) providing  $\delta^{15}\text{N}$ -PN data. In particular, we thank T. Gerke (IMBL Bimmen-Lobith), H. Petry (StUA Münster), and B. Freiheit (Senator für Umwelt, Bau, Verkehr und Europa Bremen) for coordination and help with sampling at the river sites. E. Spieck is acknowledged for corrections and helpful comments on an earlier draft.



## 4 Denitrification in coastal sediments of the German Wadden Sea

Astrid Deek, Kay Emeis, Justus van Beusekom  
resubmitted to *Biogeochemistry*

### Abstract

Although sediments of the German Wadden Sea are suspected to eliminate a considerable share of nitrate delivered to the SE North Sea, their denitrification rates have not been systematically assessed. We determined denitrification rates over seasonal cycles (February 2009 to April 2010) at two locations with two sediments types each, the first site (Meldorf Bight) receiving nitrate during all seasons from the Elbe river plume, and a second site on the island of Sylt, where nitrate is depleted during summer months. In sediments from the Sylt site, denitrification rates ranged from 16 to 32  $\mu\text{mol N}_2 \text{ m}^{-2} \text{ h}^{-1}$  in the fine sand station and from 7 and 13  $\mu\text{mol N}_2 \text{ m}^{-2} \text{ h}^{-1}$  in the coarse sand station; denitrification was not detected when nitrate was depleted in May and July of 2009. Denitrification rates in the Meldorf Bight sediments were consistently detected at higher rates (60 to 130  $\mu\text{mol N}_2 \text{ m}^{-2} \text{ h}^{-1}$  in the very fine sand station and between 14 and 30  $\mu\text{mol N}_2 \text{ m}^{-2} \text{ h}^{-1}$  in the medium sand station). Analysis of ancillary parameters suggests that major factors controlling denitrification rates in coastal sediments of the German Wadden Sea are the nitrate concentrations in the overlying water, the ambient temperature, and the organic matter content of the sediment. Extrapolating our spot measurements to the zone of nitrate availability and sediment types, we estimate an annual nitrogen removal rate around 10 kt  $\text{N y}^{-1}$  for the entire northern sector of the German Wadden Sea area. This corresponds to 12% of the annual Elbe river nitrate load.

## 4.1 Introduction

Reactive nitrogen (rN) inputs to the North Sea by rivers have increased 3-fold since the 1960's (van Beusekom and de Jonge, 2002) and are considered to be a prime reason for environmental deterioration in offshore regions of the North Sea (Owens et al. 1990) and in the Wadden Sea area (van Beusekom et al., 2001; van Beusekom und de Jonge, 2002). Mass balance estimates (Pätsch et al., 2010) suggest that increased atmospheric and riverine rN inputs are mitigated by effective sinks, such as sedimentary denitrification in subtidal and intertidal sediments of the shallow North Sea. Such sediments, which often have high organic carbon contents and are permeable so that nitrate is readily advected to suboxic depth levels, are active sites of heterotrophic and (subordinate) autotrophic denitrification, during which  $\text{NO}_3^-$  and  $\text{NO}_2^-$  are reduced via NO and  $\text{N}_2\text{O}$  to  $\text{N}_2$ . The latter escapes from the sediment to the overlying water or atmosphere by diffusion (Nixon et al., 1996) and is lost from the system (see Fig. 4.1). Together with the process of anaerobic ammonia oxidation, denitrification in sediments is the most important sink for nitrate on a global scale and a first order regulation mechanism for the nitrogen cycle of shelf seas (Middelburg et al., 1996). Controlling factors for denitrification rates in coastal sediments are amount and quality of sedimentary organic matter, concentrations of nitrate in water overlying the sediment, permeability of the sediment, and secondary factors, such as bioturbation/bio-irrigation, macrophytes and availability of manganese and iron (Cornwell et al., 1999). Although of considerable value as an ecosystem service that eliminates excess nitrate in and counteracts eutrophication of coastal zones, knowledge on denitrification rates in the sediments of the North Sea is limited. Experimental data were obtained in the 1990's with methods (the acetylene blocking technique) that may underestimate actual denitrification rates (Sørensen, 1978; Lohse et al., 1993; Lohse et al., 1996). Budget estimates generally give higher denitrification rates than available measurements (see Brion et al., 2004). Van Beusekom and de Jonge (1998) estimated annual denitrification rates of about  $900 \text{ mmol N m}^{-2} \text{ y}^{-1}$  for the Ems estuary based on nutrient-salinity relations and input data. Hydes et al. (1999) regarded the Southern North Sea as a giant estuary and estimated an average denitrification in the Southern North Sea of about  $256 \text{ mmol N m}^{-2} \text{ y}^{-1}$ . Brion et al. (2004) used similar rates for their North Sea budget. Only limited information using modern techniques like the  $\text{N}_2/\text{Ar}$  method is available to support the high denitrification rates as suggested by budget calculations. Two studies carried out within the Wadden Sea focussed on experimental techniques and reported potential denitrification rates (after addition of  $^{15}\text{N}$  labelled nitrate) (Cook et al., 2006; Gao et al., 2010). These rates were among the highest ever measured in the Wadden Sea, comparable to the above rates as derived from budgets, but lack spatial and temporal resolution.

Our objective here was to improve the estimates of denitrification rates in intertidal sediments of the Wadden Sea and to better constrain their seasonal and spatial variability. Our approach was to determine denitrification rates in spatial resolution along gradients of nitrate availability, sediment type and organic matter content and quality, and ambient temperature.

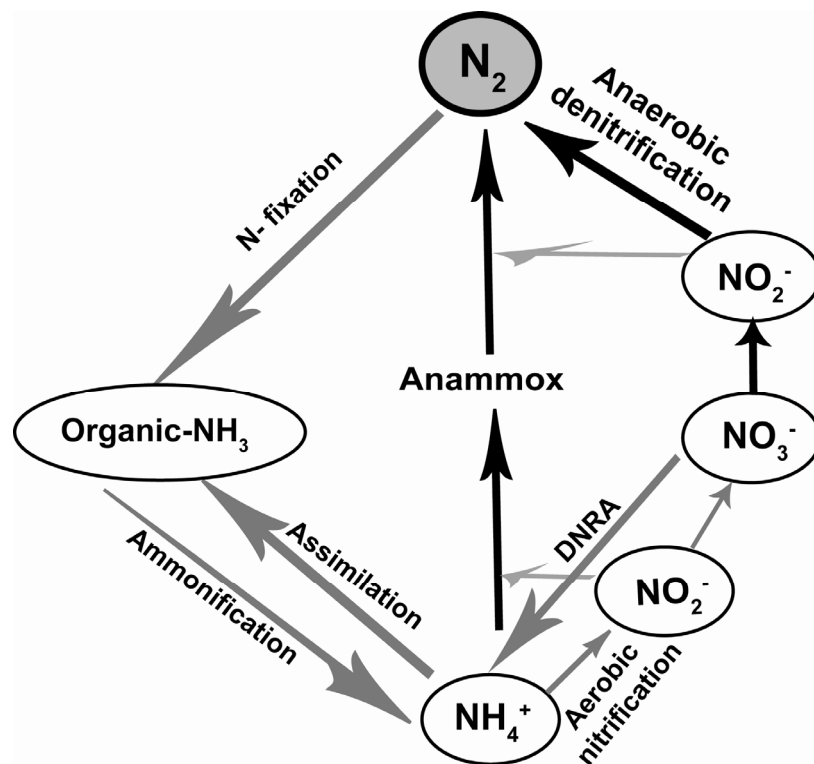


Fig. 4.1: Schematic marine N-cycle.

The processes illustrated with dark arrows indicate those pathways which produce  $N_2$  and are a net sink of reactive nitrogen.

## 4.2 Materials and Methods

We quantified denitrification rates using a direct flux approach by incubating undisturbed sediment cores in a flow-through incubation set-up (modified after Lavrentyev et al., 2000; McCarthy and Gardner, 2003) and measuring  $N_2$  fluxes by the  $N_2/Ar$  technique (Kana et al., 1994; An et al., 2001). We designed sampling campaigns and sites to bracket the most significant gradients in environmental parameters listed in the introduction (Cornwell et al., 1999).

## 4.2.1 Study sites

In the northern Wadden Sea of the German Bight, nitrate gradients are steep and mirror the decreasing influence of the Elbe River plume. We selected two study sites along the nitrate gradient: Near the plume, at study site Büsum/Meldorf Bight (Fig. 4.2), nitrate is never depleted in waters in contact with sediments. The site near the island of Sylt has no or negligible nitrate and low ammonium concentrations between July and September (van Beusekom et al., 2009). At each site, two different sediment types in terms of grain size distribution and organic matter content were sampled (Tab. 4.1): Sylt-I (fine sand) and Büsum-I (very fine sand) sediments have comparatively high organic carbon ( $C_{org}$ ) contents of 1.6 and 1.9%, respectively. Sylt-II (coarse sand) and Büsum-II (medium sand) have low  $C_{org}$  concentrations of 0.6 and 0.1%.

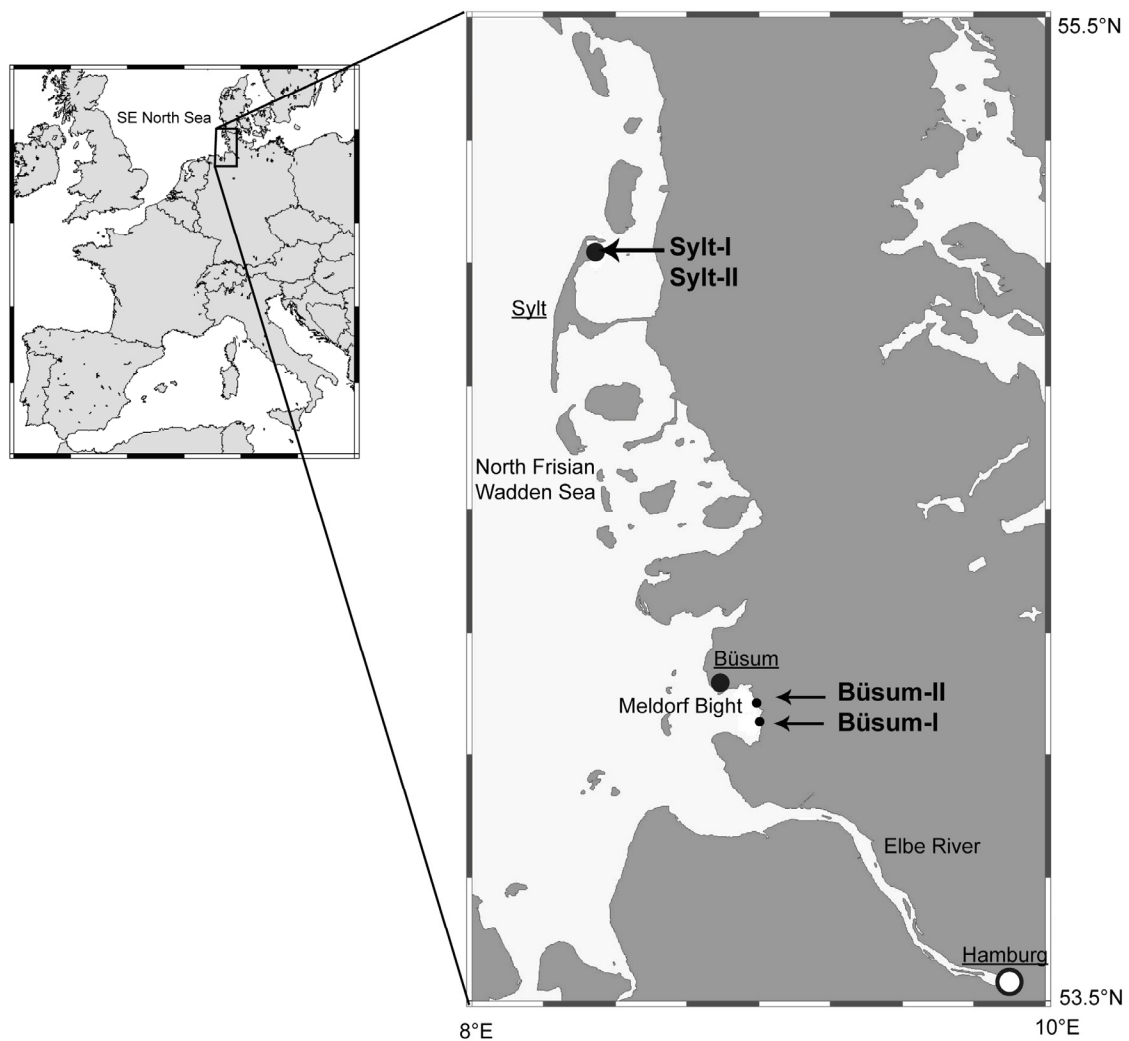


Fig. 4.2: Study sites in the North Frisian Wadden Sea.

Tab. 4.1: Sediment characteristics for the study sites Sylt-I, Sylt-II, Büsum-I and Büsum-II (Porosity, carbon content (%C), nitrogen content (%N), organic carbon content (%C<sub>org</sub>) and C/N given as average value for 0–10cm, depth resolution: 1cm,  $\delta^{15}\text{N}$  and amino acids (AA) were analyzed in surface sediment layers: 0–1cm. Sediments were classified according the Udden-Wentworth size scale (Wentworth, 1922; Pettijohn and Potter, 1972).

Date	Station	Porosity (v/v)	C [%]	N [%]	C <sub>org</sub> [%]	C/N	AA [mg g <sup>-1</sup> ]	Median grain size [ $\mu\text{m}$ ]	Sediment classification
June'09	Büsum-I	0.67	2.9	0.2	1.9	8.6	7	63	very fine sand
	Büsum-II	0.42	0.5	0.1	0.1	1.4	0.6	250	medium sand
July'09	Sylt-I	0.73	2.1	0.2	1.6	7.5	14.9	125	fine sand
	Sylt-II	0.42	0.7	0.1	0.6	12.4	0.8	500	coarse sand

#### 4.2.2 Sampling

At least six sediment cores were taken during each sampling campaign at each of the sampling stations of the two sites. These stations were sampled at the beginning of high tide, when the sediment was covered by a water column of at least 10 cm and a maximum of 30 cm. Samples (around 20 cm length) were taken manually with polyvinylchloride (PVC) tubes (60 cm length and inner diameter of 10 cm) and stoppered. After sampling, the upper rubber stopper was removed and water level overlying the sediment was adjusted to 10 cm. During transport, sediment cores were cooled and transported (<6 hours) to the temperature-controlled laboratory. At least 100 L of site water were collected in 25 L carboys to ensure sufficient site water with appropriate salinity and nitrate concentrations for the flow-through incubation. O<sub>2</sub> saturation and temperature of site water were measured with an Ecoscan DO 6 (Eutech Instruments), salinity with a handheld refractometer (Atego), and pH with an Ecoscan Ion 6 (Eutech Instruments) (Tab. 4.2).

Tab. 4.2: Site characteristics for the sampling campaigns in Sylt and Büsum.

Büsum	Watercolumn										Suspended Matter			Sediment	
	Date	T [°C]	Sal	pH	PO <sub>4</sub> <sup>-</sup> [µmol/L]	Si [µmol/L]	NH <sub>4</sub> <sup>+</sup> [µmol/L]	NO <sub>3</sub> <sup>-</sup> [µmol/L]	NO <sub>2</sub> <sup>-</sup> [µmol/L]	C [%]	N [%]	C <sub>org</sub> [%]	C/N	Büsum-I:Oxygen penetration depth [mm]	Büsum-II:Oxygen penetration depth [mm]
Büsum	February'09	4	18	8.6	6.0	18.0	23.7	67.4	1.5	3.8	0.3	3.1	10.3	1.5	2.6
	June'09	23	30	8.0	2.6	18.9	14.2	6.8	1.3	2.9	0.3	2.7	9.0	0.8	2.2
	November'09	8	20	8.0	5.2	87.3	31.0	67.2	4.2	3.0	3.1	2.4	7.9	2.6	3.0
	April'10	9	30	8.5	n.d.	20.6	1.4	85.4	4.6	4.6	0.6	4.0	6.7	1.4	1.6
Sylt	February'09	1	30	8.2	2.3	10.4	4.7	31.9	bid	3.8	0.3	2.6	8.7	2.2	3.1
	May'09	15	30	/	1.2	7.8	bid	bid	bid	5.1	0.6	4.3	7.2	1.2	1.6
	July'09	24	32	8.3	0.6	3.8	1.3	bid	bid	3.0	0.3	2.8	9.3	1.2	1.7
	November'09	8	30	8.8	1.3	10.8	10.3	12.1	0.8	7.5	0.7	6.3	9.0	1.8	/
April'10	8	30	8.5	0.2	1.7	4.8	13.0	1.3	3.2	0.3	2.2	7.3	1.2	2.0	

### 4.2.3 Sediment core incubation

After transferring the cores to a temperature controlled room or into a circulating water bath adjusted to the in-situ temperature, the supernatant water was aerated with aquarium pumps for 6 to 12 hours to reach oxygen saturation in the overlying water column before starting the incubation. The incubation set-up is illustrated in Fig. 4.3, and is a modified and larger version of the incubation set-ups described in Gardner et al. (1991), Lavrentyev et al. (2000) and McCarthy and Gardner (2003). The sediment cores were wrapped with aluminium foil to prevent variable light conditions, and were placed in a flow-through incubation system, consisting of the cores, a 25 L carboy of site water, a peristaltic pump and an outflow collection vessel. The site water reservoir was aerated constantly, because the ambient water at the study sites was always oxygen saturated during all sampling campaigns. The sediment cores were locked with a gas tight plunger with two O-rings and Tygon inflow and outflow tubes. The plunger was positioned to 5 cm above the sediment-water interface, which is equal to a water volume of 785 mL over the sediment, continuously replaced by site water at a rate of 1–2 mL min<sup>-1</sup>. Samples of inflow water and outflow water were taken every 12 hours of incubation. Two control cores without sediment were run in the same way to exclude water column denitrification. Whereas the incubations of Sylt-I and Büsum-I cores were run for 2 days, the incubations of Sylt-II and Büsum-II cores were run for 4 days. The different incubation times were necessary to account for the different sediment types: In preliminary incubation tests, sandy sediments had reached steady-state fluxes of nutrients, O<sub>2</sub> and N<sub>2</sub> only after longer incubation times, explained by deeper oxygen penetration (Tab. 4.2) and deeper denitrification zones in sandy sediments (Cook et al., 2006; Gihring et al., 2010). Three of the 6 subcores were incubated with site water enriched with 98% Na <sup>15</sup>NO<sub>3</sub><sup>-</sup> (Isotec) to a 40 to 50 µmol/L <sup>15</sup>NO<sub>3</sub><sup>-</sup> concentration. N<sub>2</sub> fluxes (m29+m30) from these amended cores were used a) to estimate N<sub>2</sub> fluxes under conditions when actual NO<sub>3</sub><sup>-</sup> limitation is eliminated through artificial <sup>15</sup>NO<sub>3</sub><sup>-</sup> addition b) to calculate denitrification rates according the isotope pairing technique (Nielsen, 1992).

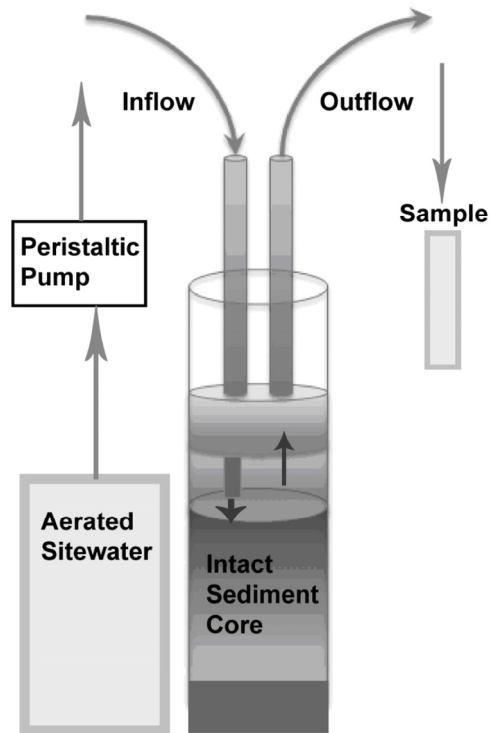


Fig. 4.3: Flow-through incubation set-up.

## 4.2.4 Laboratory Analyses

### 4.2.4.1 $N_2$ and $O_2$ concentrations

Triplicate samples from the inflow water and outflow water were taken every 12 hours with cylindrical glass vials during incubations and were analyzed immediately after collection for  $N_2$  and  $O_2$ . The concentrations of  $N_2$  and  $O_2$  were calculated from  $N_2/Ar$  and  $O_2/Ar$  ratios measured with a membrane inlet mass spectrometry (MIMS) system consisting of a Quadrupole mass spectrometer (QMS) (GAM 200, InProcess Instruments) with a modified membrane inlet from Bay Instruments. The MIMS was standardized with air saturated temperature-salinity-standards according to Kana et al. (1994) to correct measured  $N_2/Ar$  and  $O_2/Ar$  ratios to actual ratios. Concentrations were calculated by multiplying the actual Ar concentration from solubility tables (Weiss, 1970) with the corrected ratio. The QMS ion source produces  $O^+$  ions by ionizing sample gas;  $O^+$  ions may react with  $N_2$  forming  $NO_x$  (Eyre et al., 2002). This so called  $NO_x$ -effect results in higher signals on mass 28 (m28) at

low oxygen concentrations and low m28 signals at high oxygen concentrations, which may lead to a misinterpretation of actual denitrification. The  $\text{NO}_x$ -effect was tested for the MIMS system used and the extent of this effect was found to be below the standard deviation of the method (0.1%) (J. Pohlmann, pers. comm. 2010). Net  $\text{N}_2$  and  $\text{O}_2$  fluxes (fl; in  $\mu\text{mol m}^{-2} \text{h}^{-1}$ ) were calculated by subtracting inflow concentration ( $C_i$ ) from outflow concentration ( $C_o$ ) multiplied with the flow rate (f:  $\text{Lh}^{-1}$ ) and sediment surface area (a:  $\text{m}^2$ ) ratio:

$$\text{fl} = (C_o - C_i) \times f/a \quad [4.1]$$

Samples were measured simultaneously on the mass signals m28, m29 and m30, because samples from  $^{15}\text{NO}_3^-$  incubations were expected to produce  $^{29}\text{N}_2$  and  $^{30}\text{N}_2$ . These data also allowed estimation of  $\text{N}_2$  production and consumption rates based on calculations proposed by An et al. (2001) and An and Gardner (2001). By applying calculations developed for the isotope pairing technique (IPT) (Nielsen, 1992), we also estimated the proportion of nitrification-denitrification. Denitrification rates were defined as the net production of  $\text{N}_2$  which is the sum of several pathways of  $\text{N}_2$  production and  $\text{N}_2$  consumption (see also Fig. 4.1).

#### 4.2.4.2 Nutrient concentrations

During incubation, inflow and outflow samples were collected daily for nutrient analyses. Nutrient samples were filtered using a 0.2  $\mu\text{m}$  syringe filter (X50 Anlypore, PVDF), stored in 50 mL Falcon tubes and stored frozen until analyses.  $\text{NO}_3^-$ ,  $\text{NO}_2^-$  and  $\text{NH}_4^+$  concentrations were analyzed by automated continuous flow analysis using a Bran & Luebbe, Auto Analyzer 3.  $\text{NO}_3^-$  and  $\text{NO}_2^-$  were determined according to a modified method of Armstrong et al. (1967).  $\text{NH}_4^+$  concentrations were determined according a modified method of Grasshoff et al. (1983). Nutrient fluxes were calculated according to Eq. 4.1.

#### 4.2.4.3 Sediment characteristics

Before and after incubation, oxygen penetration depths were determined for one sediment core from each sampling station. Two different types of oxygen profiling setups were used during this study: A Clark-type  $\text{O}_2$  micro electrode (OX 50 and OX 100) in connection with a picoamperemeter (Unisense A/S), and an oxygen micro-optode (Oxy 50M, Pyro Science) in connection with a Microx TX3-USB (Pyro Science, Presens).

Sediment characteristics (grain size, organic carbon and amino acid concentration) were determined from sampling campaigns in June 2009 (Büsum-I and Büsum-II) and in July 2009 (Sylt-I and Sylt-II). The sediment cores were sliced into 1 cm slices and frozen for transport.

Water content and porosity were calculated from the weight before and after freeze drying and assuming a grain density of  $2.65 \text{ g cm}^{-3}$ . Grain size distribution was then determined on dry residues by sieving through mesh sizes of  $1000 \mu\text{m}$ ,  $500 \mu\text{m}$ ,  $250 \mu\text{m}$ ,  $125 \mu\text{m}$  and  $63 \mu\text{m}$ . The weight percentage of total nitrogen (TN), organic carbon ( $C_{\text{org}}$ ) were determined on the dried residues of 1cm-slices of one core from each sampling site to assess organic matter concentrations and reactivity. TN and  $C_{\text{org}}$  concentrations were determined with an Elemental Analyzer (Thermo Flash EA) calibrated against acetanilide. Total hydrolysable amino acids were analysed with a Biochrom 30 Amino Acid Analyser after hydrolysis of 30–50 mg of sediment with 6 N HCl for 22 hours at  $110^\circ\text{C}$ . HCl was then removed by evaporation and the residue was taken up by acidic buffer and injected into the analyser. After separation with a cation exchange resin, the individual monomers were detected fluorometrically. Further analytical details are given in Lahajnar et al. (2007).

### 4.3 Results

#### 4.3.1 Sediment characteristics at the different sites

Properties of sediments at each of the sample locations are listed in Tab. 4.1. These parameters were only determined once on one core from each sediment facies (see sections 4.2.1, 4.2.4). Organic matter quality is reflected by the absolute concentration of total hydrolysable amino acids and by the ratios of individual amino acid monomers (Dauwe et al., 2001; Gaye-Haake et al., 2005). In our samples, highest total hydrolysable amino acid concentrations were measured in cores of Sylt-I and Büsum-I. The data suggest that substrate quality in terms of labile particulate matter available for bacterial respiration was highest in the stations Sylt-I and Büsum-I.

#### 4.3.2 Seasonal variation of the site parameters

Stations in the Meldorf Bight (Büsum-I and Büsum-II) and on Sylt (Sylt-I and Sylt-II) experienced a pronounced seasonal variability of nutrient concentrations (Tab. 4.2). In Büsum, highest  $\text{NO}_3^-$  concentrations (April 2010:  $85 \mu\text{mol/L}$ ; February 2009 and November 2009:  $67 \mu\text{mol/L}$ ) were measured when temperature was lowest. In summer,  $\text{NO}_3^-$  concentrations were around  $7 \mu\text{mol/L}$ . At sites Sylt,  $\text{NO}_3^-$  concentrations were below detection limit during summer months; a high concentration of  $32 \mu\text{mol/L}$  was measured in February 2009.

### 4.3.3 Nutrient fluxes

Nutrient fluxes across the sediment-water interface of incubated cores are illustrated in Fig. 4.4, which depicts  $\text{NO}_3^-$  and  $\text{NH}_4^+$  fluxes (mean value of three cores) on day 2 of incubation for Büsum-I and Sylt-I and on day 4 of incubation for Büsum-II and Sylt-II (all at steady state). In Fig. 4.4  $\text{NO}_3^-$  and  $\text{NH}_4^+$  fluxes from unamended cores are compared with  $\text{NO}_3^-$  and  $\text{NH}_4^+$  fluxes from  $^{15}\text{NO}_3^-$  amended cores. For the stations Büsum-I and Büsum-II, maximum actual  $\text{NO}_3^-$  fluxes ( $-412 \text{ NO}_3^- \mu\text{mol m}^{-2} \text{ h}^{-1}$  and  $-297 \text{ NO}_3^- \mu\text{mol m}^{-2} \text{ h}^{-1}$ , respectively; negative signs denoting flux into the sediment) were measured in June 2009 and April 2010.  $\text{NO}_3^-$  fluxes in the  $^{15}\text{NO}_3^-$  amended cores were higher in June and November than actual  $\text{NO}_3^-$  fluxes. In the Sylt cores, no significant actual nitrate fluxes were measured during May and July 2009.  $\text{NO}_3^-$  fluxes in the  $^{15}\text{NO}_3^-$  amended cores were higher in Sylt-I than in Sylt-II cores, with maxima of  $-220 \mu\text{mol m}^{-2} \text{ h}^{-1}$  and  $-100 \mu\text{mol m}^{-2} \text{ h}^{-1}$ , respectively. At Sylt-I,  $\text{NH}_4^+$  effluxes from the sediment were more than  $+500 \mu\text{mol m}^{-2} \text{ h}^{-1}$  in July 2009. Ammonium effluxes were relatively low in Büsum-II and Sylt-II incubations (Fig. 4.4).

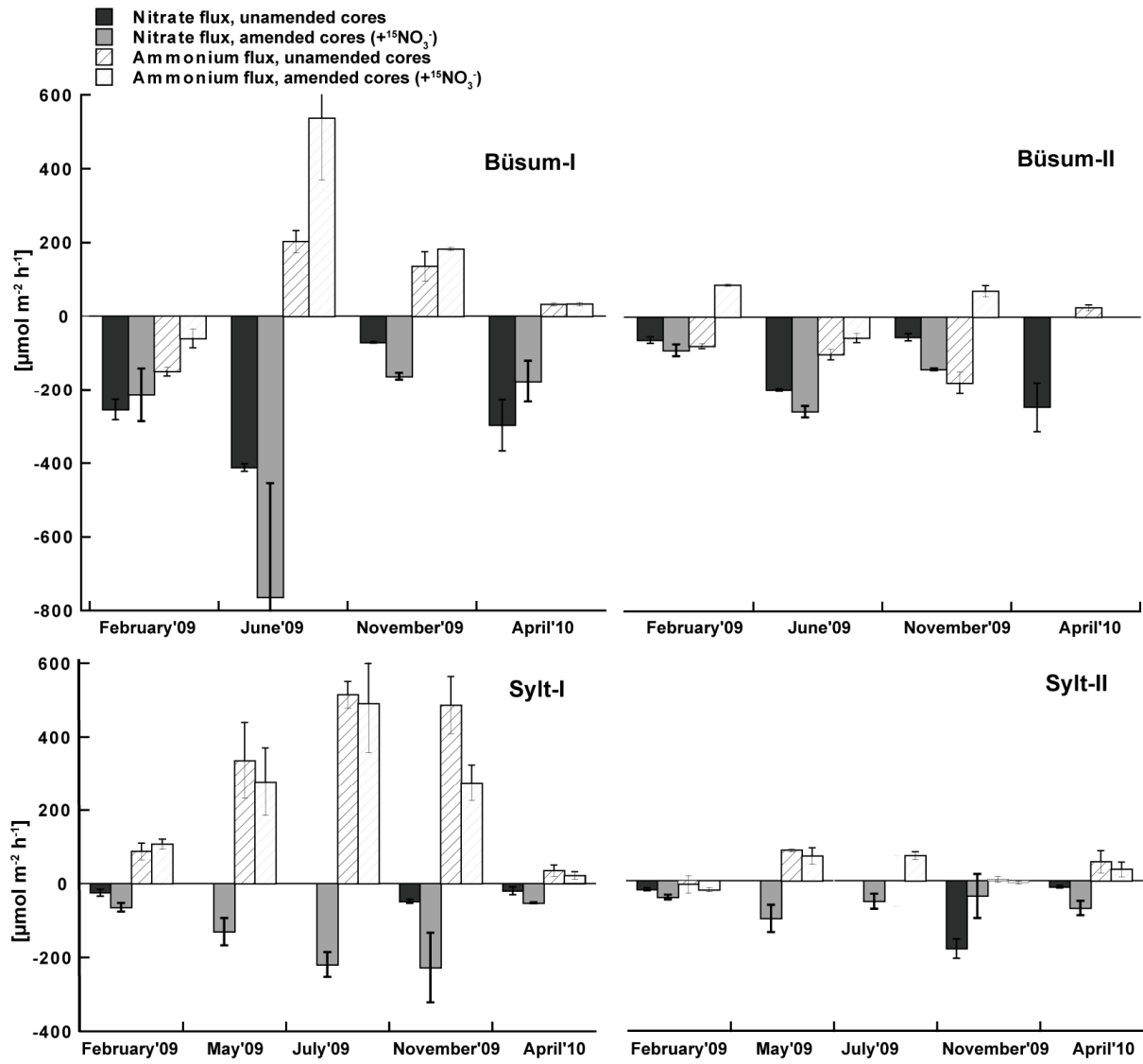


Fig. 4.4: Nitrate and ammonium fluxes.

Data are mean values of three cores (n=3) with standard deviation.

#### 4.3.4 N<sub>2</sub> and O<sub>2</sub> fluxes

N<sub>2</sub> and O<sub>2</sub> fluxes (mean value of three cores) are illustrated in Fig. 4.5a and 4.5b; again fluxes refer to day 2 of incubation for Büsum-I and Sylt-I and to day 4 of incubation for Büsum-II and Sylt-II. Sedimentary oxygen demand (SOD) was highest in November 2009 at all sampling stations (>2000  $\mu\text{mol m}^{-2} \text{h}^{-1}$  in Büsum-I and Sylt-I; around 1200  $\mu\text{mol m}^{-2} \text{h}^{-1}$  in Büsum-II and Sylt-II) (Fig. 4.5a and 4.5b).

Fig. 4.5a and 4.5b also compare four different N<sub>2</sub> fluxes obtained by the incubation experiments: Actual N<sub>2</sub> fluxes (m28) from the unamended cores, N<sub>2</sub> fluxes (m29 + m30) from amended cores where ambient  $^{14}\text{NO}_3^-$  is partially combined with added  $^{15}\text{NO}_3^-$ , and the N<sub>2</sub> production rate calculated according the isotope pairing technique (IPT) (Nielsen, 1992) from the N<sub>2</sub> fluxes (m29+m30) of the  $^{15}\text{NO}_3^-$  amended cores. The differences between calculated N<sub>2</sub> production rates on m28 and actual N<sub>2</sub> production rates on m28 are small and within the standard deviation for the respective mean N<sub>2</sub> production rates (Fig. 4.5a and 4.5b). Exceptions are fluxes during a sampling campaign at Sylt-II in February 2009, when fluxes calculated by IPT were higher (Fig. 4.5b).

Actual N<sub>2</sub> fluxes (m28) were highest in Büsum-I cores (+130  $\mu\text{mol N}_2 \text{ m}^{-2} \text{ h}^{-1}$ ) in November 2009, and varied between 15 and 30  $\mu\text{mol m}^{-2} \text{ h}^{-1}$  in Büsum-II cores. We registered no actual N<sub>2</sub> flux (m28) during May and July 2009 in Sylt-I and Sylt-II sediments; these sediments produced N<sub>2</sub> at rates of 32 and 13  $\mu\text{mol N}_2 \text{ m}^{-2} \text{ h}^{-1}$ , respectively, in February 2009. In all sediment cores, N<sub>2</sub> fluxes in the  $^{15}\text{NO}_3^-$  amended cores were higher than actual rates during summer, as indicated by maximum rates on m29 and m30 in Büsum-I (m30: 176  $\mu\text{mol N}_2 \text{ m}^{-2} \text{ h}^{-1}$ ; m29: 67  $\mu\text{mol N}_2 \text{ m}^{-2} \text{ h}^{-1}$ ) in June 2009. Büsum-II yielded 67  $\mu\text{mol N}_2$  (m30)  $\text{m}^{-2} \text{ h}^{-1}$  and 31  $\mu\text{mol N}_2$  (m29)  $\text{m}^{-2} \text{ h}^{-1}$  during the same sampling campaign (Fig. 4.5a). Maximum N<sub>2</sub> fluxes in the  $^{15}\text{NO}_3^-$  amended cores were 104  $\mu\text{mol N}_2$  (m30)  $\text{m}^{-2} \text{ h}^{-1}$  and 13  $\mu\text{mol N}_2$  (m29)  $\text{m}^{-2} \text{ h}^{-1}$  in Sylt-I cores in May 2009. Highest N<sub>2</sub> fluxes of 29  $\mu\text{mol N}_2$  (M30)  $\text{m}^{-2} \text{ h}^{-1}$  were measured in Sylt-II cores in May 2009, whereas fluxes on m30 were not observed (Fig. 4.5b).

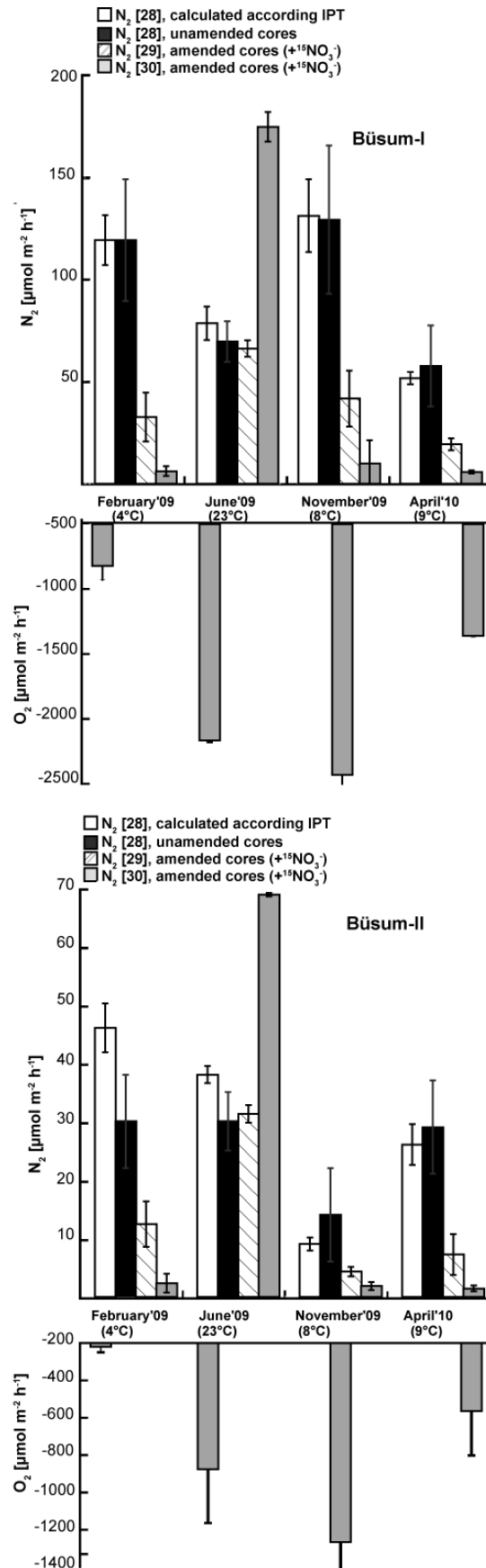


Fig. 4.5a: N<sub>2</sub> and O<sub>2</sub> fluxes for the sampling stations in Büsum.

Data are mean values of three cores (n=3) with standard deviation. Note different scale of y-axis.

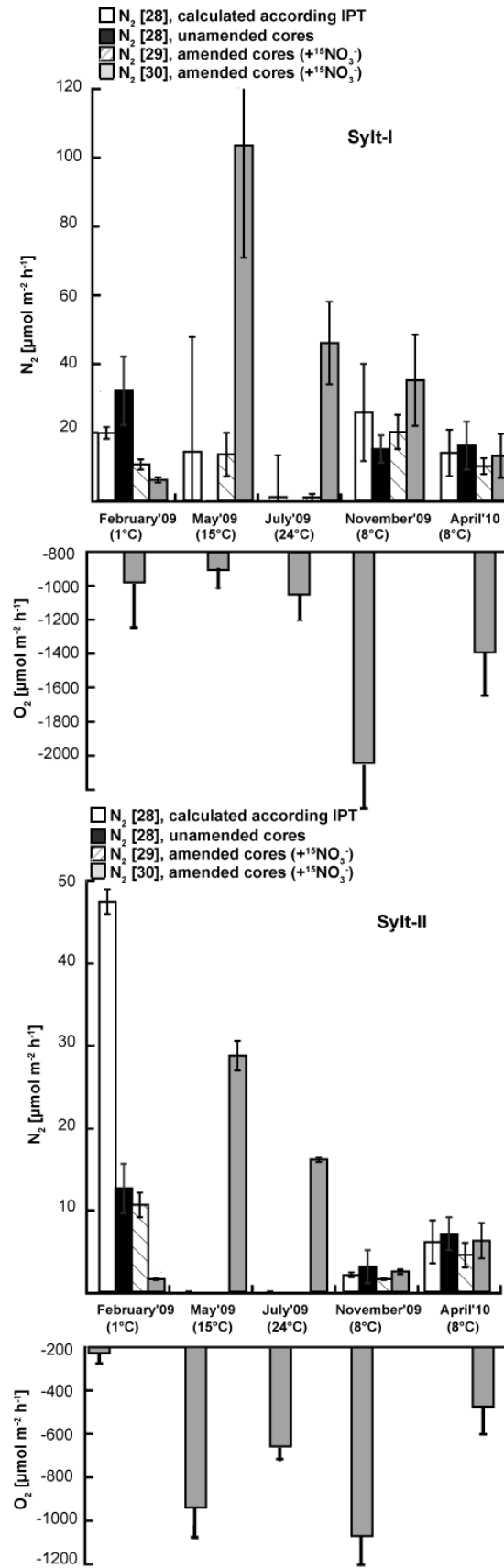


Fig. 4.5b:  $N_2$  and  $O_2$  fluxes for the sampling stations in Syllt.

Data are mean values of three cores ( $n=3$ ) with standard deviation. Note different scale of y-axis.

## 4.4 Discussion

Our data bracket a range of environmental conditions and several salient features emerge on controls of  $N_2$  fluxes (gross denitrification rates) out of Wadden Sea sediments. We focus our discussion on effects of nitrate concentrations and temperature, and further evaluate the influence of sedimentary  $C_{org}$  content on denitrification rates. But the experimental data are also suited to differentiate between different processes in the sediments at each individual location and facies. This is because the actual  $N_2$  fluxes (m28) measured in unamended sediment cores quantify net  $N_2$  production rates; whereas the mass distribution of  $N_2$  produced in  $^{15}NO_3^-$  amended cores permit application of concepts developed for the IPT. Together with observed nutrient fluxes, the data give insight into and help to quantify individual processes of the nitrogen-cycle. In the first part of our discussion, we estimate the proportion of alternative pathways of  $N_2$  production and  $N_2$  consumption, such as nitrification-denitrification and  $N_2$  fixation that contribute to the net  $N_2$  flux. Because the sediment types analysed represent the dominant sedimentary facies of the Wadden Sea, we finally estimate annual removal rates of nitrate by sediments in the northern German Wadden Sea.

### 4.4.1 Insights into N-cycling from nutrient fluxes and denitrification rates obtained by IPT

The calculated  $N_2$  fluxes (m28) obtained by IPT are in good agreement with the actual  $N_2$  fluxes (m28) measured in unamended cores (Fig. 4.5a and 4.5b) supporting that both methods yield comparable results. Moreover, the simultaneous measurement of actual  $N_2$  (m28) and nutrient fluxes, together with  $N_2$  fluxes from  $^{15}NO_3^-$  amended cores (m29+m30) allows us to estimate the amount of coupled nitrification-denitrification in the sediment, and the amount of  $N_2$  fixation.

According to An et al. (2001),  $N_2$  production rates (m28) estimated from IPT match actual  $N_2$  fluxes (m28) when no  $N_2$  fixation occurs. We applied equations derived by An et al. (2001) to calculate the amount of  $N_2$  fixation, and obtained negative solutions which denote zero  $N_2$  fixation rates.  $N_2$  fixation thus plays no or only a minor role in sediments under study. In consequence, the net  $N_2$  flux (m28) measured in the unamended cores is a good approximation of the gross  $N_2$  production, because  $N_2$  consumption can be neglected. In our approach, we do not differentiate between the two different mechanisms of  $N_2$  production (anammox and denitrification; see Fig. 4.1). Anammox has been shown to play an important role in removing rN from marine ecosystems (Thamdrup and Dalsgaard, 2002; Trimmer and

Nicholls, 2009), but within this study its contribution to the total  $N_2$  production cannot be estimated. This is because our experimental set-up did not include incubations with increasing concentrations of  $^{15}NO_3^-$  concentrations as described in Risgaard-Petersen et al. (2003). In the following, we thus defined the gross denitrification rate as the net  $N_2$  flux (m28) that includes an unknown proportion of anammox.

Because our experiments did not include incubations with different  $^{15}NO_3^-$  concentrations, requirements of the classical IPT (Nielsen, 1992; Steingruber et al., 2001) have not been met. But by applying the IPT equations and from the  $N_2$  fluxes on m29 and m30 in the  $^{15}NO_3^-$  amended cores (Fig. 4.5a and 4.5b), we can calculate the contribution of coupled nitrification-denitrification to the total  $N_2$  production (Nielsen, 1992). The calculations suggest that between 20 and 50% of  $N_2$  flux out of Büsum-I, Büsum-II and Sylt-II cores derives from coupled nitrification-denitrification, with an exceptional maximum of between 80 and 100% in Sylt-I cores in May and July 2009. This maximum calculated by IPT corresponds to  $N_2$  fluxes observed exclusively on m29 in the Sylt-I cores in May 2009 (Fig. 4.5b), when ambient  $^{14}NO_3^-$  was not available (Tab. 4.2). Fluxes on m29 are only generated when  $^{15}NO_3^-$  is mixed with  $^{14}NO_3^-$  before being reduced to  $^{29}N_2$ . The only possible source of  $^{14}NO_3^-$  to the sediment in the Sylt area in May 2009 is nitrification within the sediment, and at rates calculated to around  $15 \mu\text{mol m}^{-2} \text{h}^{-1}$ . The ammonium fluxes (up to  $500 \mu\text{mol m}^{-2} \text{h}^{-1}$ , Fig. 4.4) from Sylt-I and Büsum-I cores to oxic supernatant water suggest even higher nitrification rates, because it is estimated that 27–36% of the actual ammonium efflux may be re-oxidised to nitrate within the sediment (Sweerts et al., 1991).

The very high ammonium fluxes in the Sylt-I and Büsum-I cores coincide with the highest AA concentrations in the host sediments (Tab. 4.1), which apparently support extraordinary rates of ammonification (Fig. 4.1). But also the dissimilatory nitrate reduction to ammonium (DNRA, Fig. 4.1) may be responsible for the high ammonium fluxes in Sylt-I and Büsum-I cores (Fig. 4.4) during summer: At that time, high nitrate fluxes (around  $400 \mu\text{mol m}^{-2} \text{h}^{-1}$ ) into the unamended Büsum-I cores (Fig. 4.4) resulted in comparatively small  $N_2$  fluxes (m28) out of the sediment of  $70 \mu\text{mol m}^{-2} \text{h}^{-1}$  (Fig. 4.5a). This is good evidence that a significant share of nitrate may be reduced by DNRA and released back into the water column as ammonium (An and Gardner, 2002; Giblin et al., 2010), but it is not a sink for reactive nitrogen as are denitrification and anammox.

Compared to the high fluxes in Sylt I and Büsum I sediments, ammonium and nitrate fluxes in Sylt-II and Büsum-II cores were much smaller (Fig. 4.4), and indicated lower overall N-cycling rates; in these sediments,  $O_2$  penetration also was much deeper. Although an extended gradient of  $O_2$  in the Sylt-II and Büsum-II cores should favour complete nitrification

of effluxing ammonium, substrate limitation and a low rate of ammonification in the organic-poor sediments (Tab. 4.1) limits nitrification: According IPT calculations, coupled nitrification-denitrification in Sylt-II cores accounts for around 20% in November 2009 and April 2010, whereas no denitrification has been detected in summer (Fig. 4.5b). It is of note that we never registered a net flux of nitrate out of the sediments under study, which means that nitrification never adds more nitrate than is being immediately reduced again. Furthermore, nitrogen consumption by  $N_2$  fixation is a negligible process (see above) and net  $N_2$  fluxes are always directed out of the sediments, meaning that most of the sediments are a sink for reactive nitrogen. Exceptions are the Sylt-I sediments with ammonium fluxes of up to  $500 \mu\text{mol m}^{-2} \text{h}^{-1}$  that exceed the nitrogen consumption rate most time of the year (Fig. 4.4). Hence, Sylt-I sediments are not a net sink but a source of reactive Nitrogen.

#### 4.4.2 Nitrate and temperature effects on denitrification rates in Büsum and Sylt sediments

Denitrification rates at both locations were highest during the fall, winter, and early spring (Fig. 4.5a +4.5b), in spite of low temperatures suppressing most microbial processes (Koch et al., 1992). On the other hand, nitrate was abundant in overlying waters at these times. This observation and the fact that sediments at Sylt sites did not produce  $N_2$  (m28) when  $\text{NO}_3^-$  was depleted in summer identify nitrate availability as the overriding control on denitrification rates. Even in the small range of ambient  $\text{NO}_3^-$  concentrations encountered at Sylt-I and Sylt-II sampling sites (Fig. 4.6),  $N_2$  (m28) production appears to increase linearly with nitrate availability, which here is relatively low ( $<30 \mu\text{mol L}^{-1}$ ) and restricted to the cold seasons (Tab. 4.2). The linear positive relationships between  $N_2$  production (m28) and nitrate concentrations for the four data points for Sylt I and II sampling in Fig. 4.6 are significantly correlated for each sampling site ( $r^2 \geq 0.9$ ;  $p < 0.01$  for Sylt-I and Sylt-II), but our data lack true seasonal resolution and do not cover maximum  $\text{NO}_3^-$  concentrations of about  $50 \mu\text{mol L}^{-1}$  (van Beusekom et al., 2009). Also, the slopes differ for the two sites.  $\text{NO}_3^-$  availability is a major limiting factor in denitrification (Nedwell, 1982; Seitzinger and Nixon, 1985; Christensen et al., 1990), when other factors, such as organic matter or temperature, are not limiting (Goltermann, 2004).

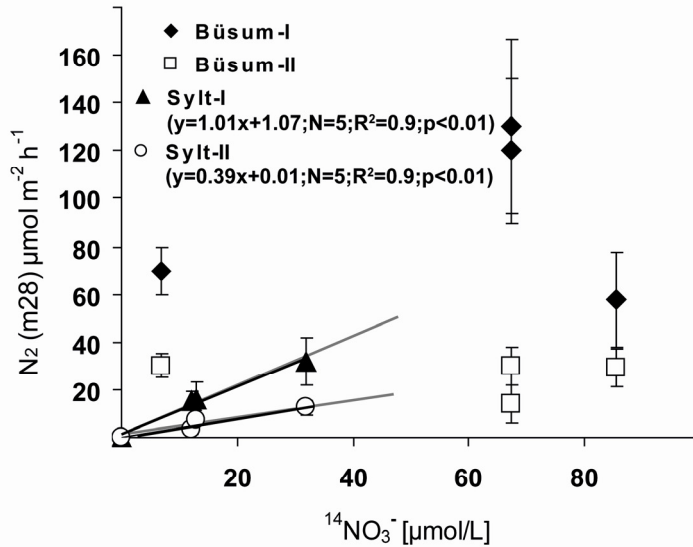


Fig. 4.6: Actual  $\text{N}_2$  production rates versus ambient  $^{15}\text{NO}_3^-$ .

In the  $^{15}\text{NO}_3^-$  amended incubations of Sylt cores (Fig. 4.5b), the  $\text{N}_2$  fluxes (m29+m30) had maxima in summer months, emphasizing that Sylt sediments are highly active when  $\text{NO}_3^-$  substrate is available. Over the last years  $\text{NO}_3^-$  concentrations have steadily decreased during summer months in the Sylt area in response to decreasing riverine nitrogen loads (van Beusekom et al., 2008), and nitrate availability was found to limit denitrification in previous investigations (Jensen et al., 1996). We conclude that denitrification (fuelled by nitrate from the overlying water column) in the nitrate-limited sector of the Wadden Sea occurs only during fall, winter, and early spring at rates between 7 and 13  $\mu\text{mol N}_2 \text{ m}^{-2} \text{ h}^{-1}$  in coarse sands (Sylt-II), and between 16 and 32  $\mu\text{mol N}_2 \text{ m}^{-2} \text{ h}^{-1}$  in fine sands (Sylt-I).

At the Büsum stations, which are permanently influenced by nitrate advected from the Elbe river plume and where nitrate is never completely depleted (Tab. 4.2), nitrate reduction in sediments proceeds during all seasons. Still,  $\text{N}_2$  fluxes (m29+m30) in the  $^{15}\text{NO}_3^-$  amended cores were higher than actual  $\text{N}_2$  (m28) fluxes in June 2008, indicating that ambient nitrate concentrations around 7  $\mu\text{mol L}^{-1}$  (Tab. 4.2) already limit denitrification during summer months. In contrast to the Sylt stations, there is no firm relationship between maximum  $\text{NO}_3^-$  concentrations and maximum actual denitrification rates (Fig. 4.6): Maximum nitrate concentrations occurred in April 2010, but were not associated with maximum  $\text{N}_2$  (m28) production rates, which were instead measured in November 2009 (Fig. 4.5a). One explanation is that temperature may control denitrification rates in the absence of  $\text{NO}_3^-$  limitation: Although water temperature was similar during sampling campaigns in November 2009 and April 2010, lower rates in April 2010 followed an exceptional long and cold winter

during this study, during which the sampling site was covered with ice and mean air temperatures of  $-1.3^{\circ}\text{C}$  chilled the coast until March (DWD, 2010).

The effect of temperature on denitrification rates is apparent from the results of the  $^{15}\text{NO}_3^-$  amended cores. Because all  $^{15}\text{NO}_3^-$  amended cores received  $40\text{--}50\ \mu\text{mol L}^{-1}$  of  $^{15}\text{NO}_3^-$ , substrate limitation can be excluded. During sampling campaigns with temperatures above  $15^{\circ}\text{C}$ ,  $\text{N}_2$  (m29+m30) fluxes were highest (Fig. 4.5a+b), indicating the positive effect of temperature on denitrification rates as shown elsewhere (Seitzinger, 1988; van Luijn et al., 1999). But the effect observed in our study may be influenced by additional factors, such as oxygen penetration depth, nitrate availability, primary productivity and hence substrate availability, which are all linked with temperature. Competing heterotrophic processes for organic matter, especially sulphate reduction and aerobic respiration, may also bias denitrification rates, so that isolated consideration of temperature only does not reflect interrelated in-situ conditions. Sørensen et al. (1979), for example, observed that denitrification rates were low at times of high temperature, but attributed this to low nitrate concentrations co-occurring with higher temperatures. Because the Büsum-II and Sylt-II cores generally have lower denitrification rates than the Büsum-I and Sylt-I cores, even at high nitrate levels in the  $^{15}\text{NO}_3^-$  experiments at in-situ temperatures above  $15^{\circ}\text{C}$ , we assume that other factors besides substrate availability and temperature may be rate-determining including organic matter content and quality or the permeability-dependent transport of nitrate to the active site of denitrification in the sediment.

#### 4.4.3 Influence of sedimentary TOC content and substrate quality

Maximum actual denitrification for the four study sites ranged between  $13$  and  $130\ \mu\text{mol N}_2\ \text{m}^{-2}\ \text{h}^{-1}$ . These rates were largely determined by nitrate availability and temperature. To assess the influence of sediment type, we grouped sediments Büsum-I and Sylt-I into one sediment facies (group I) with moderate TOC content (1.6 to 1.9%; Tab. 4.1), high bulk AA concentrations ( $7$  to  $15\ \text{mg g}^{-1}$ ; Tab. 4.1), and low oxygen penetration depths (Tab. 4.2). In contrast, the two sediment facies Büsum-II and Sylt-II have low TOC concentrations (0.1 to 0.6%), low bulk AA concentrations ( $< 1\ \text{mg g}^{-1}$ , Tab. 4.1), and higher oxygen penetration depths (Tab. 4.2). When nitrate limitation (excluded in  $^{15}\text{NO}_3^-$  amended cores) and temperature-related suppression of bacterial processes can be excluded as influences on denitrification rates in summer months (water temperatures above  $15^{\circ}\text{C}$ ; Tab. 4.2), we expected effects of sediment characteristics to emerge from the data. Indeed,  $\text{N}_2$  fluxes (m30) were highest during summer in group I sediments ( $104$  to  $176\ \mu\text{mol N}_2\ \text{m}^{-2}\ \text{h}^{-1}$ ). In

group II sediments,  $N_2$  fluxes ( $m30$ ) were also highest in summer, but significantly lower than in group-I sediments (29 to 69  $\mu\text{mol } N_2 \text{ m}^{-2} \text{ h}^{-1}$ ). There seems to be a trend of increasing denitrification rates with increasing TOC content in the group I sediments, although our data set cannot be statistically evaluated because it encompasses only four different sediment types and TOC concentrations. But the tentative trend is consistent with numerous previous studies, where denitrification rates correlated positively with the TOC content (Seitzinger, 1988; Sundbäck et al., 2000; Piña-Ochoa and Álvarez-Cobelas, 2006; Deutsch et al., 2010).

A characteristic of sediments high in TOC and high denitrification rates is a thin oxygen penetration layer. It reflects a high sedimentary oxygen demand (SOD), high microbial biomass and a high overall microbial activity. Consistent with higher SOD in group I sediments (Fig. 4.5a and 4.5b), the oxic zone in these cores is comparatively thin (Tab. 4.2). A thin oxic zone raises the denitrifying zone towards the sediment-water interface and implies a shorter diffusion path of nitrate, which increases the denitrification rate (Christensen et al., 1990), so that denitrification rates are inversely correlated with the oxygen penetration depth. We note that this relationship only holds for systems with high nitrate concentrations in overlying waters. In systems where nitrification in the sediments is the major source of nitrate for denitrification, a thick oxic layer may favour nitrification (Seitzinger, 1988) where organic matter as a substrate for ammonification is available. In our case, deep oxygen penetration in group II sediments is accompanied by low ammonium fluxes (Fig. 4.4) due to organic matter limitation, which in turn may limit nitrification.

In conclusion, denitrification rates are significantly higher in group I cores that have higher TOC content and AA concentrations, but the same supply of nitrate ( $^{15}\text{NO}_3^-$  amended cores) does not necessarily induce the same rate of denitrification. Consistent with assumptions made by Duff et al. (1984), we suggest that low TOC concentrations in Büsum-II and Sylt-II cores cause low denitrification rates, whereas high TOC amount and AA concentrations induce high denitrification rates in Büsum-I and Sylt-I.

#### 4.4.4 An estimate of annual denitrification in the north German Wadden Sea

Our ultimate goal was to quantify the role of sedimentary denitrification in the Wadden Sea, which is suspected to be a major sink for riverborne nitrate loads due to favourable boundary conditions of nitrate availability and sediment facies. Ours are the first systematic data, and although spatial and temporal resolution is admittedly rather low, we feel justified to use this data set for a first estimate of annual nitrate removal. When calculating annual denitrification

rates, our data suggest that the seasonality of  $\text{NO}_3^-$  concentrations and temperatures in the water body, and the sedimentary TOC content and quality must be considered. Of these, the dominant controlling factor in the sense of net removal from the water column is the nitrate concentration in the water column. In Fig. 4.7 we show nitrate concentrations in the northern German Wadden Sea for February 2009 and August 2009. The nitrate distribution in February 2009 is representative for the winter months (October – March) and the nitrate distribution in August 2009 represents respective concentrations for summer months (April – September). In winter, denitrification is obviously not nitrate limited, and denitrification is potentially active in the entire north German Wadden Sea area ( $2.100 \text{ km}^2$ ), whereas  $\frac{3}{4}$  of the area is nitrate limited in summer (Fig. 4.7). From these observations we assume that actual net-removal in summer is only effective in an area of about  $525 \text{ km}^2$ . Because denitrification rates also depend on permeability and the sedimentary TOC content, we have to consider the share of the individual sediment types. In the Wadden Sea, 65% of the sediments are sandy (proportion of grain size  $<63\mu\text{m}$  is less than 10%), 30% are fine sand (proportion of grain size  $<63\mu\text{m}$  is between 10 and 50%), and 5% are muddy (proportion of grain size  $<63\mu\text{m}$  is more than 50%) (Köster, 1998).

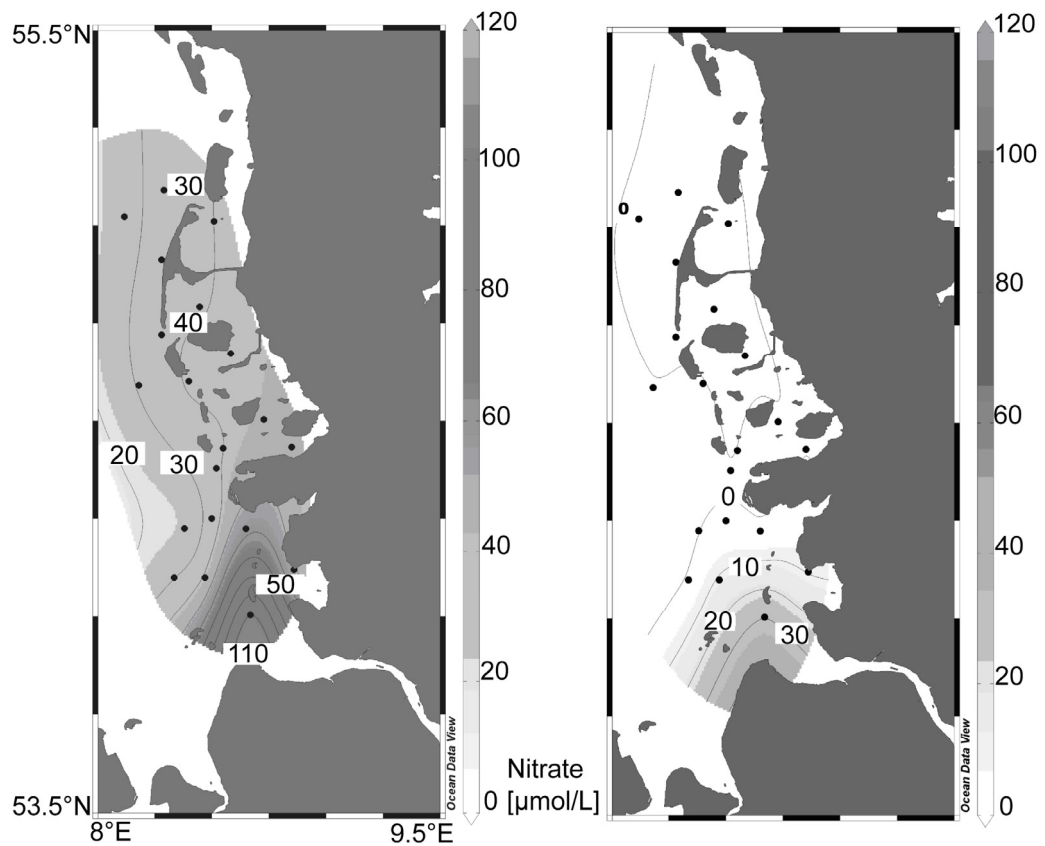


Fig. 4.7: Nitrate concentrations in the Wadden Sea area in February 2009 (left) and August 2009 (right).

Data from 21 sampling stations are from monitoring campaigns from the Landesamt für Landwirtschaft, Umwelt und ländliche Räume des Landes Schleswig-Holstein done with the RV Haithabu.

To relate the rates determined in the different sediment types studied to the gross Wadden Sea sediment composition, we assigned rates determined in group-II sediments (Büsum-II and Sylt-II) to the sandy sediment facies, and rates in the group-I sediments (Büsum-I and Sylt-I) to the fine sand facies; muddy sediments were neglected due to their limited extent. Initially, we consider the sediments detached from the actual location, so that we can estimate denitrification rates for a certain sediment group at a given season. In the present study, measured actual denitrification rates (m28) were highly dependent on location as nitrate availability is determined by the distance of the sampling site to the Elbe Estuary. By considering total denitrification rates (m28+m29+m30) from the  $^{15}\text{NO}_3^-$  amended cores, we are able to estimate denitrification rates uncoupled from nitrate limitation and location. To account for seasonal temperature variation, we separated summer (sampling campaigns in May, June and July) and winter (sampling campaigns in February, November and April) denitrification rates. From this, we calculated mean total denitrification rates (m28+m29+m30) of  $49 \mu\text{mol N}_2 \text{ m}^{-2} \text{ h}^{-1}$  (sand) and  $159 \mu\text{mol N}_2 \text{ m}^{-2} \text{ h}^{-1}$  (fine sand) in the summer, and  $25 \mu\text{mol N}_2 \text{ m}^{-2} \text{ h}^{-1}$  and  $97 \mu\text{mol N}_2 \text{ m}^{-2} \text{ h}^{-1}$ , respectively, in the winter seasons. We then assigned these mean seasonal denitrification rates to the effective area of nitrate availability in winter and summer and to the percentage of sediment types as described in Köster (1998), and obtained a nitrate removal rate of  $3.8 \text{ mmol N m}^{-2} \text{ d}^{-1}$  in the summer and of  $2.1 \text{ mmol N m}^{-2} \text{ d}^{-1}$  in the winter. Multiplied by the area ( $2.100 \text{ km}^2$  in winter and  $525 \text{ km}^2$  in summer) of nitrate availability, we calculated an annual denitrification rate of  $16 \text{ kt N y}^{-1}$  for the north German Wadden Sea area. Within this context, we have to keep in mind that  $\text{N}_2$  production is not only driven by denitrification of nitrate originating from the overlying water column, which is indeed a sink for externally supplied nitrate, but also by internal nitrification/denitrification which ultimately is an internal way of recycling deposited particulate nitrogen. Our quasi-IPT calculations suggest that around 35% (mean nitrification-denitrification rate for all sampling sites) of the total  $\text{N}_2$  efflux rate may be from nitrification-denitrification. Thus, the annual nitrate removal rate of the northern German Wadden Sea is around  $10 \text{ kt N y}^{-1}$  (annual denitrification rate of  $16 \text{ kt N y}^{-1}$  corrected for the proportion of nitrification-denitrification of around 35%) only, which comprises around 10–15% of the annual Elbe River nitrate load to the North Sea ( $82 \text{ kt N y}^{-1}$ ; Johannsen et al. 2008). But we only calculated loss in intertidal and shallow subtidal sediments of the northern sector: Considering that the entire North Sea Wadden Sea covers an area around  $8.000 \text{ km}^2$  (including the Wadden Sea south of the Elbe River and the Dutch and Danish Wadden Sea), our estimate covers only 25% of the total Wadden Sea area. And nitrate inputs from land may in addition be reduced by sedimentary denitrification in estuaries, and over an area of  $750.000 \text{ km}^2$  in the offshore North Sea that have not been evaluated in this study.

Our estimate of an annual nitrate removal rate is poorly constrained mainly because of the low number of sites examined. Furthermore, there is a source of potentially significant error in our approach and the data set, because the rates measured in the sandy sediment facies are likely to underestimate in-situ rates at the sea floor. It has been shown that permeable sediments are permanently flushed and that nitrate is continuously advected with pore water in high-energy environments (deBeer et al., 2005; Cook et al., 2006; Rao et al., 2007; 2008), which was not sufficiently imitated in the set-up of our flow-through incubations. According to Gihring et al. (2010), denitrification rates are up to ten times higher in percolated than in stirred set-ups. Recently, Gao et al. (2010) measured high potential denitrification rates ( $> 80 \mu\text{mol N}_2 \text{ m}^{-2} \text{ h}^{-1}$ ) in a percolation experiment with sediment cores from permeable sand in the southern German Wadden Sea area. Denitrification rates obtained in this study and the estimated annual nitrate loss are relatively high compared to other studies from the 1990's, which were mostly conducted in offshore sediments (van Raaphorst et al., 1990; Law and Owens, 1990; van Raaphorst et al., 1992; Lohse et al., 1993; Lohse et al., 1996). Comparable studies by Kieskamp et al. (1991) in intertidal Wadden Sea sediments estimated an average denitrification potential of  $0.3 \text{ mmol N m}^{-2} \text{ d}^{-1}$ . We attribute these relatively low rates to the acetylene-block-technique used at the time. Higher denitrification rates in Wadden Sea sediments were obtained with the isotope pairing technique (Jensen et al., 1996), who measured maximum rates of  $1.2 \text{ mmol N m}^{-2} \text{ d}^{-1}$  in spring. According to a mass-balance estimate by van Beusekom et al. (1999), the Wadden Sea was expected to remove nitrate at a (then considered excessive) rate of approximately  $1.6 \text{ mmol N m}^{-2} \text{ d}^{-1}$ . Our findings suggest even higher denitrification rates of  $2.1 - 3.8 \text{ mmol N m}^{-2} \text{ d}^{-1}$  estimated from sediment core incubations. This estimate may be still too low: No ex-situ incubation can perfectly imitate in-situ conditions, but the current stage of discussion implies that a percolation method is more adequate for reflecting actual rates in permeable sands (Gao et al., 2010). Therefore we feel that our estimate for the Wadden Sea probably underestimates the potential of sediments in the coastal ocean for nitrate removal and mitigation of river-induced eutrophication.

#### **4.5 Conclusions**

In this study we presented a first data set about seasonally varying denitrification rates in typical sediments of the German Wadden Sea. The results of our study suggest that major factors controlling denitrification rates in coastal sediments of the German Bights are the nitrate concentrations in the water body, the temperature influencing biological activity, and the organic matter content of the sediment type. Sedimentary denitrification is strongly controlled by the nitrate delivery of river Elbe and distance from that nitrate source. Whereas

denitrification in sediments at the island of Sylt are nitrate limited during summer months, denitrification proceeds during all season in the Meldorf Bight situated in the outer Elbe Estuary. Experiments with  $^{15}\text{NO}_3^-$  revealed that Wadden Sea sediments have a high potential to remove nitrate if it is abundant and available, thus providing an internal mechanism counteracting eutrophication by high river loads. In an extrapolation of seasonal mean denitrification rates classified into different sediment types, we arrive at weighted denitrification rates between 2.1 and 3.8  $\text{mmol N m}^{-2} \text{d}^{-1}$ , suggesting intense nitrate turnover in the entire Wadden Sea. Although further experiments in different sediment types and under varying conditions are required to exactly quantify nitrogen removal rates for the Greater North Sea area, it is clear that the near shore sedimentary nitrate sink accounts for a large share of the overall natural attenuation of man-induced eutrophication.

### **Acknowledgements**

We thank the GKSS Research Center, Institute for Coastal Research and the DFG (Em 37/29) for financial support. In particular, we thank W. S. Gardner and M. J. McCarthy (Marine Science Institute, University of Texas at Austin) for their helpful introduction to sediment incubation. We acknowledge N. Lahajnar and F. Langenberg (IfBM, University of Hamburg) for supervising work on the data set of sediment characteristics. We thank the FTZ Westküste, BÜsum and the AWI, List for providing laboratory space and our technician M. Ankele for assistance during field trips. A. Wieland is acknowledged for an introduction into oxygen profiling, corrections and helpful comments on an earlier draft.

## 5 Denitrification in sediments of the Elbe Estuary and adjacent coastal zones

Astrid Deek, Kay Emeis, Justus van Beusekom, Sven Meyer, Maren Voss  
in preparation

### Abstract

Denitrification rates in sediments in riparian zones along the nitrate gradient of the Elbe Estuary and in shallow areas in the adjacent coastal zone of the North Frisian Wadden Sea were determined during two sampling campaigns in March and September 2009. We quantified denitrification rates through *ex-situ* flow-through incubations of intact sediment cores and through  $N_2/Ar$  measurements in supernatant water with a modified Membrane Inlet Mass Spectrometry (MIMS) technique. We took sediment samples within the Elbe at four stations with high nitrate concentrations during both sampling campaigns ( $90\text{--}280 \mu\text{mol NO}_3^- \text{L}^{-1}$ ). Denitrification rates were constantly high in the sediments of the inner Elbe Estuary ( $10\text{--}78 \mu\text{mol N}_2 \text{m}^{-2} \text{h}^{-1}$ ) with similar rates in March and September. Nitrate availability was a limiting factor for denitrification in the sediments of the adjacent coastal zone in September 2009. In March, sedimentary oxygen demand (SOD) was generally lower (with a maximum SOD of  $750 \mu\text{mol O}_2 \text{m}^{-2} \text{h}^{-1}$ ) than in September (with a maximum of  $1450 \mu\text{mol O}_2 \text{m}^{-2} \text{h}^{-1}$ ). Significant positive correlations exist between denitrification rates and sedimentary oxygen demand (SOD) validating previous estimates of denitrification rates based on the SOD. Direct interrelations between putative controlling factors and denitrification rates were not pronounced at stations in the Elbe Estuary. Including coastal study sites with larger distance to the outer Elbe Estuary revealed that nitrate concentration in the overlying water body and sedimentary organic matter content were controlling factors for denitrification rates along the nitrate gradient directing northwards the North Frisian coast. Extrapolating average denitrification rates of  $2.9 \text{ mmol m}^{-2} \text{d}^{-1}$  for sediments in the Elbe River results in nitrate removal rates between 1.6 and 3.3 kt N during spring and summer months reducing the nitrate load of the Elbe River ( $79 \text{ kt y}^{-1}$ ) by around 5%.

## 5.1 Introduction

Sedimentary denitrification converts nitrate and nitrite to the gaseous products  $N_2O$  and  $N_2$ , which escape from the sediment to the overlying water or atmosphere by diffusion (Nixon et al., 1996) and are lost from the system. Together with the process of anaerobic ammonia oxidation, denitrification in sediments is the most important sink for nitrate on a global scale and a first order regulation mechanism for the nitrogen cycle of estuaries and adjacent coastal ecosystems (Seitzinger, 1988; Middelburg et al., 1996). Recent studies suggest that estuaries have partly lost their capacity to neutralise reactive nitrogen (rN) compounds due to the loss of intertidal flats and areas of low flow velocity as a result of continuous deepening of rivers to comply economic demands of container shipping (Jickells et al., 2000; Dähnke et al., 2008). This is at odds with assumptions that estuaries are sites of massive nitrogen turnover (Seitzinger et al., 2006).

The Elbe River is an example of a highly impacted river system transporting high rN loads to the adjacent coastal areas of the North Sea. The riverbed of the Elbe River has been continuously dredged to maintain the water route to Germany's largest port in Hamburg (Lozàn and Kausch 1996; Heise et al., 2005). It appears as if the Elbe River has become a mere channel flushing nitrate loads into the river mouth without significant turnover processes (Dähnke et al., 2008). Construction activities and the associated loss of sediment types effective in terms of denitrification compromise the natural ability of the Elbe River to counteract anthropogenic nitrate loads. The aim of this study was to re-evaluate the denitrification capacity in extant riparian zones of the Elbe Estuary and in impacted coastal areas receiving nitrate loads of the Elbe River plume. The role of sedimentary denitrification has previously been assessed by Schröder et al. (1996) who quantified denitrification processes in four typical shallow water areas in the Elbe Estuary during 1984 – 1991. In the present study, we sampled these four sites for a direct comparison with a previous data set. Additionally, we included stations in the outer Elbe Estuary and along the North Frisian Wadden Sea to estimate the extent of sedimentary denitrification activity in compensating the riverine nitrate load.

## 5.2 Materials and methods

### 5.2.1 Study site

The Elbe River is one of the main water routes of central Europe connecting the port of Hamburg with a highly industrialized hinterland. The Elbe is highly impacted by human activities; about 25 million inhabitants live in its catchment area (Lozàn and Kausch 1996). With an average fresh water discharge of  $731 \text{ m}^3 \text{ s}^{-1}$  and an annual nitrate load of 79 kt (ARGE, 2005), the Elbe River delivers high loads of reactive nitrogen (rN) into the North Sea. The nitrate delivery of the Elbe River plume varies with season. In summer, nitrate loads are constrained to the Meldorf Bight (Fig. 5.1), whereas in winter, nitrate loads of the Elbe River plume extend to the northern Wadden Sea as far as the Island of Sylt (van Beusekom et al., 2009).

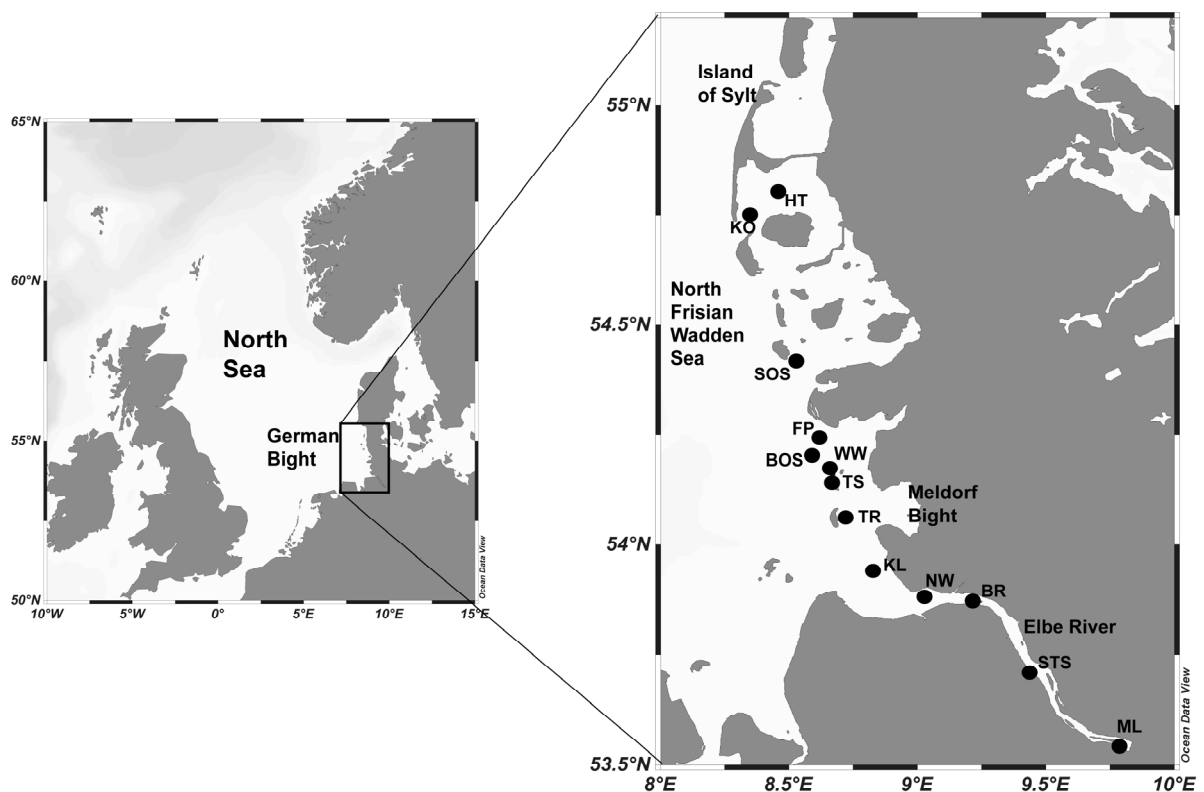


Fig. 5.1: Study site.

## 5.2.2 Sampling

Sampling campaigns were carried out with the RV Ludwig Prandtl in March and September 2009. In March 2009, 7 stations were sampled (ML-WW), and in September 2009, 12 stations (ML-HT) were occupied (Fig. 5.1). On board ship, water temperature, salinity and O<sub>2</sub> saturation were measured with a multiprobe (OTS 1500, ME Meerestechnik-Elektronik).

Surface sediment cores (around 20 cm length) were taken with polyvinylchloride (PVC) tubes (60 cm length and inner diameter of 10 cm) with a Multicorer (MUC). After sampling, water level overlying the sediment in the tubes was adjusted to 10 cm. During transport, sediment cores were cooled and transported (<6 hours) to the temperature-controlled laboratory. At least 100 L of site water was collected in 25 L carboys to ensure sufficient site water with appropriate salinity and nitrate concentrations for the flow-through incubation.

## 5.2.3 Sediment core incubation

### 5.2.3.1 Flow through incubation and direct flux measurement

After transferring the cores to a temperature controlled room or into a circulating water bath adjusted to the in-situ temperature, the supernatant water was aerated with aquarium pumps for 6 to 12 hours to reach oxygen saturation in the overlying water column before starting the incubation. The incubation set-up is illustrated in Fig. 5.2, and is a modified and larger version of the incubation set-ups described in Gardner et al. (1991), Lavrentyev et al. (2000) and McCarthy and Gardner (2003). The sediment cores were wrapped with aluminium foil to prevent variable light conditions, and were placed in a flow-through incubation system, consisting of the cores, a 25 L carboy of site water, a peristaltic pump and an outflow collection vessel. The site water reservoir was aerated constantly, because the ambient water at the study sites was always oxygen saturated during all sampling campaigns. The sediment cores were locked with a gas tight plunger with two O-rings and Tygon inflow and outflow tubes. The plunger was positioned to 5 cm above the sediment-water interface, which is equal to a water volume of 785 mL over the sediment, continuously replaced by site water at a rate of 1–2 mL min<sup>-1</sup>. Inflowing and outflowing water were sampled every 24 hours of incubation for 3 days. Three of the 6 subcores were incubated with site water enriched with 98% Na <sup>15</sup>NO<sub>3</sub><sup>-</sup> (Isotec) to a 40 to 50 μmol L<sup>-1</sup> <sup>15</sup>NO<sub>3</sub><sup>-</sup> concentration. N<sub>2</sub> fluxes (m28) from unamended cores were used to measure directly net N<sub>2</sub> production rates. N<sub>2</sub> fluxes (m29+m30) from <sup>15</sup>NO<sub>3</sub><sup>-</sup> amended cores were used a) to estimate N<sub>2</sub> fluxes under conditions when actual NO<sub>3</sub><sup>-</sup> limitation is eliminated through artificial <sup>15</sup>NO<sub>3</sub><sup>-</sup> addition b) to estimate

denitrification rates and the proportion of nitrification-denitrification and  $N_2$  fixation applying calculations according the isotope pairing technique (Nielsen, 1992) and An et al. (2001).

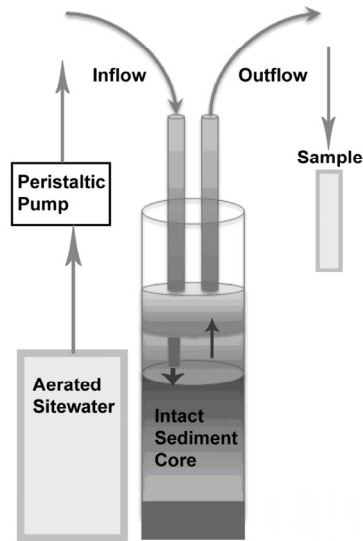


Fig. 5.2: Flow-through incubation set-up.

#### 5.2.3.2 Sub core incubation and isotope pairing technique

Additionally to the flow through incubation technique, sedimentary denitrification was determined using the classical isotope pairing technique (Nielsen, 1992; Risgaard-Petersen et al., 2003) at seven stations in September 2009. Three sub cores (25 cm length, 3.6 cm diameter) were taken from the MUC cores. The isotope pairing experiments were performed as concentration series;  $K^{15}NO_3^-$  solution was added to the cores at a final concentration of 25, 50, 100 and 150  $\mu\text{mol L}^{-1}$ , respectively. The cores were then capped with stirring devices, and incubated in the dark at in-situ temperature for maximum 24 h. After the incubation, the sediment of each core was homogenized. Triplicate samples of the sediment slurry were stored preserved with 100  $\mu\text{L ZnCl}_2$  in 15mL glass vials and measured within 24 hours with the MIMS technique described in the next section.

## 5.2.4 Laboratory analyses

### 5.2.4.1 N<sub>2</sub> and O<sub>2</sub> concentrations with MIMS

During flow-through incubation, triplicate samples from the inflow water and outflow water were taken every 24 hours with cylindrical glass vials and were analyzed immediately after collection for N<sub>2</sub> and O<sub>2</sub>. From the sub core incubation, triplicate samples were measured within 24 hours.

The concentrations of N<sub>2</sub> and O<sub>2</sub> were calculated from N<sub>2</sub>/Ar and O<sub>2</sub>/Ar ratios measured with a membrane inlet mass spectrometry (MIMS) system consisting of a Quadrupole mass spectrometer (QMS) (GAM 200, InProcess Instruments) with a modified membrane inlet from Bay Instruments. The MIMS was standardized with air saturated temperature-salinity-standards according to Kana et al. (1994) to correct measured N<sub>2</sub>/Ar and O<sub>2</sub>/Ar ratios to actual ratios. Concentrations were calculated by multiplying the actual Ar concentration from solubility tables (Weiss, 1970) with the corrected ratio. The QMS ion source produces O<sup>+</sup> ions by ionizing sample gas; O<sup>+</sup> ions may react with N<sub>2</sub> forming NO<sub>x</sub> (Eyre et al., 2002). This so called NO<sub>x</sub>-effect results in higher signals on mass 28 (m28) at low oxygen concentrations and low m28 signals at high oxygen concentrations, which may lead to a misinterpretation of actual denitrification. The NO<sub>x</sub>-effect was tested for the MIMS system used and the extent of this effect was found to be below the standard deviation of the method (0.1%) (J. Pohlmann, pers. comm. 2010).

From the flow-through incubation, net N<sub>2</sub> and O<sub>2</sub> fluxes (fl; in μmol m<sup>-2</sup> h<sup>-1</sup>) were calculated by subtracting inflow concentration (C<sub>i</sub>) from outflow concentration (C<sub>o</sub>) multiplied with the flow rate (f: Lh<sup>-1</sup>) and sediment surface area (a: m<sup>2</sup>) ratio:

$$fl = (C_o - C_i) \times f/a \quad [5.1]$$

Samples were measured simultaneously on the mass signals m28, m29 and m30, because samples from <sup>15</sup>NO<sub>3</sub><sup>-</sup> incubations were expected to produce <sup>29</sup>N<sub>2</sub> and <sup>30</sup>N<sub>2</sub>. For the sub core incubations, denitrification rates were calculated according Nielsen (1992).

### 5.2.4.2 Nutrient concentrations

During flow-through incubation, inflow and outflow samples were collected daily for nutrient analyses. Nutrient samples were filtered using a 0.2 μm syringe filter (X50 Analytore, PVDF), stored frozen in 50 mL Falcon tubes until analyses. NO<sub>3</sub><sup>-</sup>, NO<sub>2</sub><sup>-</sup> and NH<sub>4</sub><sup>+</sup> concentrations were analyzed by automated continuous flow analysis using a Bran &

Luebbe, Auto Analyzer 3.  $\text{NO}_3^-$  and  $\text{NO}_2^-$  were determined according a modified method of Armstrong et al. (1967).  $\text{NH}_4^+$  concentrations were determined according a modified method of Grasshoff et al. (1983). Nutrient fluxes were calculated according to Eq. 5.1.

#### 5.2.4.3 Sediment characteristics

Before incubation, oxygen penetration depths were determined for one sediment core from each sampling station. Two different types of oxygen profiling setups were used during this study: A Clark-type  $\text{O}_2$  micro electrode (OX 50 and OX 100) in connection with a Picoamperemeter (Unisense A/S), and an Oxygen micro-optode device (Oxy 50M, Pyroscience) in connection with a Microx TX3-USB (Pyroscience).

Sediment characteristics were also determined at each sampling site. The sediment cores were sliced into 1 cm slices and frozen for transport. Water content and porosity was calculated from the weight before and after freeze drying and assuming a grain density of  $2.65 \text{ g cm}^{-3}$ . Grain size distribution was then determined on dry residues by sieving through mesh sizes of 1000  $\mu\text{m}$ , 500  $\mu\text{m}$ , 250  $\mu\text{m}$ , 125  $\mu\text{m}$  and 63  $\mu\text{m}$ .

To assess organic matter concentrations and reactivity, the weight percentage of total nitrogen (TN), organic carbon ( $C_{\text{org}}$ ) and amino acid concentrations (AA) were determined on the dried and ground residues of 1cm-slices of one core from each sampling site. TN and  $C_{\text{org}}$  concentrations were determined with an Elemental Analyzer (Thermo Flash EA) calibrated against acetanilide.

### 5.3 Results

#### 5.3.1 Sediment characteristics

Properties of sediments at each of the sample locations are listed in Tab. 5.1. The locations are shown in Fig. 5.1.

#### 5.3.2 Seasonal variation of the site parameters

The site parameters of the respective sampling locations are given in Tab. 5.2. In general, dissolved nutrient concentrations in site water are higher in March than in September. During March, maximum nitrate concentrations of  $263 \mu\text{mol L}^{-1}$  were measured at ML (upper estuary) with decreasing concentration to  $58 \mu\text{mol L}^{-1}$  at station WW in the outer Elbe

Estuary. In September nitrate concentration at ML was around  $87 \mu\text{mol L}^{-1}$ , decreasing to concentrations between 2 and  $8 \mu\text{mol L}^{-1}$  in the outer Elbe Estuary (TR, TS).

Tab. 5.1: Sediment characteristics of the sampling stations.

Date [mm/dd/yy]	Station	Longitude [°E]	Latitude [°N]	Porosity (v/v)	C [%]	N [%]	C <sub>org</sub> [%]	Oxygen penetration depth [mm]	AA [mg/g]	Median grain size [ $\mu\text{m}$ ]	Sediment classification
03/23/09	ML	9.79	53.54	0.8	3.7	0.2	2.4	2.9	9.05	<63	silt
03/24/09	STS	9.44	53.71	0.7	1.3	0.1	0.7	>35	0.3	63	very fine sand
03/25/09	BR	9.22	53.87	0.6	2.5	0.1	1.5	3.2	2.6	63	very fine sand
03/26/09	NW	9.03	53.88	0.5	0.9	0.02	0.3	3.7	0.54	63	very fine sand
04/01/09	KL	8.94	55.27	0.5	1.1	0.1	0.6	3.6	0.42	63	very fine sand
03/30/09	TS	8.67	54.16	0.4	0.2	bdl	0.1	6.5	-	125	fine sand
03/29/09	WW	8.71	54.06	0.4	0.2	bdl	0.06	4.2	0.2	125	fine sand
09/08/09	ML*	9.80	53.55	0.9	4.4	0.4	3.4	1.9	9.0	<63	silt
09/09/09	STS*	9.43	53.73	0.7	1.3	0.1	0.7	4.2	0.25	63	very fine sand
09/10/09	BR*	9.22	53.87	0.4	0.5	bdl	0.1	3.6	0.51	63	very fine sand
09/11/09	NW*	9.04	53.88	0.7	2.3	0.1	1.4	1.3	4.55	63	very fine sand
09/12/09	KL*	8.70	53.97	0.5	0.7	0.03	0.3	2.9	1.15	63	very fine sand
09/13/09	TR	8.71	54.06	0.5	0.5	0.02	0.2	3.5	2.75	125	fine sand
09/14/09	TS*	8.67	54.17	0.5	0.5	0.03	0.1	2.1	0.97	63	very fine sand
09/15/09	BOS	8.59	54.20	0.4	0.4	0.03	0.2	2.3	0.77	125	fine sand
09/16/09	FP	8.62	54.24	0.4	0.2	0.02	bdl	3.2	0.14	125	fine sand
09/17/09	SOS	8.52	54.42	0.4	0.2	bdl	bdl	-	0.14	125	fine sand
09/18/09	KO	8.35	54.75	0.4	0.1	bdl	bdl	2.4	-	125	fine sand
09/18/09	HT	8.46	54.80	0.4	0.1	bdl	bdl	-	-	125	fine sand

Tab. 5.2: Site characteristics of the sampling stations.

Date [mm/dd/yy]	Station	Watercolumn										Suspended Matter				
		T [°C]	Sal	pH	PO <sub>4</sub> <sup>-</sup> [µmol/L]	Si [µmol/L]	NH <sub>4</sub> <sup>+</sup> [µmol/L]	NO <sub>3</sub> <sup>-</sup> [µmol/L]	NO <sub>2</sub> <sup>-</sup> [µmol/L]	C [%]	N [%]	C <sub>org</sub> [%]				
03/23/09	ML	6.7	0.3	8.3	2.9	120.5	8.7	263	1.6	7.9	0.7	6.6				
03/24/09	STS	6.6	0.4	8.2	2.6	122.7	5.7	278	2.0	8.1	0.6	6.6				
03/25/09	BR	4.8	0.5	8.4	2.6	107.5	3.7	284	3.0	7.0	0.5	5.9				
03/26/09	NW	6.3	0.6	8.2	3.0	145.2	3.3	285	2.6	6.5	0.5	5.7				
04/01/09	KL	6.5	10.2	8.3	3.6	84.4	4.0	194	2.6	4.5	0.3	3.5				
03/30/09	TS	5.8	21.8	8.4	2.9	32.4	4.9	89	1.9	3.2	0.2	2.0				
03/29/09	WW	5.8	22.9	8.4	2.0	34.0	5.8	58	1.3	2.5	0.2	1.8				
09/08/09	ML*	18.2	0.4	7.5	1.2	25.5	8.4	86.8	3.1	8.3	0.8	8.1				
09/09/09	STS*	18.9	0.8	7.8	2.8	13.1	0.4	99.9	bdl	5.7	0.5	9.4				
09/10/09	BR*	18.1	5.2	7.9	4.4	33.7	1.2	96.6	0.4	4.4	0.3	11.5				
09/11/09	NW*	18.0	8.0	8.0	4.5	34.7	1.5	88.1	0.5	7.3	0.6	10.4				
09/12/09	KL*	16.7	22.9	8.2	3.0	11.1	2.1	30.1	0.6	3.0	0.3	10.1				
09/13/09	TR	16.1	28.2	8.2	2.0	4.0	4.0	7.9	0.7	3.3	0.3	8.1				
09/14/09	TS*	16.3	28.9	8.3	1.3	1.4	2.0	2.2	bdl	2.6	0.3	8.5				
09/15/09	BOS	16.1	29.4	8.3	1.2	1.0	1.7	bdl	bdl	1.8	0.2	9.0				
09/16/09	FP	16.0	30.2	8.3	0.7	0.8	1.2	bdl	bdl	2.3	0.2	9.3				
09/17/09	SOS	15.7	30.0	8.2	0.7	1.1	1.3	bdl	bdl	2.6	0.3	9.0				
09/18/09	KO	15.9	31.0	8.3	0.4	0.9	1.2	bdl	bdl	2.5	0.3	8.5				
09/18/09	HT	16.1	31.0	8.3	0.6	0.9	1.1	bdl	bdl	2.4	0.2	9.2				

### 5.3.3 Nutrient fluxes

Nutrient fluxes across the sediment-water interface of incubated cores (mean value of three cores) on day 3 of incubation are illustrated in Fig. 5.3. Nitrate fluxes are directed into the sediment during both sampling campaigns. Highest nitrate fluxes of  $-187 \pm 46 \mu\text{mol m}^{-2} \text{h}^{-1}$  (negative signs denoting flux into the sediment) were measured in ML in September 2009 and are similar to nitrate fluxes in March ( $-182 \pm 23 \mu\text{mol m}^{-2} \text{h}^{-1}$ ). Nitrate fluxes were not detected for BOS and stations further northwards. Ammonium fluxes were directed out of the sediment during September (up to  $343 \pm 10 \mu\text{mol m}^{-2} \text{h}^{-1}$ ), whereas ammonium fluxes were directed into the sediment during March (up to  $-97 \pm 15 \mu\text{mol m}^{-2} \text{h}^{-1}$ ).

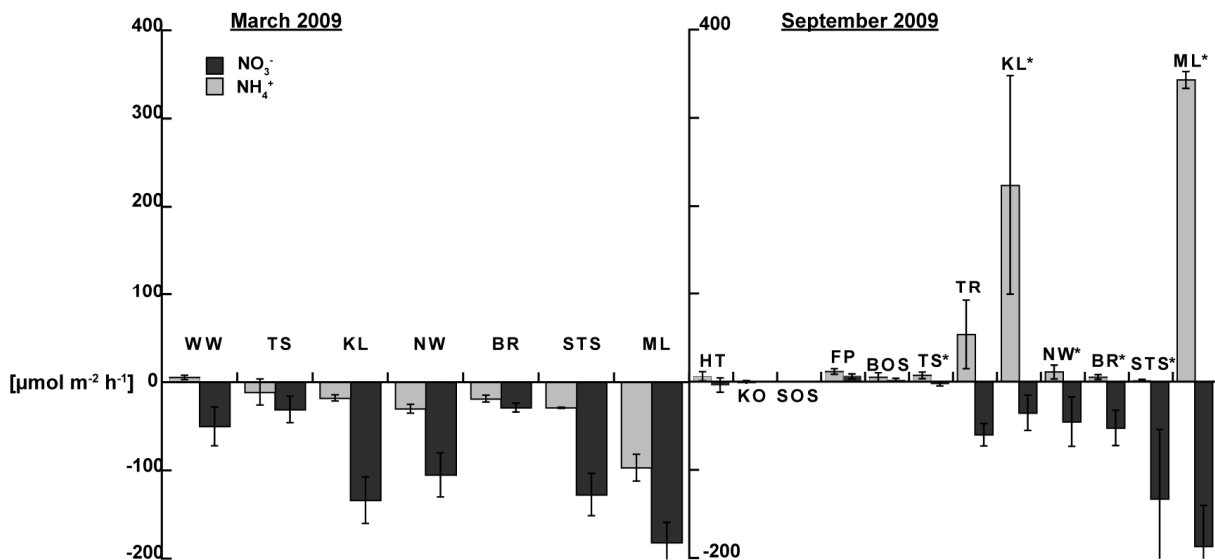


Fig. 5.3: Ammonium and nitrate fluxes during flow-through incubation of unamended sediment cores.

### 5.3.4 N<sub>2</sub> and O<sub>2</sub> fluxes during flow-through incubation

N<sub>2</sub> and O<sub>2</sub> fluxes (mean value of three cores) are illustrated in Fig. 5.4; again fluxes refer to day 3 of incubation. Fig. 5.4 compares N<sub>2</sub> fluxes (m28) from unamended cores with N<sub>2</sub> fluxes (m29 + m30) from <sup>15</sup>NO<sub>3</sub><sup>-</sup> amended cores where <sup>15</sup>NO<sub>3</sub><sup>-</sup> is combined with ambient <sup>14</sup>NO<sub>3</sub><sup>-</sup>. The sedimentary oxygen demand (SOD) was generally higher in September (e.g. ML:  $1940 \pm 398 \mu\text{mol O}_2 \text{m}^{-2} \text{h}^{-1}$ ) than in March (e.g. ML:  $1080 \pm 72 \mu\text{mol O}_2 \text{m}^{-2} \text{h}^{-1}$ ). In September, SOD decreased towards the sea in parallel with the C<sub>org</sub> content of the sediment (Tab.

5.1). Variations of  $N_2$  (m28) production rates were relatively small at the four stations within the Elbe Estuary, with similar rates in March and September. At TS in the Meldorf Bight,  $N_2$  (m28) production was higher in March than in September (Fig. 5.4) corresponding to a steep nitrate decrease at TR/TS in September (Tab. 5.2).  $N_2$  (m28) production was not detected in FP and further northwards, whereas  $N_2$  production rates on m30 was detected at relatively low levels with maximum rates of  $3 \mu\text{mol } N_2 \text{ m}^{-2} \text{ h}^{-1}$  (Fig. 5.4).

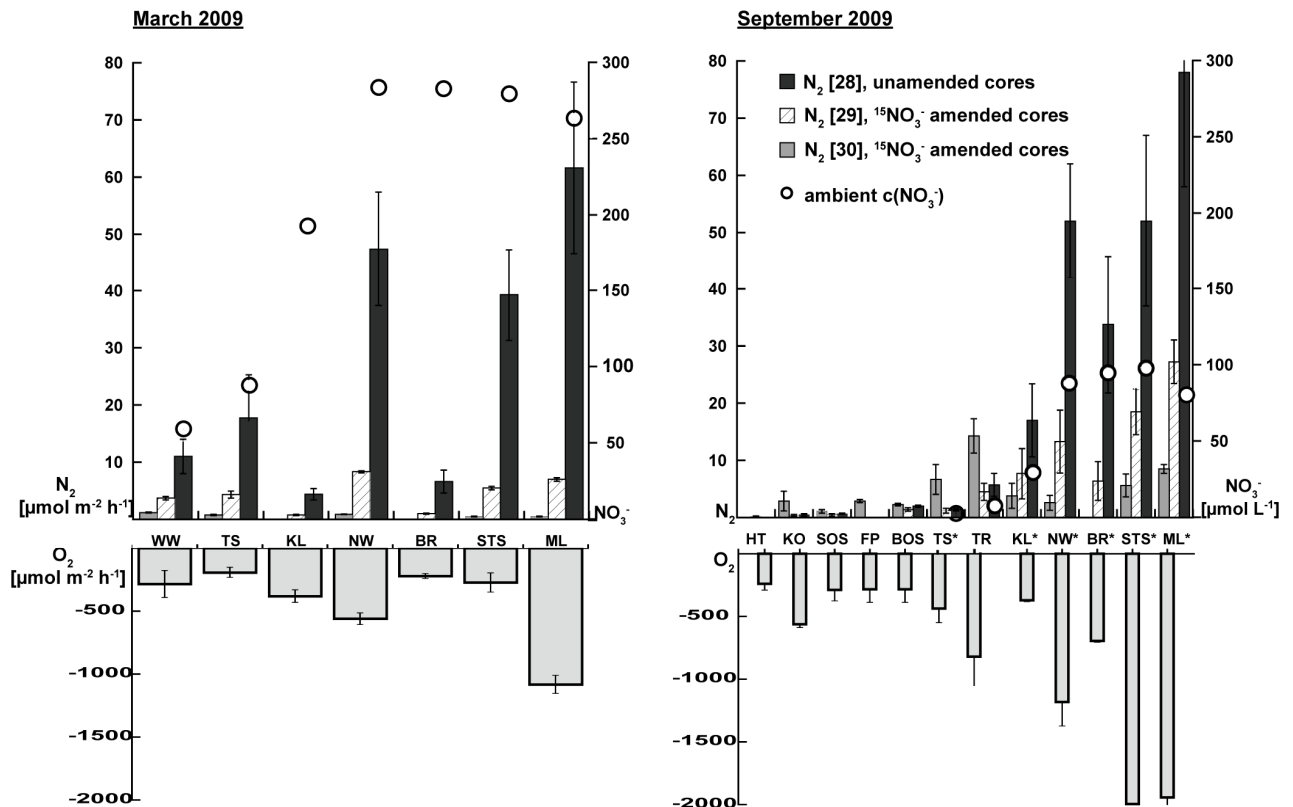


Fig. 5.4:  $N_2$  and  $\text{O}_2$  fluxes during flow-through incubation of unamended sediment cores (m28) and  $^{15}\text{NO}_3^-$  amended sediment cores (m29+m30).

$\text{O}_2$  flux is the mean flux of unamended and  $^{15}\text{NO}_3^-$  amended sediment cores.

## 5.3.4 Denitrification rates obtained by sub core incubation and IPT

To verify the results obtained by flow-through incubation and direct  $N_2$  (m28) measurement, we sampled seven stations in September 2009 additionally for the determination of denitrification rates applying the isotope pairing technique in sub core incubations (Nielsen, 1992; Risgaard-Petersen et al., 2003). The comparison of both methods is illustrated in Fig. 5.5. The difference between both data sets is within the standard deviation for the respective mean denitrification rates, except for KL which was slightly higher determined with the flow-through incubation technique. These data support that under the given conditions both methods yield comparable results.

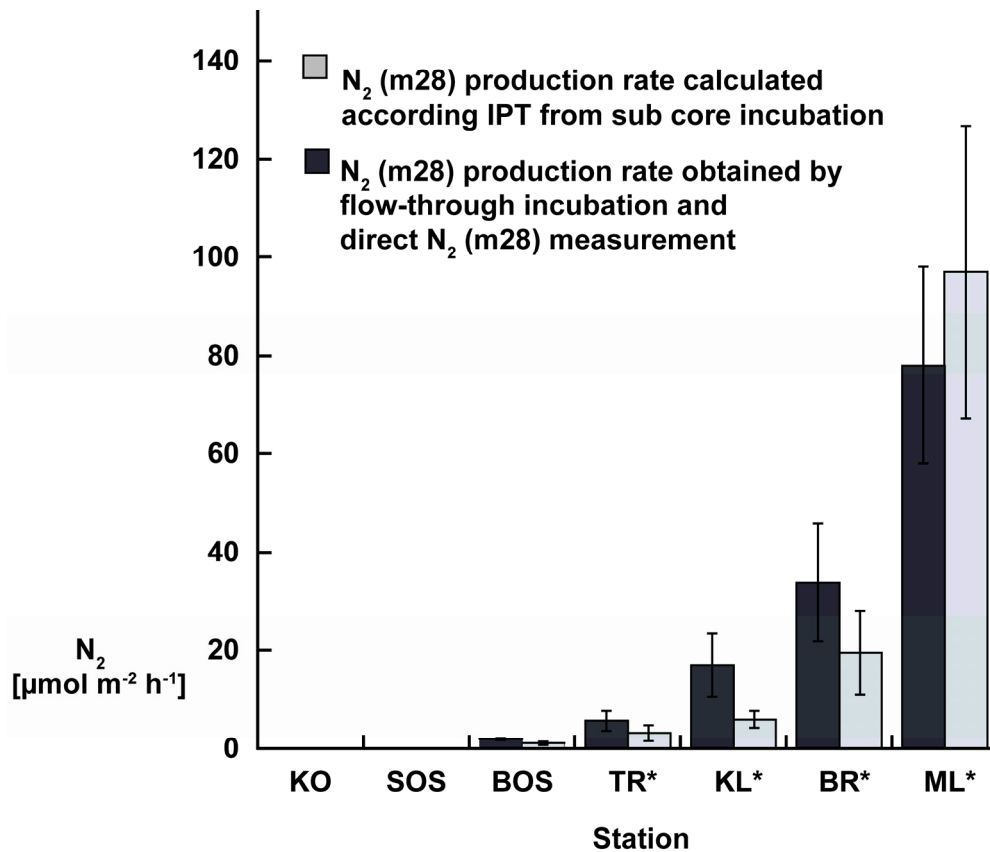


Fig. 5.5: Comparison of  $N_2$  production (m28) calculated according IPT from  $N_2$  fluxes (m29+m30) in sub core incubations and  $N_2$  production (m28) obtained by flow-through incubation and direct  $N_2$  (m28) measurement.

## 5.4 Discussion

In our study we evaluate denitrification rates in riparian zones of the Elbe Estuary and adjacent coastal zone exposed to the nitrate load of the Elbe River plume. Further, the experimental data are also suited to differentiate between different N conversions in the sediment. This is because the actual N<sub>2</sub> fluxes (m28) measured in unamended sediment cores quantify net N<sub>2</sub> production rates; whereas the mass distribution of N<sub>2</sub> produced in <sup>15</sup>NO<sub>3</sub><sup>-</sup> amended cores permit calculations according IPT. Together with observed nutrient fluxes, the data give insight into individual processes of the nitrogen-cycle. In the first part of our discussion, we estimate the proportion of alternative pathways that contribute to the net N<sub>2</sub> flux. Further, we focus our discussion on factors interrelating with sedimentary denitrification such as nitrate concentration, the organic matter availability, and sedimentary oxygen demand (SOD). Finally, we estimate annual nitrate removal rates in the shallow water zones in the tidal Elbe Estuary and adjacent coastal zone, and their capacity to counteract the N-load of the Elbe River plume.

### 5.4.1 Pathways of N<sub>2</sub> production and N<sub>2</sub> consumption

The comparison between N<sub>2</sub> production rates (m28) from direct N<sub>2</sub> (m28) measurements and N<sub>2</sub> fluxes (m28) obtained by IPT from sub core incubation (Fig. 5.5) illustrates that two different methods yield comparable results. Besides methodical comparison, the simultaneous measurement of actual N<sub>2</sub> (m28) and nutrient fluxes, together with N<sub>2</sub> fluxes from <sup>15</sup>NO<sub>3</sub><sup>-</sup> amended cores (m29+m30) during flow-through incubation and from sub core incubation allows us to estimate the amount of coupled nitrification-denitrification in the sediment, and the amount of N<sub>2</sub> fixation.

According to An et al. (2001), N<sub>2</sub> production rates (m28) estimated from IPT match actual N<sub>2</sub> fluxes (m28) when no N<sub>2</sub> fixation occurs. Because we conducted two different experiments with <sup>15</sup>NO<sub>3</sub><sup>-</sup> addition, we applied IPT calculations on: a) the N<sub>2</sub> fluxes from <sup>15</sup>NO<sub>3</sub><sup>-</sup> amended cores during flow-through incubation conducted in March and September 2009 (m29+m30, Fig. 5.4), and on b) the N<sub>2</sub> production from <sup>15</sup>NO<sub>3</sub><sup>-</sup> amended cores (m29+m30, not shown) during sub core incubation of seven stations in September 2009. The calculation of N<sub>2</sub> production rates (m28) according Nielsen (1992) from both <sup>15</sup>NO<sub>3</sub><sup>-</sup> amended cores during flow-through incubation (m28, not shown) and from <sup>15</sup>NO<sub>3</sub><sup>-</sup> amended cores during sub core incubation (m28, Fig. 5.5) results in m28 fluxes comparable with actual N<sub>2</sub> fluxes (m28). Thus, we applied equations derived by An et al. (2001) to calculate the amount of N<sub>2</sub> fixation, and obtained negative solutions which denote zero N<sub>2</sub> fixation rates. N<sub>2</sub> fixation thus plays no

or only a minor role in sediments under study. In consequence, the net  $N_2$  flux (m28) measured in the unamended cores is a good approximation of the gross  $N_2$  production, because  $N_2$  consumption can be neglected.

As previously demonstrated (Thamdrup and Dalsgaard 2002; Trimmer and Nicholls 2009), denitrification is not the only pathway for rN removal from estuaries: Anammox which couples the reduction of  $NO_2^-$  to the oxidation of  $NH_4^+$  produces  $N_2$  gas as well. But due to the experimental set-up within this study we did not differentiate between anammox and denitrification driven  $N_2$  production. In the following, we thus defined the gross denitrification rate as the net  $N_2$  flux (m28) that includes an unknown proportion of anammox.

But by applying the IPT equations on the  $N_2$  fluxes from  $^{15}NO_3^-$  amended cores during flow-through incubation (m29+m30, Fig. 5.4) and on the  $N_2$  production from  $^{15}NO_3^-$  amended cores (m29+m30, not shown) during sub core incubation, we can calculate the contribution of coupled nitrification-denitrification to the total  $N_2$  production (Nielsen 1992). The calculations from the flow-through incubations suggest that denitrification in sediments of the inner Elbe (ML–KL) is mainly fuelled by nitrate from the overlying water column. At stations ML–KL (Fig. 5.1) between 5% and 30% of the overall  $N_2$  flux (m28) is driven by nitrification-denitrification; a seasonal pattern was not pronounced. The proportion of nitrification-denitrification increases with distance to the Elbe river plume: in TS, WW and BOS sediments, the proportion of nitrification-denitrification contributing to the  $N_2$  flux (m28) is between 25% and 90%. It is reasonable that indirect denitrification (nitrification-denitrification) becomes a relatively more important component of total denitrification with distance to the Elbe Estuary due to the lower nitrate concentration in the overlying water column (Tab. 5.2).

Considering the rN fluxes in Fig. 5.3, we observed significant ammonium fluxes at station KL and TR with highest ammonium efflux at station ML ( $340 \mu\text{mol m}^{-2} \text{h}^{-1}$ ) in September 2009. Ammonium fluxes to the oxic zone of the sediment and to oxic supernatant water may fuel nitrification within the sediment or in the overlying water column. According Sweerts et al. (1991) around 30% of ammonium efflux is assumed to be re-oxidized within the sediment. From the high ammonium fluxes at ML (Fig. 5.4), we assume that a relatively high proportion of ammonium may have been already recycled to nitrate within the sediment (around  $100 \mu\text{mol m}^{-2} \text{h}^{-1}$ ). However, we did not register a net flux of nitrate out of the sediment at any stations including ML, which we take as an indication that nitrification does not produce more nitrate than is being reduced again. On the other hand, it is obvious that ammonium fluxes of  $340 \mu\text{mol m}^{-2} \text{h}^{-1}$  exceed the net nitrate consumption rate ( $-187 \mu\text{mol m}^{-2} \text{h}^{-1}$ ) at ML. Hence, in summer, ML sediments are not a net sink but a source of rN even though denitrification rates were the highest measured within this study ( $78 \mu\text{mol } N_2 \text{ m}^{-2} \text{h}^{-1}$ ).

#### 5.4.2 Factors driving denitrification in the Elbe Estuary

In general, low temperatures are assumed to suppress most microbial processes (Koch et al., 1992). Thus, we assumed at first that denitrification rates would be higher in September (16–18°C, Tab. 5.2) than in March (around 6°C, Tab. 5.2). However, a consistent seasonal pattern of higher  $N_2$  fluxes (m28) with increasing temperature was not observed: at stations ML, STS and NW,  $N_2$  fluxes (m28) did not vary significantly (Fig. 5.4), at BR and KL,  $N_2$  fluxes (m28) were two to three times higher in September than in March, whereas at TS,  $N_2$  fluxes (m28) were even higher in March than September (Fig. 5.4).

Beginning with this observation, we suggest other driving factors for denitrification such as the  $C_{org}$  content of the sediments and the nitrate concentration in the overlying water column that have been observed in previous studies (Seitzinger and Nixon, 1985; Seitzinger, 1988; van Luijn et al., 1999, Deutsch, 2010). Thus, we set up a multiple regression matrix separately for the March and September data (Tab. 5.3).

For the data set raised in March (stations: ML–WW), there was no indication for a consistent factor that controls denitrification rates; significant correlations between denitrification rates and sediment characteristics or water column properties were not obtained for this sampling campaign (Tab. 5.3).

However, multiple regression analyses conducted for September data (stations: ML–HT; including coastal stations spanning a more extended gradient in sediment types and nitrate availability) demonstrates that  $N_2$  production rates are strongly related to the  $C_{org}$  content ( $R^2=0.83$ ;  $N=12$ ;  $p<0.01$ ) and water column nitrate concentration ( $R^2=0.92$ ;  $N=12$ ;  $p<0.01$ ). This is in accordance with the highest  $N_2$  fluxes (m28) observed in sediments (ML–NW) within the Elbe Estuary (7–78  $\mu\text{mol } N_2 \text{ m}^{-2} \text{ h}^{-1}$ ); receiving highest nitrate loads (Tab. 5.2) and having medium to high  $C_{org}$  content (Tab. 5.1).

Tab. 5.3: Correlation matrix including  $N_2$  fluxes, sedimentary characteristics and  $NO_3^-$  availability for the sampling campaigns in March 2009 and September 2009 (\*\*correlation is significant ( $p < 0.01$ ), \*correlation is significant ( $p < 0.05$ )).

c (AA) (sediment)	Porosity (sediment)	$C_{org}$ (sediment)	$C_{org}$ (suspension)	c ( $NO_3^-$ ) (water column)	$NO_3^-$ flux	SOD	$N_2$ (30) production	$N_2$ (28) production	March 2009 (N=7)
-0.264	0.351	-0.122	0.351	0.252	0.195	-0.271	-0.031	0.214	Oxygen penetration depth (sediment)
	0.761*	0.525	0.525	0.383	0.561	0.867*	-0.216	0.596	c (AA) (sediment)
		0.690	0.876*	0.742	0.699	0.641	-0.431	0.656	Porosity (sediment)
			0.690	0.588	0.513	0.703	-0.503	0.455	$C_{org}$ (sediment)
				0.959*	0.556	0.489	-0.415	0.645	$C_{org}$ (suspension)
					0.486	0.383	-0.530	0.505	c ( $NO_3^-$ ) (water column)
						0.782*	-0.256	-0.681	$NO_3^-$ flux
							-0.015	0.784*	SOD
								0.236	$N_2$ (30) production

c (AA) (sediment)	Porosity (sediment)	$C_{org}$ (sediment)	$C_{org}$ (suspension)	c ( $NO_3^-$ ) (water column)	$NO_3^-$ flux	SOD	$N_2$ (30) production	$N_2$ (28) production	September 2009 (N=12)
-0.452	-0.684	-0.486	-0.264	0.105	0.151	0.076	0.116	-0.134	Oxygen penetration depth (sediment)
	0.519	0.311	0.424	0.298	0.322	0.234	0.365	0.323	c (AA) (sediment)
		0.913**	0.702*	0.370	0.650*	0.467	0.369	0.646*	Porosity (sediment)
			0.843**	0.561	0.758**	0.712**	0.328	0.834**	$C_{org}$ (sediment)
				0.868**	0.809**	0.880**	0.177	0.972**	$C_{org}$ (suspension)
					0.709**	0.804**	0.013	0.916**	c ( $NO_3^-$ ) (water column)
						0.777**	-0.354	0.851**	$NO_3^-$ flux
							0.417	0.901**	SOD
								0.184	$N_2$ (30) production

That nitrate is indeed a major controlling factor for denitrification in sediments under study is seen when comparing  $N_2$  fluxes in unamended cores and  $^{15}NO_3^-$  amended cores in September 2009 (Fig. 5.4): Beginning at station TR, where ambient  $^{14}NO_3^-$  decreases to  $8 \mu\text{mol L}^{-1}$  (Tab. 5.2), the  $N_2$  production on m30 in  $^{15}NO_3^-$  amended cores was higher than on m28 in unamended cores; an indication that coastal sediments are potentially active when  $NO_3^-$  substrate is available. Nitrate availability thus limits actual denitrification during summer

months in coastal areas of the northern Wadden Sea which has been previously shown elsewhere. Deek et al. (2010) and Sørensen et al. (1979) observed that denitrification rates were low at times of high temperature in marine coastal sediments, and attributed this to low nitrate concentrations co-occurring with higher temperatures.

Interestingly, within the nitrate limited coastal sampling sites (TR–HT) in September 2009, the addition of relatively high  $^{15}\text{NO}_3^-$  concentration (40–50  $\mu\text{mol L}^{-1}$ ) did not necessarily result in high  $\text{N}_2$  fluxes (m29+m30). This is in accordance with the comparatively low  $C_{\text{org}}$  content of the respective sediment types.  $C_{\text{org}}$  was around 0.1–0.2% in TR, TS and BOS, and even below detection limit at FP and further northwards.

In conclusion, we note that actual  $\text{N}_2$  production rates are higher in sediments of the inner Elbe Estuary than in sediments of the adjacent coastal zone. High denitrification rates in Elbe Estuary sediments are fuelled by high ambient nitrate concentrations and higher  $C_{\text{org}}$  content compared to sediments in the coastal area.

#### 5.4.3 Estimating denitrification rates based on SOD

Another interesting aspect found by the multiple regression analyses of both March and September data is a linear relationship with a strong positive correlation between denitrification and sedimentary oxygen demand (SOD) (in March:  $R^2=0.78$ ;  $N=7$ ;  $p<0.05$  and in September:  $R^2=0.9$ ;  $N=12$ ;  $p<0.001$ ; Tab. 5.3). This relationship has been previously observed (Seitzinger, 1990) and applied by Seitzinger and Giblin (1996). In Fig. 5.6 we plotted overall denitrification rates (sum of m28+m29+m30) against SOD for both sampling campaigns ( $N=19$ ) and obtained a significant positive correlation ( $R^2=0.86$ ;  $y=0.075-0.4$ ;  $p<0.01$ ). Additionally, we plotted calculated denitrification rates based on the equation suggested by Seitzinger and Giblin (1996) with a slope of 0.142 for denitrification including coupled nitrification/denitrification (indirect denitrification) and through nitrate from the overlying water (direct denitrification). Actual rates obtained in March and September 2009 are around 50% lower than rates predicted by Seitzinger and Giblin (1996) (Fig. 5.6). Possibly, the relationship between denitrification and SOD may differ regionally depending on the amount of direct denitrification and indirect denitrification. Thus, a valid model to estimate spatial and temporal denitrification derived from SOD may be very specific and requires being adapted for the salient factors regulating denitrification. We note that within this study, the raised data points are still too low in resolution to set up an estimative SOD-denitrification model, the tentative trend and exact slope should be verified for robustness.

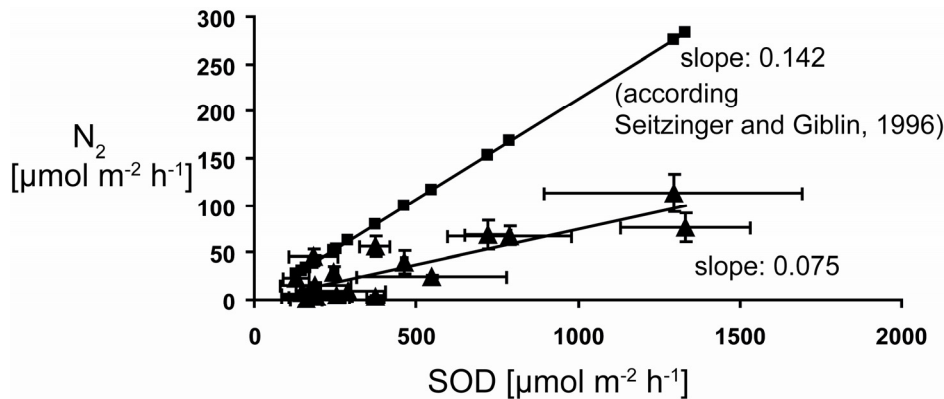


Fig. 5.6:  $\text{N}_2$  production (m28+m29+m30) versus SOD.

Comparison with calculated denitrification rates according Seitzinger and Giblin, 1996.

#### 5.4.4 Effective nitrate sink vs. total N budget of the Elbe River

The rates measured during the present study are generally smaller than the rates reported by Schröder et al. (1996) who determined an average denitrification rate around  $208 \mu\text{mol N}_2 \text{ m}^{-2} \text{ h}^{-1}$  for the same stations (ML–NW). The method applied by Schröder et al. (1996) integrates N fluxes from incubations under in situ conditions and anoxic incubations, the latter tending to overestimate actual  $\text{N}_2$  fluxes in systems with high nitrate concentrations fuelling direct denitrification. During anoxic incubations the sedimentary oxic zone decreases and raises the denitrifying zone towards the sediment-water interface; this implies a shorter diffusion path of nitrate enhancing direct denitrification (Christensen et al., 1990). Because denitrification at stations ML–NW is mainly driven by nitrate from the overlying water column, we assume that anoxic incubations resulted in relatively high denitrification rates compared to the rates we obtained by oxic incubations.

However, based on  $\text{N}_2$  fluxes obtained within this study, we give a rough estimation of nitrate removal rates during spring and summer time based upon the area where potentially denitrification may take place.

Construction activities such as diking and deepening of the river led to an increase in the tidal range (from 2.6 m in 1963 to 3.6 m in 2004) and to a reduction in shallow areas and tidal flood plains (Heise et al., 2005). Side branches of the Elbe like the Mühlenberger Loch (study site: ML) were partially or even completely removed. One negative side effect of these

activities has been the decrease of the low tide level which led to a steep increase of water level with beginning of high tide resulting in higher current velocities (ARGE, 2004). A deep channel has been formed, removing fine grained sediment types from the navigational route and exposing underlying sandy layers (Kerner and Jacobi, 2005). Still, remaining shallow water sediments areas may be very effective in terms of rN removal. When estimating the significance of sedimentary denitrification as an effective sink within the nitrogen cycle of the Elbe River, we have to account these areas. According to Schröder et al. (1996), shallow water sediments (areas with depth  $\leq 3$  m at low tide) between Hamburg and Cuxhaven cover about 300 km<sup>2</sup>.

Because N<sub>2</sub> fluxes (m28) were not significantly different comparing March and September data (Fig. 5.4), we average N<sub>2</sub> fluxes (m28) of the inner Elbe Estuary sediments (ML–NW) for both sampling campaigns and obtained a mean denitrification rate of 2.9 mmol N m<sup>-2</sup> d<sup>-1</sup> ( $\pm 1.1$  mmol N m<sup>-2</sup> d<sup>-1</sup>). When assigning this admittedly high variable denitrification rate to the shallow water area of the Elbe Estuary, between 1.6 and 3.6 kt N may be removed from Elbe River sediments during spring and summer months (March–September). Compared to the N discharge of the Elbe River, which is around 79 kt N y<sup>-1</sup> (ARGE, 2005); only a maximum around 5% of the total rN is converted to N<sub>2</sub> on transit to the river estuary.

Our estimation lacks the amount of denitrification possibly taking place in prevailing coarse grained sediment types, because N<sub>2</sub> fluxes within the navigational route were not examined. Recently, high potential denitrification rates ( $> 80 \mu\text{mol N}_2 \text{ m}^{-2} \text{ h}^{-1}$ ) in permeable sand facies of the southern German Wadden Sea have been observed (Gao et al., 2010). On the other site, considering the inner Elbe Estuary, high current velocities and channel like behaviour of the water body may hamper high rates of nitrate turnover within the navigational route (Alexander et al., 2000). Our assumptions are in accord with a study by Dähnke et al. (2008) who stated that nitrate behaves strictly conservatively along the salinity gradient of the Elbe Estuary today. The estuarine ability to reduce nutrient loads must have changed during the last 25 years, when the Elbe Estuary functioned as a larger rN sink (Dähnke et al., 2008). Obviously, rN sinks do not balance prevailing massive rN inputs in the present situation. Hence, massive NO<sub>3</sub><sup>-</sup> loads are discharged into the outer Elbe Estuary which may be partially buffered by the rN removal capacity of coastal sediments.

Considering N<sub>2</sub> fluxes measured in coastal sediments in September 2009 (KL–HT, Fig. 5.4), we measured denitrification rates up to 17  $\mu\text{mol N}_2 \text{ m}^{-2} \text{ h}^{-1}$  with most coastal sediments inactive in terms of denitrification due to nitrate limitation at this season (Fig 5.4). With respect to the inconsistent variations of the coastal denitrification rates and relatively low seasonal and spatial resolution, an extrapolation of these data would not be representative

for the adjacent coastal zone. However, from a recent accompanying study about denitrification rates in Wadden Sea sediments (Deek et al., 2010), an overall annual nitrate removal rate of  $10 \text{ kt N y}^{-1}$  for the north German Wadden Sea area has been estimated. Again, compared to the rN input of the Elbe River ( $79 \text{ kt N y}^{-1}$ ; ARGE, 2005), denitrification in adjacent coastal sediments comprises only 10–15% of the rN load of the Elbe River plume.

### 5.5 Conclusions

Human activity has markedly increased the rN inputs into the Elbe River and adjacent coastal zone of the German Bight. However, the natural capacity of the Elbe Estuary to retain nutrients by denitrification has been reduced by morphological changes accompanied by the reduction of shallow water areas. Indeed, sediments of the inner Elbe Estuary are effective sinks for nitrate: with a relatively high average rN removal rate around  $2.9 \text{ mmol N m}^{-2} \text{ d}^{-1}$ . Extrapolated, shallow water sediments remove between 1.6 and 3.6 kt N during spring and summer months that comprises around 5% of the total rN load of the Elbe River. Thus, most rN is channeled to the open North Sea. Coastal stations partly buffer nitrate in the overlying water delivered by the Elbe River plume but we observe that in summer months, nitrate availability limits sediment denitrification indicating an additional capacity to remove  $\text{NO}_3^-$  from the water column. In contrast, the overall high denitrification rates within the Elbe Estuary that do not vary significantly with temperature and nitrate concentrations suggest that a plateau of highest denitrification rates is reached within the riparian zones of the Elbe Estuary. Thus, an increase in nitrate delivery is not accompanied by an increase in denitrification rates that would counteract eutrophication pressures.

### Acknowledgements

We thank the GKSS Research Center, Institute for Coastal Research and the DFG (Em 37/29) for financial support. The IfBM, University of Hamburg and the FTZ Westküste, BÜsum are acknowledged for providing laboratory space.

In particular, we thank W. S. Gardner and M. J. McCarthy (Marine Science Institute, University of Texas at Austin) for their helpful introduction into sediment incubation. We thank the captain, H. Bornhöft and the crew of the RV Ludwig Prandtl for help and assistance during our sampling campaigns, and we acknowledge N. Lahajnar and F. Langenberg (IfBM, University of Hamburg) for supervising work on the data set of sediment characteristics.

## 6 Conclusions and Outlook

### 6.1 Conclusions

In this thesis, riverine sources of reactive nitrogen have been identified by means of the stable isotope composition of nitrate. The generally enriched  $\delta^{15}\text{N}$  signal of nitrate in five German rivers under study (Rhine, Elbe, Weser, Ems and Eider) suggests that riverine nitrate sources derive mainly from soil nitrification, sewage and manure. In all rivers,  $\delta^{15}\text{N}$  and  $\delta^{18}\text{O}$  values undergo a seasonal cycle which is characterized by elevated isotope values in summer and is caused by assimilative processes active at higher temperatures. The consumption of nitrate and its fractionation rate depends strongly on the riverine current velocity with highest nitrate consumption rates accompanied by high isotopic variation in smaller rivers. In contrast to the biological effects on nitrate in summer seasons, nitrate isotope values are generally lower in winter and reflect the source signal more closely. Nitrate isotopic composition is strongly influenced by the land use patterns in the respective river catchments, resulting in a strong positive correlation between  $\delta^{15}\text{N}$  in nitrate and proportion of urban and agricultural land use.

Excessive riverine nitrate loads to the North Sea are potentially denitrified in estuaries before they are discharged into the German Bight, or may be eliminated in adjacent coastal zones.

To estimate the amount of nitrate denitrified in riparian zones of the Elbe estuary, denitrification rates were determined in spring and summer for the year 2009 along the nitrate concentration gradient in the estuary. Major factors controlling denitrification rates in sediment sites were the nitrate concentrations in the overlying water body and the organic matter content of the sediment. Within the inner Elbe Estuary, shallow water areas and mud flats of the estuary are effective sink for nitrate, but their capacity is limited by their small extent that has steadily declined over the last decades due to construction activities to maintain a competitive container port in the city of Hamburg. Compared to the N discharge of the Elbe River, only a maximum around 5% of the total rN is converted to  $\text{N}_2$  on transit to the river estuary.

Hence, most riverine nitrate is passively transported to the coastal North Sea, where riverborne nitrate is apparently eliminated by sedimentary denitrification in intertidal and shallow subtidal sediments.

Denitrification rates in these types of sediments have been studied in seasonal resolution at two locations with different sediment compositions and ambient nitrate concentrations. In summer months, denitrification in the northern Wadden Sea is nitrate limited having an

additional capacity to degrade nitrate. In winter, low temperature slows down the denitrification rates in sediments considerably. Extrapolating seasonal denitrification rates for the entire northern sector of the Wadden Sea results in an annual nitrate removal rate of 10 kt y<sup>-1</sup>, which eliminates around 10–15% of the annual Elbe River nitrate load.

These findings give evidence that a high proportion of riverborne nitrate escapes the coastal and estuarine nitrate sinks, and remains biologically available within the rN-cycle of the German Bight.

## 6.2 Outlook

The results on the isotopic composition of nitrate in German rivers have demonstrated the importance of soil nitrification, which apparently contributes massively to the riverine nitrate pools. But little is known about the proportion of nitrate generated within the river by water-column nitrification. As a follow-up to this study, a next logical step would be the determination of water column nitrification rates within the different rivers, and including the maximum turbidity zone of the estuaries. There is evidence for significant nitrate production by nitrification in the turbidity maximum of the Elbe estuary (Dähnke et al., 2008; Schlarbaum et al., 2010), but no conclusive measurements have been conducted yet.

Within this context, many questions remain unanswered with regard to the isotope effects of nitrification. Recent studies suggested that the sources of oxygen and the fractionation of dissolved oxygen contributing to nitrate vary considerably depending on environmental conditions and microorganisms involved. Further work on isotopic fractionation in pure cultures studies and on in-situ nitrification rates is necessary to better quantify the amount of nitrification by means of stable isotopes (Wankel et al., 2006; Sigman et al., 2005, 2009, Buchwald and Casciotti, 2010).

Furthermore, the role of estuaries in degrading rN fluxes from land to sea is not well constrained. While the general consensus has been that estuaries remove 20–50% of riverine nitrate loads (Seitzinger et al., 2006), estuaries of several river systems apparently do no longer act as a nitrate sink (Jickells et al., 2000; Dähnke et al., 2009). Studies on the nitrate retention capacity of tidal estuaries draining into the German Bight are sparse, and it would be important to quantify nitrate removal in estuaries of large (Elbe, Weser, Rhine) and smaller rivers (Ems) to compare nitrate consumption rates in relation to discharge regime and catchment characteristics.

One first effort towards a better constraint of factors affecting sediment denitrification rates has been presented in this thesis. But considering that the quantification of sedimentary denitrification is of high economical and environmental relevance, the present study suffers from relatively low spatial and temporal resolution caused by the elaborate sediment incubation technique used. In future studies, sample resolution in space and time need to be spatial enhanced. This is difficult to do with the incubation technique used here, and a desired denser data set of denitrification rates, site parameters and sediment characteristics that would support a statistically robust estimate of denitrification rates in the German Bight requires that other methods be explored. Thus, an adaption of the incubation set-up with sub cores would be more feasible. Another promising approach to raise large data sets on denitrification rates would be the vertical profiling of  $N_2/Ar$  in undisturbed sediment cores using a needle probe MIMS inlet (Hilairy and Seitzinger, 2003) followed by modelling of  $N_2$  production rates. The present study completely lacks denitrification rate estimates for offshore sites of the German Bight, and a more effective technique would permit to extend the data from nearshore environments to vast areas in the North Sea where TOC availability in sediments is relatively low.

The experimental approach used here considers only net- $N_2$  fluxes, and denitrification rates within this study are defined as the sum of various processes which produce or consume  $N_2$ . With modifications in the experimental design and use of various isotopically labelled N-substrates in the incubation experiments, it would be possible to determine the partition of anammox contributing to the overall  $N_2$  flux. Anammox has been shown to occur in various sediments of shelf seas (e.g. Thamdrup and Dalsgaard, 2002), but until present, the significance of anammox in the German Bight has not been assessed in detail.

In the end, the obtained data set and derived insights should find their way into a model that parameterises and quantifies N sources and sinks in the German Bight by an isotope tracking module (Pätsch et al., 2010, Serna et al., 2010). With this model it is possible to reconstruct pristine conditions in order to provide quality targets for environmental legislation. Further, the effects of future human actions on land, in rivers, and in estuaries with respect to their likely environmental consequences could be estimated.

To conclude, the assessment of nitrification within riverine N cycling, the quantification of anammox in sediments of the German Bight and the optimization of sediment incubations to obtain a higher resolution of denitrification rates would be very promising to gain further insights into N-cycling of the German Bight.

**Figure captions**

Fig. 1.1: The marine nitrogen cycle .....	2
Fig. 1.2: Biogeochemical zonation in marine sediments and respective free energy changes .....	7
Fig. 2.1: Locations of sampling stations at rivers in the north western part of Germany. ....	13
Fig. 2.2: The annual cycle of discharge, nitrate concentrations and $\delta^{15}\text{N}/\delta^{18}\text{O}$ of nitrate for the river Ems, March 2006–March 2007. ....	18
Fig. 2.3: The annual cycle of discharge, nitrate concentrations and $\delta^{15}\text{N}/\delta^{18}\text{O}$ of nitrate for the river Rhine, March 2006–March 2007. ....	18
Fig. 2.4: The annual cycle of discharge, nitrate concentrations and $\delta^{15}\text{N}/\delta^{18}\text{O}$ of nitrate for the river Weser, March 2006–March 2007. ....	19
Fig. 2.5: The annual cycle of discharge, nitrate concentrations and $\delta^{15}\text{N}/\delta^{18}\text{O}$ of nitrate for the river Elbe, January 2006–December 2006. ....	19
Fig. 2.6: The annual cycle of discharge, nitrate concentrations and $\delta^{15}\text{N}/\delta^{18}\text{O}$ of nitrate for the river Eider, March 2006–March 2007. ....	20
Fig. 2.7: $\delta^{15}\text{N}-\text{NO}_3^-$ plotted against agricultural and urban land use values for rivers in North America and Europe. ....	23
Fig. 2.8: General fingerprints of $\text{NO}_3^-$ sources in a diagram of $\delta^{15}\text{N}$ and $\delta^{18}\text{O}$ (modified from Kendall, 1998) and character of nitrate isotopic composition in the rivers examined here. ....	24
Fig. 2.9: Plot of isotopic values against nitrate concentrations. ....	27
Fig. 3.1: Sampling locations at the river Rhine, Weser and Ems. ....	37
Fig. 3.2a: Seasonal cycles of $\text{NO}_3^-$ concentrations, $\delta^{15}\text{N}-\text{NO}_3^-$ , $\delta^{18}\text{O}-\text{NO}_3^-$ , $\delta^{15}\text{N}-\text{PN}$ and $\delta^{18}\text{O}-\text{H}_2\text{O}$ of the Rhine River. ....	40
Fig. 3.2b: Seasonal cycles of $\text{NO}_3^-$ concentrations, $\delta^{15}\text{N}-\text{NO}_3^-$ , $\delta^{18}\text{O}-\text{NO}_3^-$ , $\delta^{15}\text{N}-\text{PN}$ and $\delta^{18}\text{O}-\text{H}_2\text{O}$ of the river Weser. ....	41
Fig. 3.2c: Seasonal cycles of $\text{NO}_3^-$ concentrations, $\delta^{15}\text{N}-\text{NO}_3^-$ , $\delta^{18}\text{O}-\text{NO}_3^-$ , $\delta^{15}\text{N}-\text{PN}$ and $\delta^{18}\text{O}-\text{H}_2\text{O}$ of the river Ems. ....	42
Fig. 3.3: Temporal variation in discharge in relation to nitrate concentrations and nitrate load. ....	44
Fig. 3.4: Nitrate discharge relationship in comparison with the theoretical dilution curve. ....	53

Fig. 3.5: Variation in $\delta^{18}\text{O-NO}_3^-$ in relation to $\delta^{15}\text{N-NO}_3^-$ for the Rhine, Weser and Ems.....	55
Fig. 3.6: Change in $\delta^{15}\text{N-NO}_3^-$ and $\delta^{18}\text{O-NO}_3^-$ relative to the fraction of the remaining reactant ( $\text{NO}_3^-$ ) pool.....	57
Fig. 4.1: Schematic marine N-cycle.....	63
Fig. 4.2: Study sites in the North Frisian Wadden Sea.....	64
Fig. 4.3: Flow-through incubation set-up.....	68
Fig. 4.4: Nitrate and ammonium fluxes.....	72
Fig. 4.5a: $\text{N}_2$ and $\text{O}_2$ fluxes for the sampling stations in Büsum.....	74
Fig. 4.5b: $\text{N}_2$ and $\text{O}_2$ fluxes for the sampling stations in Sylt.....	75
Fig. 4.6: Actual $\text{N}_2$ production rates versus ambient $^{15}\text{NO}_3^-$ .....	79
Fig. 4.7: Nitrate concentrations in the Wadden Sea area in February 2009 (left) and August 2009 (right).....	83
Fig. 5.1: Study site.....	89
Fig. 5.2: Flow-through incubation set-up.....	91
Fig. 5.3: Ammonium and nitrate fluxes during flow-through incubation of unamended sediment cores.....	96
Fig. 5.4: $\text{N}_2$ and $\text{O}_2$ fluxes during flow-through incubation of unamended sediment cores (m28) and $^{15}\text{NO}_3^-$ amended sediment cores (m29+m30).....	97
Fig. 5.5: Comparison of $\text{N}_2$ production (m28) calculated according IPT from $\text{N}_2$ fluxes (m29+m30) in sub core incubations and $\text{N}_2$ production (m28) obtained by flow-through incubation and direct $\text{N}_2$ (m28) measurement.....	98
Fig. 5.6: $\text{N}_2$ production (m28+m29+m30) versus SOD.....	104

## Table captions

Tab. 1.1: Fractionation factors for microbial processes in pure culture.....	5
Tab. 2.1: Load weighted annual isotope values in reference to the mean summer and winter isotope values. ....	22
Tab. 2.2: Land use of the sub-basins according to CORINE landcover (Statistisches Bundesamt, 1990).....	23
Tab. 3.1: N-NO <sub>3</sub> <sup>-</sup> discharge and load weighted isotope values for the respective sampling periods subdivided into seasons.....	43
Tab. 3.2.: Correlation matrix (Pearson's) of biogeochemical parameters of the rivers Rhine, Weser and Ems. ....	46
Tab. 4.1: Sediment characteristics for the study sites Sylt-I, Sylt-II, Büsum-I and Büsum-II.....	65
Tab. 4.2: Site characteristics for the sampling campaigns in Sylt and Büsum.....	66
Tab. 5.1: Sediment characteristics of the sampling stations.....	94
Tab. 5.2: Site characteristics of the sampling stations.....	95
Tab. 5.3: Correlation matrix .....	102

## List of abbreviations

AA:	amino acid
Anammox:	anaerobic ammonium oxidation
ARGE:	Arbeitsgemeinschaft zur Reinhaltung der Elbe
ATP:	adenosine triphosphate
AOA:	ammonia-oxidizing archaea
AOB:	ammonia-oxidizing bacteria
bdl:	below detection limit
C <sub>org</sub> :	organic carbon
DIN:	dissolved inorganic nitrogen
DNRA:	dissimilatory nitrate reduction to ammonium
DON:	dissolved organic nitrogen
ε:	fractionation factor
EA:	Elemental Analyzer
GISP:	Greenland Ice Sheet Precipitation
IAEA:	International Atomic Energy Agency
IPT:	isotope pairing technique
kt:	kilotons
MUC:	multicorer
MIMS:	membrane inlet mass spectrometry
m28:	mass 28
m29:	mass 29
m30:	mass 30
n.a.:	not analyzed
NLÖ:	Niedersächsisches Landesamt für Ökologie
OSPAR:	Convention for the Protection of the Marine Environment of the North-East Atlantic (combines <u>O</u> slo and <u>P</u> aris Convention)
PN:	particulate nitrogen
PON:	particulate organic nitrogen
PVC:	polyvinylchloride
QMS:	Quadrupole mass spectrometer
R:	isotope ratio
rN:	reactive nitrogen
RV:	research vessel
SLAP:	Standard Light Antarctic Precipitation

## List of abbreviations

---

SOD:	sedimentary oxygen demand
TDN:	total dissolved nitrogen
TN:	total nitrogen
TOC:	total organic carbon
UBA:	Umweltbundesamt
WFD:	European Water Framework Directive

---

## References

- Ahad, J. M. E., Ganeshram, R. S., Spencer, R. G. M., Uher, G., Upstill-Goddard, R. C., Cowie, G. L., 2006. Evaluating the sources and fate of anthropogenic dissolved inorganic nitrogen (DIN) in two contrasting North Sea estuaries. *Science of the Total Environment*, 372(1), 317–333.
- Alexander, R. B., Smith, R. A., Schwarz, G. E., 2000. Effect of stream channel size on the delivery of nitrogen to the Gulf of Mexico. *Nature*, 403, 758–761.
- Altabet, M. A., Deuser, W. G., Honjo, S., Stienen, C., 1991. Seasonal and depth-related changes in the source of sinking particles in the North Atlantic. *Nature*, 354, 136–139.
- Amberger, A., Schmidt, H. L., 1987. Natürliche Isotopengehalte von Nitrat als Indikatoren für dessen Herkunft. *Geochimica et Cosmochimica Acta*, 51(10), 2699–2705.
- An, S., Gardner, W. S., Kana, T., 2001. Simultaneous measurement of denitrification and nitrogen fixation using isotope pairing with membrane inlet mass spectrometry analysis. *Applied Environmental Microbiology*, 67 1171–1178.
- An, S., Gardner, W. S., 2002. Dissimilatory nitrate reduction to ammonium (DNRA) as a nitrogen link versus denitrification as a sink in a shallow estuary (Laguna Madre/Baffin Bay, Texas). *Marine Ecology Progress Series*, 237, 41–50.
- Anderson, K. K., Philson, S. B., Hooper, A. B., 1982.  $^{18}\text{O}$  isotope shift in  $^{15}\text{N}$  NMR analysis of biological N-oxidations:  $\text{H}_2\text{O}$ - $\text{NO}_2^-$  exchange in the ammonia-oxidizing bacterium *Nitrosomonas*. *Proceedings of the National Academy of Sciences of the United States of America*, 79, 5871–5875.
- Anderson, K. K., Hooper, A. B., 1983.  $\text{O}_2$  and  $\text{H}_2\text{O}$  are each the source of one O in  $\text{NO}_2^-$  produced from  $\text{NH}_3$  by *Nitrosomonas*.  $^{15}\text{N}$ -NMR evidence. *FEBS Letters*, 164, 236–240.
- Aravena, R., Evans, M. L., Cherry, J. A., 1993. Stable Isotopes of Oxygen and Nitrogen in Source Identification of Nitrate from Septic Systems. *Ground Water*, 31(2), 180–186.
- Arbeitsgemeinschaft für die Reinerhaltung der Elbe (ARGE), 2004. Sauerstoffhaushalt der Tideelbe.  
<http://www.arge-elbe.de/wge/Download/Texte/O2HaushTide.pdf> [14.02.2010].
- Arbeitsgemeinschaft für die Reinerhaltung der Elbe (ARGE), 2005. Gewässergütebericht der Elbe 2004.
- Armstrong, F. A. J., Sterns, C. R., Strickland, J. D. H., 1967. The measurement of upwelling and subsequent biological processes by means of the Technicon AutoAnalyzer and associated equipment. *Deep-Sea Research*, 14, 381–389.
- Attard, E., Poly, F., Commeaux, C., Laurent, F., Terada, A., Smets, B. F., Recous, S., Le Roux, X., 2010. Shifts between Nitrospira- and Nitrobacter-like nitrite oxidizers

- underlie the response of soil potential nitrite oxidation to changes in tillage practices. *Environmental Microbiology*, 12, 315–326.
- Bach, M., Frede, H. G., Schwankart, U., Huber, A., 1998. Regional differenzierte Bilanzierung der Stickstoff- und Phosphorüberschüsse der Landwirtschaft in den Gemeinden/Kreisen in Deutschland. Forschungs- und Entwicklungsvorhaben 10204515 des Umweltbundesamtes.
- Bakker, J. F., Bartelds, W., Becker, P. H., Bester, K., Dijkhuizen, K., Frederiks, B., Reineking, B., 1999. Chapter 4: Marine Chemistry. The Wadden Sea Quality Status Report. Common Wadden Sea Secretariat. Trilateral Monitoring and Assessment Group. Quality Status Report Group., Wilhelmshaven.
- Bartosch, S., Hartwig, C., Spieck, E., Bock, E., 2002. Immunological detection of Nitrospirilla-like bacteria in various soils, *Microbial Ecology*, 43, 26–33.
- Beddig, S., Brockmann, U., Dannecker, W., Körner, D., Pohlmann, T., Puls, W., Radach, G., Rebers, A., Rick, H.-J., Schatzmann, M., Schlünzen, H., Schulz, M., 1997. Nitrogen fluxes in the German Bight. *Marine Pollution Bulletin*, 34, 382–394.
- Behrendt, H., 1996. Inventories of point and diffuse sources and estimated nutrient loads – a comparison for different river basins in Central Europe. *Water Science and Technology*, 33(4–5), 99–107.
- Behrendt, H., Kornmilch, M., Opitz, D., Schmoll, O., Scholz, G., 2002. Estimation of the nutrient inputs into river systems – experiences from German rivers. *Regional Environmental Change*, V3(1), 107–117.
- Berounsky, V.M., Nixon, S.W., 1985. Eutrophication and the rate of net nitrification in a coastal marine ecosystem. *Estuarine, Coastal and Shelf Science*, 20(6), 773–781.
- Blume, H. P., 2004. *Handbuch des Bodenschutzes: Bodenökologie und -belastung, vorbeugende und abwehrende Schutzmaßnahmen.*
- Böhlke, J. K., Coplen, T. B., 1995. Reference and Intercomparison Materials for Stable Isotopes of Light Elements (IAEA-TECDOC-825). International Atomic Energy Agency. Vienna, 51–66.
- Böhlke, J. K., S. J. Mroczkowski, Coplen, T. B., 2003. Oxygen isotopes in nitrate: new reference materials for O-18:O-17 : O-16 measurements and observations on nitrate-water equilibration. *Rapid Communications in Mass Spectrometry*, 17, 1835–1846.
- Böttcher, J., Strebel, O., Voerkelius, S., Schmidt, H. L., 1990. Using isotope fractionation of nitrate-nitrogen and nitrate-oxygen for evaluation of microbial denitrification in a sandy aquifer. *Journal of Hydrology*, 114, 413–424.
- Bowen, G.J., Revenaugh, J., 2003. Interpolating the isotopic composition of modern meteoric precipitation. *Water Research*, 39(10), 1299. doi:10.1029/2003WR002086

- Bowen, G.J., Wassenaar, L.I. and Hobson, K.A., 2005. Global application of stable hydrogen and oxygen isotopes to wildlife forensics. *Oecologia*, 143, 337–348.
- Bowen, G.J., Wilkinson, B., 2002. Spatial distribution of  $\delta^{18}\text{O}$  in meteoric precipitation. *Geology*, 30(4), 315–318.
- Bran & Luebke, 2000. Nitrate and Nitrite in Soil Extracts and Water. Method No.G-067-92 Rev.2, Auto Analyzer Applications. Operation Manual.Publication No. MT7-3OEN-O3.
- Brandes, J. A. and Devol, A. H., 1997. Isotopic fractionation of oxygen and nitrogen in coastal marine sediments. *Geochimica et Cosmochimica Acta*, 61 (9), 1793–1801.
- Brion, N., Baeyens, W., De Galan, S., Elskens, M. and Laane, R. W. P. M., 2004. The North Sea: source or sink for nitrogen and phosphorus to the Atlantic Ocean? *Biogeochemistry*, 68, 277–296.
- Bristow, L. A., 2009. Tracing nitrogen flows across the Southern North Sea: A stable isotope approach, PhD thesis, University of East Anglia, School of Environmental Sciences.
- Bronk, D. A., 2002. Dynamics of DON in: Hansell, D. A., Carlson, C. A. (Eds.), *Biogeochemistry of Marine Dissolved Organic Matter*, pp. 153–249.
- Buchwald, C., Casciotti, K. L., 2010. Oxygen isotopic fractionation and exchange during bacterial nitrite oxidation. *Limnology and Oceanography*, 55, 1064–1074.
- Buhl, D., Neuser, R.D., Richter, D. K., Riedel, D., Roberts, B., Strauss, H., Veizer, J., 1991. Nature and nurture: Environmental isotope story of the River Rhine. *Naturwissenschaften*, V78 (8), 337–346.
- Burdige, D. J., 1993. The biogeochemistry of manganese and iron reduction in marine sediments. *Earth-Science Reviews*, 35, 249–284.
- Burdige, D. J., 2006. *Geochemistry of Marine Sediments*. xix + 609 pp. Princeton University Press.
- Burns, D. A., Kendall, C., 2002. Analysis of sources of  $^{15}\text{N}$  and  $^{18}\text{O}$  to differentiate  $\text{NO}_3^-$  sources in runoff at two watersheds in the Catskill Mountains of New York. *Water Resources Research*, 5, 1051, doi:10.1029/2001WR000292.
- Canfield, D. E., Thamdrup, B., Kristensen, E., 2005. The nitrogen cycle in: Southward, A.J., Tyler, P. A., Young, C. M., Fuiman, L. A. (Eds.), *Aquatic Geomicrobiology. Advances in Marine Biology*. Elsevier Academic Press, pp. 205–267.
- Capone, D. G., 2000. The marine microbial nitrogen cycle in: Kirchmann, D. L. (Ed.), *Microbial ecology of the oceans*, Wiley Series in Ecological and Applied Microbiology, pp. 455–493.
- Casciotti, K. L., Sigman, D. M., Hastings, M. G., Bohlke, J. K. and Hilkert, A., 2002. Measurement of the Oxygen Isotopic Composition of Nitrate in Seawater and Freshwater Using the Denitrifier Method. *Analytical Chemistry*, 74(19), 4905–4912.

- Casciotti, K. L., 2009. Inverse kinetic isotope fractionation during bacterial nitrite oxidation. *Geochimica et Cosmochimica Acta*, 73, 2061–2076.
- Christensen, P. B., Nielsen, L. P., Sørensen, J., Revsbech, N. P., 1990. Denitrification in nitrate rich streams: Diurnal and seasonal variation related to benthic oxygen metabolism. *Limnology and Oceanography*, 35, 640–651.
- Cloern, J. E., 2001. Our evolving conceptual model of the coastal eutrophication problem. *Marine Ecology Progress Series*, 210, 223–253.
- Cook, P. L. M., Wenzhöfer, F., Rysgaard, S., Galaktionov, O. S., Meysman, F. J. R., Eyre, B. D., Cornwell, J., Huettel, M., Glud, R. N., 2006. Quantification of denitrification in permeable sediments: Insights from a two-dimensional simulation analysis and experimental data. *Limnology and Oceanography Methods*, 4, 294–307.
- Cornwell, J. C., Kemp, W. M., Kana, T. M., 1999. Denitrification in coastal ecosystems. *Aquatic Ecology*, 33, 41–54.
- Dähnke, K., Bahlmann, E., Emeis, K., 2008. A nitrate sink in estuaries? An assessment by means of stable nitrate isotopes in the Elbe estuary, *Limnology and Oceanography*, 53, 1504–1511.
- Dauwe, B., Middelburg, J. J., Herman, P. M. J., 2001. Effect of oxygen on the degradability of organic matter in subtidal and intertidal sediments of the North Sea area, *Marine Ecology Progress Series*, 215, 13–22.
- Davis, J. S., Keller, H. M., 1983. Dissolved loads in streams and rivers-discharge and seasonally related variations in Dissolved Loads of Rivers and Surface Water Quantity-Quality Relationships. *IAHS Publication*, 141, 79–89.
- de Beer, D., Wenzhöfer, F., Ferdelman, T. G., Boehme, S. E., Huettel, M., van Beusekom, J. E. E., Böttcher, M. E., Musat, N., Dubilier, N., 2005. Transport and mineralization rates in North Sea sandy intertidal sediments, Sylt-Rømø Basin, Waddensea. *Limnology and Oceanography*, 50, 113–127.
- Deek, A., Emeis, K., van Beusekom, J., 2010. Denitrification in coastal sediments of the German Wadden Sea, resubmitted to *Biogeochemistry*.
- de Jonge, V. N., 1995. The Ems Estuary, in: *Eutrophic shallow estuaries and lagoons*, McComb, A. J., CRC Press, U.S.A., 81–105.
- Descy, J.-P., Servais, P., Smitz, J. S., Billen, G., Everbecq, E., 1987. Phytoplankton biomass and production in the River Meuse (Belgium). *Water Research*, 21, 1557–1566.
- Deutsch, B., Liskow, I., Kahle, P., Voss, M., 2005. Variations in the  $\delta^{15}\text{N}$  and  $\delta^{18}\text{O}$  values of nitrate in drainage water of two fertilized fields in Mecklenburg-Vorpommern (Germany). *Aquatic Sciences*, 67, 156–165.

- Deutsch, B., Mewes, M., Liskow, I., Voss, M., 2006. Quantification of diffuse nitrate inputs into a small river system using stable isotopes of oxygen and nitrogen in nitrate. *Organic Geochemistry*, 37(10), 1333–1342.
- Deutsch, B., Forster, S., Wilhelm, M., Dippner, J. W., Voss, M., 2010. Denitrification in sediments as a major nitrogen sink in the Baltic Sea: an extrapolation using sediment characteristics. *Biogeosciences Discussions*, 7, 2487–2521.
- de Wilde, H. P. J. and De Bie, M. J. M., 2000. Nitrous oxide in the Schelde estuary: production by nitrification and emission to the atmosphere. *Marine Chemistry*, 69(3-4), 203–216.
- Dijkzeul, A., 1982. The quality of Rhine water in The Netherlands in the period 1970-1981 (in Dutch). Report 82061. DBW-RIZA, Lelystad, The Netherlands.
- Dispirito, A. A., Lipscomb, J. D., Hooper, A. B., 1986. Cytochrome aa<sub>3</sub> from *Nitrosomonas europaea*. *The Journal of Biological Chemistry*, 261, 17048–17056.
- Durka, W., Schulze, E.-D., Gebauer, G., Voerkelius S., 1994. Effects of forest decline on uptake and leaching of deposited nitrate determined from 15N and 18O measurements. *Nature*, 372, 765–767.
- Duff, J. H., Triska, F. J., Oremland, R. S., 1984. Denitrification associated with stream Periphyton: Chamber estimates from undisturbed communities. *Journal of Environmental Quality*, 13, 514–518.
- DWD, 2010. Deutscher Wetterdienst, Presse- und Öffentlichkeitsarbeit. Deutschlandwetter im Winter 2009/2010.  
[http://www.dwd.de/bvbw/generator/DWDWWW/Content/Presse/Pressemitteilungen/2010/20100226\\_Deutschlandwetter\\_Winter\\_2009\\_2010,templateId=raw,property=publicationFile.pdf/20100226\\_Deutschlandwetter\\_Winter\\_2009\\_2010.pdf](http://www.dwd.de/bvbw/generator/DWDWWW/Content/Presse/Pressemitteilungen/2010/20100226_Deutschlandwetter_Winter_2009_2010,templateId=raw,property=publicationFile.pdf/20100226_Deutschlandwetter_Winter_2009_2010.pdf)  
[07.06. 2010].
- Emeis, K.-C, Bahlmann, E., Paetsch, J., Serna, A., Dähnke, K., Schlarbaum, T., 2006. Der Stickstoffkreislauf in der Deutschen Bucht: Woher und Wohin? Eine isotopengeochemische Perspektive. In: Nies, S. (Ed.). *Überwachung der Meeresumwelt*, BSH, Hamburg.
- Erguder, T. H., Boon, N., Wittebolle, L., Marzorati, M., Verstraete, W., 2009. Environmental factors shaping the ecological niches of ammonia-oxidizing archaea. *FEMS Microbiology Reviews*, 33, 855–869.
- Erisman, J. W., Sutton, M. A., 2008. Reduced nitrogen in ecology and the environment. *Special Issue of Environmental Pollution*, 154 (3), 357–508.
- Eyre, B. D., Rysgaard, S., Dalsgaard, T., Christensen, P. B., 2002. Comparison of Isotope Pairing and N<sub>2</sub>:Ar methods for measuring sediment denitrification—Assumptions, modifications, and implications. *Estuaries*, 25, 1077–1087.

- Faure, G., Mensing, T. M., 2005. *Isotope: principles and applications*, third edition. John Wiley & Sons.
- FGG-Weser, 2005. Flussgebietsgemeinschaft Weser. EG-Wasserrahmenrichtlinie. Bewirtschaftungsplan der Flussgebietseinheit Weser. Bestandsaufnahme 2005.
- Focht, D. D., Verstraete, W., 1977. Biochemical ecology of nitrification and denitrification. *Advanced Microbial Ecology*, 1, 135–214.
- Fogg, G. E., Rolston, D. E., Decker, D. L., Louie, D. T., Grismer, M. E., 1998. Spatial variation in nitrogen isotope values beneath nitrate contamination sources, *Groundwater*, 36, 418–426.
- Francis, C. A., Beman, J. M., Kuypers, M. M. M., 2007. New processes and players in the nitrogen cycle: the microbial ecology of anaerobic and archaeal ammonia oxidation. *The ISME Journal* 1, 19–27.
- Frank, D., Evans, R. D., Tracy, B., 2004. The role of ammonia volatilization in controlling the natural  $^{15}\text{N}$  abundance of a grazed grassland. *Biogeochemistry*, 68, 169–178.
- Frankignoulle, M., Middelburg, J. J., 2002. Biogases in tidal European Estuaries: the Biogest project. *Biogeochemistry*, 59, 1–4.
- Freyer, H.D., 1991. Seasonal variation of  $^{15}\text{N}/^{14}\text{N}$  ratios in atmospheric nitrate species. *Tellus Series B: Chemical and Physical Meteorology*, 43, 30–44.
- Froelich, P. N., Klinkhammer, G. P., Bender, M. L., Luedtke, N. A., Heath, G. R., Cullen, D., Dauphin, P., Hammond, D., Hartman, B., Maynard, V., 1979. Early oxidation of organic matter in pelagic sediments of the eastern equatorial Atlantic: suboxic diagenesis, *Geochimica et Cosmochimica Acta*, 43, 1075–1090.
- Fulweiler, R. W., Nixon, S. W., Buckley, B. A., Granger, S. L., 2007. Reversal of the net dinitrogen gas flux in coastal marine sediments. *Nature*, 448, 180–182.
- Galloway, J. N., Schlesinger, W. H., Levy, H., Michaels, A., Schnoor, J. L., 1995: Nitrogen fixation: Anthropogenic enhancement-environmental response. *Global Biogeochemical Cycles*, 9, 235–252.
- Galloway, J.N. and Cowling, E.B., 2002. Reactive nitrogen and the world: 200 years of change. *Ambio*, 31, 64–71.
- Galloway, J. N., 2003. The global nitrogen cycle, in: *Treatise on Geochemistry*, Schlesinger; W. H, Elsevier, 557–583.
- Galloway, J. N., Townsend, A. R., Erisman, J. W., Bekunda, M., Cai, Z., Freney, J. R., Martinelli, L. A., Seitzinger, S. P., Sutton, M. A., 2008. Transformation of the nitrogen cycle: Recent trends, questions and potential solution. *Science*, 320, 889–892.
- Gao, H., Schreiber, F., Collins, G., Jensen, M. M., Kostka, J. E., Lavik, G., de Beer, D., Zhou, H., Kuypers, M. M. M., 2010. Aerobic denitrification in permeable Wadden Sea sediments. *The ISME Journal*, 417–426.

- Gardner, W. S., Seitzinger, S. P., Malczyk, J. M., 1991. The effects of sea salts on the forms of nitrogen released from estuarine and freshwater sediments: does ion pairing affect ammonium flux? *Estuaries*, 14, 157–166.
- Gaye-Haake, B., Lahajnar, N., Emeis, K., Unger, D., Rixen, T., Suthhof, A., Ramaswamy, V., Schulz, H., Paropkari, A. L., Guptha, M. V. S., Ittekkot, V., 2005. Stable nitrogen isotopic ratios of sinking particles and sediments from the northern Indian Ocean. *Marine Chemistry*, 96, 243–255.
- Giblin, A. E., Weston, N. B., Banta, G. T., Tucker, J., Hopkinson, C. S., 2010. The Effects of Salinity on Nitrogen Losses from an Oligohaline Estuarine Sediment. *Estuaries and Coast*, 33, 1054–1068.
- Gihring, T. M., Canion, A., Riggs, A., Huettel, M., Kostka, J. E., 2010. Denitrification in shallow, sublittoral Gulf of Mexico permeable sediments. *Limnology and Oceanography*, 55, 43–54.
- Golterman, H. L., 2004. *The Chemistry of Phosphate and Nitrogen Compounds in Sediments*. Dordrecht, Kluwer Academic Publishers.
- Gömann, H., Kreins, P., Kunkel, R., Wendland, F., 2005. Model based impact analysis of policy options aiming at reducing diffuse pollution by agriculture - a case study for the river Ems and a sub-catchment of the Rhine. *Environmental Modelling & Software*, 20, 261–271.
- Granger, J., Sigman, D. M., Needoba, J. A., Harrison, J. A., 2004. Coupled nitrogen and oxygen isotope fractionation of nitrate during assimilation by cultures of marine phytoplankton. *Limnology and Oceanography*, 49(5), 1763–1773.
- Grasshoff, K., Ehrhardt, M., Kremling, K., 1983. *Methods of seawater analysis*. Verlag Chemie. Weinheim.
- Grischek, T., Hiscock, K. M., Metschies, T., Dennis, P. F., Nestler, W., 1997. Factors affecting denitrification during infiltration of river water into a sand and gravel aquifer in Saxony, Germany. *Water Research*, 32 (2), 450–460.
- Gruber, N., Galloway, J. N., 2008. An earth-system perspective of the global nitrogen cycle. *Nature*, 451, 293–296.
- Gupta, P., Noone, D., Galewsky, J., Sweeney, C., Vaughn, B. H., 2009. Demonstration of high-precision continuous measurements of water vapor isotopologues in laboratory and remote field deployments using wavelength-scanned cavity ring-down spectroscopy (WS-CRDS) technology. *Rapid Communications in Mass Spectrometry*, 23, 2534–2542.
- Hales, H., Ross, D., Lini, A., 2007. Isotopic signature of nitrate in two contrasting watersheds of Brush Brook, Vermont, USA. *Biogeochemistry*, 84, 51–66.

- Hamilton, S. K., Tank, J. L., Raikow, D. F., Wollheim, W. M., Peterson, B. J., Webster, J. R., 2001. Nitrogen uptake and transformation in a midwestern U.S. stream: A stable isotope enrichment study. *Biogeochemistry*, 54(3), 297–340.
- Hamm, A., 1996. Wie und woher kommen die Nährstoffe in die Flüsse? In: Warnsignale aus Flüssen und Ästuaren, Lozán, J. L., Kausch, H., Parey Buchverlag Berlin, 105–110.
- Harrington, B. P., Chamberlain, C. P., Blum, J. D. and Folt, C. L., 1998.  $^{15}\text{N}$  enrichment in agricultural catchments: field patterns and applications to tracking Atlantic salmon (*Salmo salar*). *Chemical Geology*, 147, 281–294.
- Heaton, T.H.E., 1986. Isotopic studies of nitrogen pollution in the hydrosphere and atmosphere: A review. *Chemical Geology: Isotope Geoscience section*, 59: 87–102.
- Hebbel, H. and Steuer, D. 2006. Empirische Untersuchungen zur Berechnung von Frachten in Fließgewässern in: Hauptmann, H., Krumbholz, W. (Eds.), *Discussion Papers in Statistics and Quantitative Economics*, Hamburg.
- Heise, S., Calmano, W., Ahlf, W., Leal, W., Krahn, D., 2005. Environmental challenges for the Hamburg stretch of the River Elbe and its catchment with regard to the Water Framework Directive. Hamburg University of Technology / TuTech Innovation GmbH Centre for Integrated Sediment Management. [http://www.watersketch.net/WP4\\_Dissemination\\_of\\_results/Handbook/vdo\\_ws\\_05\\_study\\_germany\\_elbe.pdf](http://www.watersketch.net/WP4_Dissemination_of_results/Handbook/vdo_ws_05_study_germany_elbe.pdf) [17.08.10].
- Herfort, L., Kim, J. H., Coolen, M. J. L., Abbas, B., Schouten, S., Herndl, G. J., Sinninghe Damsté, J. S., 2009. Diversity of *Archaea* and detection of crenarchaeotal *amoA* genes in the rivers Rhine and Têt. *Aquatic Microbial Ecology*, 55, 189–201.
- Hickel, W., Mangelsdorf, P., Berg, J., 1993. The human impact in the German Bight: Eutrophication during three decades (1962–1991). *Helgoland Marine Research*, 47, 243–263.
- Hilairy, E. H., Seitzinger, S. P., 2003. High-Resolution nitrogen gas profiles in sediment porewaters using a new membrane probe for membrane-inlet mass spectrometry (MIMS). *Marine Chemistry*, 83, 23–30.
- Hirschfeld, M., 2003. Isotopen- und Hydrochemie des Rheinsystems: Saisonale Variationen als Konsequenz dynamischer Prozessabläufe des kontinentalen Kohlenstoff- und Wasserkreislaufes, *Kölner Forum Geol. Paläontol.*, 12.
- Hoefs, J., 2004. *Stable Isotope Geochemistry*, 5th revised and updated edition. Springer.
- Hoffman, J. C., Bronk, D. A., 2006. Interannual variation in stable carbon and nitrogen isotope biogeochemistry of the Mattaponi River, Virginia. *Limnology and Oceanography*, 51, 2319–2332.

- Hollocher, T. C., 1984. Source of the oxygen atoms of nitrate in the oxidation of nitrate by *Nitrobacter agilis* and evidence against a P-O-N anhydride mechanism in oxidative phosphorylation. *Archives of Biochemistry and Biophysics*, 233, 721–727.
- Horrigan, S. G., Montoya, J. P., Nevins, J. L., McCarthy, J. J., 1990. Natural isotopic composition of dissolved inorganic nitrogen in the Chesapeake Bay. *Estuarine, Coastal and Shelf Science*, 30, 393–410.
- Howarth, R. W., Billen, G., Swaney, D., Townsend, A., Jarowski, N., Lajtha, K., Downing, J. A., Elmgren, R., Caracao, N., Jordan, T., Berendse, F., Freney, J., Kudeyarov, V., Murdoch, P., Zhao-Ling, Z., 1996. Regional nitrogen budgets and riverine N & P fluxes for the drainages to the North Atlantic Ocean: natural and human influences. *Biogeochemistry*, 35, 75–139.
- Howarth, R. W., Anderson, D., Cloern, J., Elfring, C., Hopkinson, C., Lapointe, B., Malone, T., Marcus, N., McGlathery, K., Sharpley, A., Walker, D., 2000. Nutrient pollution of coastal rivers, bays and seas. *Issues in Ecology 7*. Ecological Society of America, Washington DC.
- Howarth, R.W., Marino, R., 2006. Nitrogen as the limiting nutrient for eutrophication in coastal marine ecosystems: Evolving views over three decades. *Limnology and Oceanography*, 51((1, part 2)), 364–376.
- Huntenburg, S., Zahrt, K., Ricklefs, K., Stüben, D., 1995. Untersuchungen zu Schwermetallkonzentrationen im Eider-Ästuar. *Meyniana*, 47, 21–43.
- Hydes, D. J., Kelly-Gerreyn, B. A., Le Gall, A. C., Proctor, R., 1999. The balance of supply of nutrients and demands of biological production and denitrification in a temperate latitude shelf sea – a treatment of the southern North Sea as an extended estuary. *Marine Chemistry*, 68, 117–131.
- James, W. F., Richardson, W. B., Soballe, D. M., Barko, J. W., Eakin, H. L., 2006. Effect of Residence Time on Net Nitrate Retention in Flow-Regulated Backwaters of the Upper Mississippi River. ERDC TN-SWWRP-06-1.
- Jensen, K. M., Jensen, M. H., Kristensen, E., 1996. Nitrification and denitrification in Wadden Sea sediments (Königshafen, Island of Sylt, Germany) as measured by nitrogen isotope pairing and isotope dilution. *Aquatic Microbial Ecology*, 11, 181–191.
- Jickells, T. D., 1998. Nutrient biogeochemistry of the Coastal Zone. *Science*, 281, 217–222.
- Jickells, T., and others, 2000. Nutrient fluxes through the Humber estuary—past, present and future. *Ambio*, 29, 130–135.
- Johannsen, A., Dähnke, K., Emeis, K., 2008. Isotopic composition of nitrate in five German rivers discharging into the North Sea. *Organic Geochemistry*, 39, 1678–1689.
- Jones, F.H., 1984. The dynamics of suspended algal populations in the lower Wye catchment. *Water Research*, 18, 25–35.

- Kadlec, R.H., 1994. Detention and mixing in free water wetlands. *Ecological Engineering*, 3, 345–380.
- Kana, T. M., Darkangelo, C., Hunt, M. D., Oldham, J. B., Bennett, G. E., Cornwell, J. C., 1994. Membrane inlet mass spectrometer for rapid high-precision determination of N<sub>2</sub>, O<sub>2</sub>, and Ar in environmental water samples. *Analytical Chemistry*, 66, 4166–4170.
- Kattan, Z., Salleron, J. L., Probst, J.-L., 1986. Bilans et dynamiques de transfert de azote et du phosphore sur le bassin de la Moselle (Nord-Est de la France). *Science de l'eau*, 5, 435–459.
- Kaushik, N. K., Robinson, J. B., Stammers, W. N., Whitely, H. R., 1981. Aspects of nitrogen transport and transformation in headwater streams in: Lock, M. A., Williams, D. D. (Eds.), *Perspectives in Running Water Ecology*. Plenum Press, New York, 113–139.
- Kellman, L., Hillaire-Marcel, C., 1998. Nitrate cycling in streams: using natural abundances of  $\delta^{15}\text{N}$ -nitrate to measure in situ denitrification. *Biogeochemistry*, 43, 273–292.
- Kempe, S., Krahe, P., 2005. Water and Biogeochemical fluxes in the River Rhine catchment, *Erdkunde*, 59, 216–250.
- Kendall, C., Campbell, D. H., Burns, D. A., Shanley, J. B., Silva, S. R., Chang, C. C. Y., 1995. Tracing sources of nitrate in snowmelt runoff using the oxygen and nitrogen isotopic compositions of nitrate, *Biogeochemistry of Seasonally Snow-Covered Catchments (Proceedings of a Boulder Symposium, July 1995)*, 339–347.
- Kendall, C., 1998. Tracing nitrogen sources and cycling in catchments in: Kendall, C., McDonnell, J.J. (Eds.), *Isotope tracers in catchment hydrology*. Elsevier Science, Amsterdam, pp. 517–576.
- Kerner, M., Jacobi, A., 2005. Die Elbevertiefung von 1999, Tatsächliche und prognostizierte Auswirkungen, WWF Deutschland, Frankfurt am Main.
- Kieskamp, W. M., Lohse, L., Epping, E., Helder, W., 1991. Seasonal variation of denitrification rates and nitrous oxide fluxes in intertidal sediments of the western Wadden Sea. *Marine Ecology Progress Series*, 72, 145–151.
- Koch, M. S., Maltby, E., Oliver, G. A., Bakker, S. A., 1992. Factors controlling denitrification rates of tidal mudflats and fringing salt marshes in south-west England. *Estuarine Coastal and Shelf Science*, 34, 471–485.
- Köster, R., 1998. Wattedimente. In: *Umweltatlas Wattenmeer*, Bd I: Nordfriesisches und Dithmarscher Wattenmeer. Ulmer-Verlag, Stuttgart, pp. 40–41.
- Komor, S. C., Anderson, H. W., 1993. Nitrogen Isotopes as Indicators of Nitrate Sources in Minnesota Sand-Plain Aquifers. *Ground Water*, 31(2), 260–270.
- Kool, D. M., Wrage, N., Oenema, O., Dolfing, J., Van Groenigen, J. W., 2007. Oxygen exchange between (de)nitritication intermediates and H<sub>2</sub>O and its implications for

- source determination of  $\text{NO}_3^-$ : a review. *Rapid Communications in Mass Spectrometry*, 21, 3569–3578.
- Kroopnick, P., Craig, H., 1972. Atmospheric oxygen: Isotopic composition and solubility fractionation. *Science*, 175, 54–55.
- Kumar, S. Nicholas, D. J. D., Williams, E. H., 1983. Definitive  $^{15}\text{N}$  NMR evidence that water serves as a source of 'O' during nitrite oxidation by *Nitrobacter agilis*, *FEBS Letters*, 152, 71–74.
- Kunkel, R., 2006. Diffuse Nitrateinträge in die Grund- und Oberflächengewässer von Rhein und Ems: Ist-Zustands- und Maßnahmenanalysen. Schriften des Forschungszentrum Jülich, Reihe Umwelt/Environment.
- Laane, R., Brockmann, U, Van Liere, L., Bovelander, R., 2005. Immission targets for nutrients (N and P) in catchments and coastal zones: a North Sea assessment. *Estuarine Coastal and Shelf Science*, 62, 495–505.
- Lack, T. J., 1971. Quantitative studies on the phytoplankton of the Rivers Thames and Kennet at Reading. *Freshwater Biology*, 1, 213–224.
- Lahajnar, N., Wiesner, M. G., Gaye, B., 2007. Fluxes of amino acids and hexosamines to the deep South China Sea. *Deep Sea Research PT I*, 54, 2120–2144.
- Lancelot, C., Billen, G., Sournia, A., Weisse, T., Colijn, F., Veldhuis, M.J.W., Davies, A., Wassman, P., 1987. Phaeocystis blooms and nutrient enrichment in the continental coastal zones of the North Sea. *Ambio*, 16, 38–46.
- Lavrentyev, P. J., Gardner, W. S., Yang, L., 2000. Effects of the zebra mussel on nitrogen dynamics and the microbial community at the sediment–water interface. *Aquatic Microbial Ecology*, 21, 187–194.
- Law, C. S., Owens, N. J. P., 1992. Denitrification and nitrous oxide in the North Sea. *Netherlands Journal of Sea Research*, 25, 65–74.
- Lehmann, M. F., Reichert, P, Bernasconi, S. M., Barbieri, A., McKenzie, J. A., 2003. Modelling nitrogen and oxygen isotope fractionation during denitrification in a lacustrine redox-transition zone. *Geochimica et Cosmochimica Acta*, 67(14), 2529–2542.
- Lehmann, M. F., Sigman, D. M., McCorkle, D. C., Granger, J., Hoffmann, S., Cane, G., Brunelle, B. G., 2007. The distribution of nitrate  $^{15}\text{N}/^{14}\text{N}$  in marine sediments and the impact of benthic nitrogen loss on the isotopic composition of oceanic nitrate. *Geochimica et Cosmochimica Acta*, 71, 5384–5404.
- Leininger, S., Urich, T., Schloter, M., Schwark, L., Qi, J., Nicol, G. W., Prosser, J. I., Schuster, S. C., Schleppen, C., 2006. Archaea predominate among ammonia oxidizing prokaryotes in soils. *Nature*, 442, 806–809.

- Lenhart, H. J., Pohlmann, T. H., 1997. The ICES-boxes approach in relation to results of a North Sea Circulation model. *Tellus*, 49A, 139–160.
- Liersch, S., Volk, M., 2009. How realistic is the implementation of the European Water Framework Directive in river basins dominated by agriculture? The example of the Upper Ems River Basin (Germany), International Conference: Megacities: Risk, Vulnerability and Sustainable development, Leipzig, Germany.
- Lohse, L., Malschaert, J. F. P., Slomp, C. P., Helder, W., van Raaphorst, W., 1993. Nitrogen cycling in North Sea sediments: interaction of denitrification and nitrification in offshore and coastal areas. *Marine Ecology Progress Series*, 101, 283–296.
- Lohse, L., Kloosterhuis, R., van Raaphorst, W., Helder, W., 1996. Denitrification rates in continental shelf sediments of the North Sea: acetylene block technique versus isotope pairing. *Marine Ecology Progress Series*, 132, 169–179.
- Lòzan, J.L., Kausch, H., 1996. Warnsignale aus Flüssen und Ästuaren. *Wissenschaftliche Fakten*. Parey Buch Verlag, Berlin.
- Luc, R., Bernhard, M., 2006. Nitrogen budget for the Oldman River Basin, southern Alberta, Canada. *Nutrient Cycling in Agroecosystems*, V75(1), 147–162.
- Macko, S. A., Ostrom, N. E., 1994. Pollution studies using stable isotopes, in: *Stable Isotopes in Ecology and Environmental Sciences*, Lajtha, K., Michener, R.H., Blackwell, 45–62.
- Mariotti, A., Germon, P., Hubert, P., Kaiser, P., Letolle, R., Tardieux, A., Tardieux, P., 1981. Experimental determination of nitrogen kinetic isotope fractionation: Some principles, illustrations for denitrification and nitrification. *Plant and Soil Science*, 62, 413–430.
- Mayer, B., Bollwerk, S. M., Mansfeldt, T., Hütter, B., Veizer, J., 2001. The oxygen isotope composition of nitrate generated by nitrification in acid forest floors. *Geochimica et Cosmochimica Acta*, 65, 2743–56.
- Mayer, B., Boyer, E. W., Goodale, C., Jaworski, N. A., van Breemen, N., Howarth, R.W., Seitzinger, S., Billen, G., Lajtha, K., Nadelhoffer, K., van Dam, D., Hetling, L. J., Nosal, M., Paustian, K., 2002. Sources of nitrate in rivers draining sixteen watersheds in the northeastern U.S.: Isotopic constraints. *Biogeochemistry*, V57-58(1), 171–197.
- McCarthy, M. J., Gardner, W. S., 2003. An application of membrane inlet mass spectrometry to measure denitrification in a recirculating mariculture system. *Aquaculture*, 218, 341–355.
- Mengis, M., Walther, U., Bernasconi, S., Wehrli, B., 2001. Limitations of using  $\delta^{18}\text{O}$  for the source identification of nitrate in agricultural soils. *Environmental Science & Technology*, 35, 1840–1844.
- Middelburg, J. J., Soetaert, K., Herman, P. M. J., Heip, C., 1996. Denitrification in marine sediments: a model study. *Global Biogeochemical Cycles*, 10, 661–673.

- Middelburg, J. J., Nieuwenhuize, J., 1998. Carbon and nitrogen stable isotopes in suspended matter and sediments from the Schelde Estuary. *Marine Chemistry*, 60, 217–225.
- Nedwell, D. B., 1982. Exchange of nitrate, and the products of bacterial nitrate reduction, between seawater and sediment from a U.K. saltmarsh. *Estuarine Coastal and Shelf Science*, 14, 557–566.
- Nielsen, L. P., 1992. Denitrification in sediment determined from nitrogen isotope pairing. *FEMS Microbiology Letters*, 86, 357–362.
- Nishikawa, J., Kohzu, A., Boontanon, N., Iwata, T., Tanaka, T., Ogawa, N. O., Ishii, R., Wada, E., 2009. Isotopic composition of nitrogenous compounds with emphasis on anthropogenic loading in river ecosystems, *Isotopes in Environmental and Health Studies*, 45, 27–40.
- Nixon, S. W., Atkinson, L. P., Berounsky, V. M., Billén, G., Boicourt, W. C., Boynton, W. R., Church, T. M., Ditoro, D. M., Elmgren, R., Garber, J. H., Giblin, A. E., Jahnke, R. A., Owens, N. J. P., Pilson, M. E. Q., Seitzinger, S. P., 1996. The fate of nitrogen and phosphorus at the land-sea margin of the North Atlantic Ocean. *Biogeochemistry*, 35, 141–180.
- NLÖ, 1995. Niedersächsisches Landesamt für Ökologie: Deutsches gewässerkundliches Jahrbuch. Weser-Emsgebiet. Abflußjahr 1990., Hildesheim.
- OIPC, 2007. Online Isotopes in Precipitation Calculator, copyrighted by Bowen, G.J. URL: [www.wateriso.eas.purdue.edu/waterisotopes/pages/data\\_access/oipc.html](http://www.wateriso.eas.purdue.edu/waterisotopes/pages/data_access/oipc.html)
- OSPAR, 2003. OSPAR integrated report 2003 on the Eutrophication Status of the OSPAR Maritime Area based upon the first application of the Comprehensive Procedure, OSPAR Commission 2003.
- OSPAR, 2008. Second OSPAR Integrated Report on the Eutrophication Status of the OSPAR Maritime Area. OSPAR Commission, 2008. OSPAR Publication Number 372/2008, pp. 107.
- Osterkamp, S., Kraft, D., Schirmer, M., 2001. Climate change and the ecology of the Weser estuary region: assessing the impact of an abrupt change in climate. *Climate Research*, 18, 97–104.
- Ostrom, N. E., Macko, S. A., Deibel, D., Thompson, R. J., 1997. Seasonal variation in the stable carbon and nitrogen isotope biogeochemistry of a coastal cold ocean environment. *Geochimica et Cosmochimica Acta*, 61, 2929–2942.
- Owens, N. J. P., Woodward, E. M. S., Aiken, J., Bellan, I. E., Rees, A. P., 1990. Primary production and nitrogen assimilation in the North Sea during July 1987. *Netherlands Journal of Sea Research*, 25, 143–154.

- Pätsch, J., Radach, G., 1997. Long-term simulation of the eutrophication of the North Sea: temporal development of nutrients, chlorophyll and primary production in comparison to observations. *Journal of Sea Research*, 38, 275–310.
- Pätsch, J., Serna, A., Dähnke, K., Schlarbaum, T., Johannsen, A., Emeis, K., 2010. Nitrogen cycling in the German Bight (SE North Sea) – Clues from modelling stable nitrogen isotopes. *Continental Shelf Research*, 30, 203–213.
- Painter, H.A., 1970. A review of literature on inorganic nitrogen metabolism in microorganisms. *Water Research*, 4, 393–450.
- Pardo, L.H., Kendall, C., Pett-Ridge, J., Chang, C.C.Y., 2004. Evaluating the source of streamwater nitrate using  $\delta^{15}\text{N}$  and  $\delta^{18}\text{O}$  in nitrate in two watersheds in New Hampshire, USA. *Hydrological Processes*, 18, 2699–2712.
- Peterson, B. J., Wollheim, W. M., Mulholland, P. J., Webster, J. R., Meyer, J. L., Tank, J. L., Marti, E., Bowden, W. B., Valett, H. M., Hershey, A. E., McDowell, W. H., Dodds, W. K., Hamilton, S. K., Gregory, S., Morrall, D. D., 2001. Control of nitrogen export from watersheds by headwater streams. *Science*, 292, 86–90.
- Pettijohn, F. J., Potter, P. E., 1972. *Sand and sandstone*. Springer, New York.
- Piña-Ochoa, E., Álvarez-Cobelas, M., 2006. Denitrification in Aquatic Environments: A Cross-system Analysis. *Biogeochemistry*, 81, 111–130.
- Probst, J.-L., 1985. Nitrogen and phosphorus exportation in the Garonne Basin (France). *Journal of Hydrology*, 76, 281–305.
- Rabalais, N., 2002. Nitrogen in aquatic systems. *Ambio* 31, 102–112.
- Rachor, E., Albrecht, H., 1983. Sauerstoff-Mangel im Bodenwasser der Deutschen Bucht. Veröff. Inst. Meeresforsch. Bremerhaven, 19, 209–227.
- Radach, G., Pätsch, J., 2007. Variability of Continental Riverine Freshwater Inputs into the North Sea for the Years 1977-2000 and Its Consequences for the Assessment of Eutrophication. *Estuaries and Coasts*, 30 (1), 66–81.
- Rao, A, M, F., McCarthy, M. J., Gardner, W. S., Jahnke, A., 2007. Respiration and denitrification in permeable continental shelf deposits on the South Atlantic Bight: Rates of carbon and nitrogen cycling from sediment column experiments. *Continental Shelf Research*, 27, 1801–1819.
- Rao, A, M, F., McCarthy, M. J., Gardner, W. S., Jahnke, A., 2008. Respiration and denitrification in permeable continental shelf deposits on the South Atlantic Bight:  $\text{N}_2:\text{Ar}$  and isotope pairing measurements in sediment column experiments. *Continental Shelf Research*, 28, 602–613.
- Reinhardt, M., Müller, B., Gächter, R., Wehrli, B. 2006. Nitrogen Removal in a Small Constructed Wetland: An Isotope Mass Balance Approach. *Environmental Science and Technology*, 40, 3313–3319.

- Reise, K., Jager, Z., Jong, D.J., van Katwijk, M., Schanz, A., 2005. Seagrass. Wadden Sea Quality Status Report 2004. Wadden Sea Ecosystem No. 19, Trilateral Monitoring and Assessment Group. Common Wadden Sea Secretariat, Wilhelmshaven, Germany.
- Reise, K., Siebert, I., 1997. Grünalgenausbreitung im Wattenmeer. Umweltbundesamt Texte 21.
- Renger, A., 2002. Sicker- und Fließzeiten von Nitrat aus dem Wurzelraum ins Grundwasser. Arbeitsbericht Nr. 223 / November 2002, Akademie für Technikfolgenabschätzung in Baden-Württemberg.
- Révész, K., Böhlke, J. K., Yoshinari, T., 1997. Determination of  $\delta^{18}\text{O}$  and  $\delta^{15}\text{N}$  in Nitrate. *Analytical Chemistry*, 69, 4375–4380.
- Révész, K., Böhlke, J.-K., 2002. Comparison of  $\delta^{18}\text{O}$  measurements in nitrate by different combustion techniques. *Analytical Chemistry*, 74, 5410–5413.
- Risgaard Petersen, N. L. P., Nielsen, S., Rysgaard, D. T., Meyer, R. L., 2003. Application of the isotope pairing technique in sediments where anammox and denitrification coexist. *Limnology and Oceanography: Methods*, 1, 63–73.
- Rysgaard, S., Risgaard-Petersen, N., Sloth, N. P., Jensen, K., Nielsen, L. P., 1994. Oxygen regulation of nitrification and denitrification in sediments. *Limnology and Oceanography*, 39, 1643–1652.
- Savage, C. 2005. Tracing the influence of sewage nitrogen in a coastal ecosystem using stable nitrogen isotopes. *Ambio*, 34, 145–150.
- Schlarbaum, T., Daehnke, K., Emeis, K., 2010. Turnover of combined dissolved organic nitrogen and ammonium in the Elbe estuary/NW Europe: Results of nitrogen isotope investigations. *Marine Chemistry*, 119, 91–107.
- Schröder, F., Wiltshire, K. H., Klages, D., Mathieu, M., Blöcker, G., Knauth, H. D., 1996. Nitrogen and oxygen processes in sediments of the Elbe estuary. *Archiv für Hydrobiologie*, 110, 311–328.
- Sebilo, M., Billen, G., Grably, M., Mariotti, A., 2003. Isotopic composition of nitrate-nitrogen as a marker of riparian and benthic denitrification at the scale of the whole Seine River system. *Biogeochemistry*, 63, 35–51.
- Sebilo, M., Billen, G., Mayer, B., Billiou, D., Grably, M., Garnier, J., Mariotti, A., 2006. Assessing nitrification and denitrification in the Seine river and estuary using chemical and isotopic techniques. *Ecosystems*, 9, 564–577.
- Seitzinger, S. P., Nixon, S. W., 1985. Eutrophication and the rate of denitrification and  $\text{N}_2\text{O}$  production in coastal marine sediments. *Limnology and Oceanography*, 30, 1332–1339.

- Seitzinger, S. P., 1988. Denitrification in freshwater and coastal marine ecosystems: Ecological and geochemical significance. *Limnology and Oceanography*, 33, 702–724.
- Seitzinger, S. P., 1990. Denitrification in Aquatic Sediments in: Denitrification in Soil and Sediment, Revsbech, N. P., Sørensen, J., FEMS Symposium, 301–322.
- Seitzinger, S. P., Giblin, A. E., 1996. Estimating denitrification in North Atlantic continental shelf sediments. *Biogeochemistry*, 35, 301–322.
- Seitzinger, S. P., and others. 2006. Denitrification across landscapes and waterscapes: A synthesis. *Ecological Applications*, 16, 2064–2090.
- Serna, A., Pätsch, J., Dähnke, K., Wiesner, M.G., Hass, H. C. Z., Hebbeln, M. D., Emeis, K.-C., 2010. History of anthropogenic nitrogen input to the German Bight/SE North Sea as reflected by nitrogen isotope composition of surface sediments, sediment cores and hindcast models. *Continental Shelf Research*, 30(15), 1626–1638.
- Sigleo, A. C., Macko, S. A., 2002. Carbon and Nitrogen Isotopes in Suspended Particles and Colloids, Chesapeake and San Francisco Estuaries, U.S.A. *Estuarine, Coastal and Shelf Science*, 54, 701–711.
- Sigman, D. M., Altabet, M. A., McCorkle, D. C., Francois, R., Fischer, G., 1999. The  $\delta^{15}\text{N}$  of nitrate in the Southern Ocean: Consumption of nitrate in surface waters. *Global Biogeochemical Cycles*, 13, 1149–1166.
- Sigman, D. M., Casciotti, K. L., 2001. Nitrogen isotopes in the ocean in: *Encyclopedia of Ocean Sciences*, pp. 1884–1894.
- Sigman, D. M., Casciotti, K. L., Andreani, M., Barford, C., Galanter, M., Bohlke, J. K., 2001. A Bacterial Method for the Nitrogen Isotopic Analysis of Nitrate in Seawater and Freshwater. *Analytical Chemistry*, 73(17), 4145–4153.
- Sigman, D. M., Granger, J., DiFiore, P. J., Lehmann, M. F., Ho, R., Cane, G., Van Geen, A., 2005. Coupled nitrogen and oxygen isotope measurements of nitrate along the eastern North Pacific margin. *Global Biogeochemical Cycles*, 19, 1–14.
- Sigman, D. M., Karsh, K. L., Casciotti, K. L., 2009. Nitrogen isotopes in the ocean. In: *Encyclopedia of Ocean Sciences* (update from 2001), edited by Steele, J.H., Turekian, K.K., Thorpe, S. A. Academic Press, London.
- Silva, S. R., Kendall, C., Wilkison, D. H., Ziegler, A. C., Chang, C. C. Y., Avanzino, R., 2000. A new method for collection of nitrate from fresh water and the analysis of nitrogen and oxygen isotope ratios. *Journal of Hydrology*, 228, 22–36.
- Skogen, M. D., Soiland, H., Svendsen, E., 2004. Effects of changing nutrient loads to the North Sea. *Journal of Marine Systems*, 46(1-4), 23–38.
- Smith S.V., Boudreau P.R. Ruardij, P. 1997. NP budget for the southern North Sea. LOICZ paper. URL: <http://data.ecolgy.su.se/MNODE/Europe?NorthSea/NORTHSEA.htm>

- Sørensen, J., 1978. Denitrification rates in a marine sediment as measured by the acetylene inhibition technique. *Applied Environmental Microbiology*, 36, 139–143.
- Sørensen, J., Jørgensen, B. B., Revsbech, N. P., 1979. A comparison of oxygen, nitrate and sulfate respiration in coastal marine sediments. *Marine Ecology*, 5, 105–115.
- Spoelstra, J., Schiff, S. L., Hazlett, P. W., Jeffries, D. S., Semkin, R. G., 2007. The isotopic composition of nitrate produced from nitrification in a hardwood forest floor. *Geochimica et Cosmochimica et Acta*, 71, 3757–3771.
- Stal, L. J., Grossberger, S., Krumbein, W. E., 1984. Nitrogen fixation associated with the cyanobacterial mat of a marine laminated microbial ecosystem. *Marine Biology*, 82, 217–224.
- Statistisches Bundesamt, 1990. Coordination of Information on the Environment CORINE Landcover. Digitale Landnutzungskarten 1:100.000 für die Bundesrepublik Deutschland. Europäische Umweltagentur EUA, Wiesbaden.
- Stichler, W., Trimborn, P., Schotterer, U., Leuenberger, M., Kozel, R., Schürch, M., 2005. The stable isotope composition along the river Rhine as characterized by its individual catchment areas. *Geophysical Research Abstracts*, 7, 10687.
- Steingruber, S. M., Friedrich, J., Gächter, R., Wehrli, B., 2001. Measurement of Denitrification with the  $^{15}\text{N}$  Isotope Pairing Technique. *Applied Environmental Microbiology*, 9, 3771–3778.
- Sundbäck, K., Miles, A., Göransson, E., 2000. Nitrogen fluxes, denitrification and the role of micro-phytobenthos in microtidal shallow-water sediments: an annual study. *Marine Ecology Progress Series*, 200, 59–76.
- Sweerts, J. P., Bär-Gilissen, M. J., Cornelese, A. A., Cappenberg, T. E., 1991. Oxygen-consuming processes at the profundal and littoral sediment-water interface of a small meso-eutrophic lake (Lake Vechten, The Netherlands). *Limnology and Oceanography*, 36, 1124–1133.
- Thamdrup, B., Dalsgaard, T., 2002. Production of  $\text{N}_2$  through anaerobic ammonium oxidation coupled to nitrate reduction in marine sediments. *Applied Environmental Microbiology*, 68, 1312–1318.
- Thomas, D. J., 2004. Evidence for deep-water production in the North Atlantic Ocean during the early Cenozoic warm interval. *Nature*, 430, 65–68.
- Trimmer, M., Nicholls, J. C., 2009. Production of nitrogen gas via anammox and denitrification in intact sediment cores along a continental shelf to slope transect in the North Atlantic. *Limnology and Oceanography*, 54, 577–589.
- Trudeau, V., Rasmussen, B., 2003. The effect of water velocity on stable carbon and nitrogen isotope signatures of periphyton. *Limnology and Oceanography*, 48, 2194–2199.

- UBA, 2006. Umweltbundesamt. Wasser, Trinkwasser und Gewässerschutz. Oberflächengewässer und Hydrographie.  
URL: [http://www.umweltbundesamt.de/wasser/themen/ow\\_s1.htm](http://www.umweltbundesamt.de/wasser/themen/ow_s1.htm) [01.04.2007].
- UBA, 2009. Umweltbundesamt: Thema: Biologische Vielfalt, Naturhaushalt und Landschaft, Unterthema: Belastung der Umweltmedien und Lebensräume durch Stoffe; Boden, Indikator: Stickstoffüberschuss, <http://www.umweltbundesamt-daten-zur-umwelt.de/umweltdaten/public/theme.do?nodeIdent=2879> [04.04.2010].
- van Beusekom, J. E. E., 2005. A historic perspective on Wadden Sea eutrophication. *Helgoland Marine Research*, 59, 45–54.
- van Beusekom, J. E. E., de Jonge, V. E., 1998. Retention of Phosphorus and Nitrogen in the Ems Estuary. *Estuaries*, 21(4A), 527–539.
- van Beusekom, J. E. E., Brockmann, U. H., Hesse, K. J., Hickel, W., Poremba, K., Tillmann, U., 1999. The importance of sediments in the transformation and turnover of nutrients and organic matter in the Wadden Sea and German Bight. *German Journal of Hydrography*, 51, 245–266.
- van Beusekom, J. E. E., Fock, H., de Jong, F., Diel-Christiansen, S., Christiansen, B., 2001. Wadden Sea specific eutrophication criteria, *Wadden Sea Ecosystem*, pp. 1–115.
- van Beusekom, J. E. E., de Jonge, V. N., 2002. Long-term changes in Wadden Sea nutrient cycles: importance of organic matter import from the North Sea. *Hydrobiologia* 475/476, 185–194.
- van Beusekom, J., Weigelt-Krenz, S., Martens, P., 2008. Long-term variability of winter nitrate concentrations in the Northern Wadden Sea driven by freshwater discharge, decreasing riverine loads and denitrification. *Helgoland Marine Research*, 62, 49–57.
- van Beusekom, J. E. E., Loebel, M., Martens, P., 2009. Distant riverine nutrient supply and local temperature drive the long-term phytoplankton development in a temperate coastal basin. *Journal of Sea Research*, 61, 26–33.
- van Breemen, N., Boyer, E. W., Goodale, C. L., Jaworski, N. A., Paustian, K., Seitzinger, S. P., Lajtha, K., Mayer, B., van Dam, D., Howarth, R. W., Nadelhoffer, K. J., Eve, M., Billen, G., 2002. Where did all the nitrogen go? Fate of nitrogen inputs to large watersheds in the northeastern U.S.A. *Biogeochemistry*, 57–58 (1), 267–293.
- van Luijn, F., Boers, C. M., Lijklema, L., Sweerts, J. P. R. A., 1999. Nitrogen fluxes and processes in sandy and muddy sediments from a shallow eutrophic lake. *Water Research*, 33, 33–42.
- van Raaphorst, W., Kloosterhuis, H. T., Cramer, A., Bakker, K. J. M., 1990. Nutrient early diagenesis in the sediments of the Dogger Bank area, North Sea: pore water results. *Netherlands Journal of Sea Research*, 26, 25–52.

- van Raaphorst, W., Kloosterhuis, H. T., Berghuis, E. M. Gieles, A. J. M., Malschaert, J. F. P., van Noort, G. J., 1992. Nitrogen cycling in two types of sediments of the Southern North Sea (Frisian Front, Broadfourteens): field data and mesocosm results. *Netherlands Journal of Sea Research*, 28, 293–316.
- Voss, M., Deutsch, B., Elmgren, R., Humborg, C., Kuuppo, P., Pastuszak, M., Rolff, C., Schulte, U, 2006. Source identification of nitrate by means of isotopic tracers in the Baltic Sea catchments. *Biogeosciences Discussions*, 3, 663–676.
- Wada, E., Hattori, A., 1978. Nitrogen isotope effects in the assimilation of inorganic nitrogenous compounds by marine diatoms. *Geomicrobiology*, 1, 85–101.
- Wankel, S. D., Kendall, C., Francis, C. A., Paytan, A., 2006. Nitrogen sources and cycling in the San Francisco Bay Estuary: A nitrate dual isotopic composition approach. *Limnology and Oceanography*, 51(4), 1654–1664.
- Wankel, S. D., Kendall, C. Paytan, A., 2009. Using nitrate dual isotopic composition ( $\delta^{15}\text{N}$  and  $\delta^{18}\text{O}$ ) as a tool for exploring sources and cycling of nitrate in an estuarine system: Elkhorn Slough, California. *Journal of Geophysical Research*, 114, G01011, doi:10.1029/2008JG000729.
- Wassenaar, L. I., 1995. Evaluation of the origin and fate of nitrate in the Abbotsford Aquifer using the isotopes of  $^{15}\text{N}$  and  $^{18}\text{O}$  in  $\text{NO}_3^-$ . *Applied Geochemistry*, 10(4), 391–405.
- Weigelt-Krenz, S., Hanslik, M., Pätsch, J., Petenati, T., van Beusekom, J. E. E., 2010. Nährstoffe im deutschen Wattenmeer und in der Deutschen Bucht. *Meeresumwelt Aktuell Nord- und Ostsee*, 2010/1, Bundesamt für Seeschifffahrt und Hydrographie.
- Weiss, R. F., 1970. The solubility of nitrogen, oxygen and argon in water and seawater. *Deep Sea Research and Oceanographic Abstracts*, 17, 721–735.
- Wendland F., Albert, H., Bach, M., Schmidt, R., 1993. Atlas zum Nitratstrom in der Bundesrepublik Deutschland - Rasterkarten zu geowissenschaftlichen Grundlagen, Stickstoffbilanzgrößen und Modellergebnissen. Springer, Berlin, Heidelberg, New York.
- Wentworth, C. K., 1922. A scale of grade and class terms for clastic sediments. *The Journal of Geology*, 30, 377–392.
- Weston, K., Jickells, T. D., Fernand, L., Parker, E. R., 2004. Nitrogen cycling in the southern North Sea: consequences for total nitrogen transport. *Estuarine, Coastal and Shelf Science*, 59, 559–573.
- WFD, 2000. Water Framework Directive, Richtlinie 2000/60/EG des Europäischen Parlamentes und des Rates vom 23. Oktober 2000 zur Schaffung eines Ordnungsrahmens für Maßnahmen der Gemeinschaft im Bereich der Wasserpolitik. *Amtsblatt der Europäischen Gemeinschaften*.p.1–72. L327, EC.

- Winner, J.M., 1975. Zooplankton in: Whitton, B.A. (Ed.), *River Ecology*. Blackwell, Oxford, pp155–169.
- Wollheim, W. M., Peterson, B. J., Deegan, L. A., Hobbie, J. E., Hooker, B., Bowden, W. B., Edwardson, K. J., Arscott, D. B., Hershey, A. E., Finlay, J., 2001. Influence of stream size on ammonium and suspended particulate nitrogen processing. *Limnology and Oceanography*, 46, 1, 1–13.
- Wu, J., Calvert, S. E., Wong, C. S., 1997. Nitrogen isotope variations in the subarctic northeast Pacific: relationships to nitrate utilization and trophic structure. *Deep Sea Research I* 44, 287–314.
- Yoshinari, T. and Wahlen, M., 1985. Oxygen isotope ratios in N<sub>2</sub>O from nitrification at a waste water treatment facility. *Nature*, 317, 349–50.
- Yurtsever, Y., 1975. Worldwide survey of stable isotopes in precipitation, Rept. Section of Isotope Hydrology, IAEA, 1975.

## Acknowledgements

First, I would like to take this opportunity to thank Prof. Kay Emeis for the supervision of this thesis, his insight and catching enthusiasm for nitrogen cycling. I also appreciate the opportunity to join several research cruises and conferences.

I thank Dr. Justus van Beusekom for co-supervision, together with Dr. Andrea Wieland for the inspiring discussions and helpful ideas.

A special thank goes to Prof. Ralf Ebinghaus for the opportunity to work under excellent conditions at the GKSS, Institute for Coastal Research. I thank my colleagues at the GKSS for the nice work atmosphere and support whenever I needed. In particular I would like to thank T. Pieplow for endless nutrient analyses. A special thank goes to the students who helped me during sampling campaigns and in the laboratory: Markus Ankele, Angela Nawrocki, Jan Pohlmann, Jonna Rieck, Steffi Pommerening, Anika Riedel and many other helpful hands! Thanks to Dr. Kirstin Dähnke for support especially during my beginning at the GKSS and to Dr. Carsten Frank for the nice atmosphere in our office.

Many thanks to the captain, Helmut Bornhöft and the crew of the RV Ludwig Prandtl who greatly supported this project. I also acknowledge the technicians Karin Wirth, Gerd Blöcker and Steffen Schmidt who shared their experience with me.

I would also like to thank Dr. Niko Lahajnar and Frauke Langeberg who organized the analyses of sediment samples.

I also acknowledge T. Gerke (IMBL Bimmen-Lobith), Dr. H. Schimmer and H. Petry (Bezirksregierung Münster), Dr. F. Schulz (LANU, Schleswig-Holstein) and B. Freiheit (Senator für Bau, Umwelt und Verkehr in Bremen) for their cooperation and help with sampling at the river sites.

Mark J. McCarthy and Prof. Wayne S. Gardner are acknowledged for the invitation to the UTMSI and the opportunity to learn the incubation and MIMS technique.

Thank you, Rany!

## Curriculum Vitae

### CONTACT INFORMATION

---

Astrid Deek, née Johannsen  
Auf der Bojewiese 17  
D-21033 Hamburg

### PERSONAL INFORMATION

---

Date of Birth: 12.02.1979  
Place of Birth: Reinbek, Germany  
Citizenship: German

### EDUCATION

---

1999	Abitur at Gymnasium Glinde
09/99 – 03/02	Apprenticeship: Biological Laboratory Assistant, Research Centre Borstel, Centre for Medicine and Biological Science,
10/02 – 07/07	Study of Environmental Science, University of Lüneburg, Scholarship: SDW (Stiftung der Deutschen Wirtschaft), Certificate: <u>Diploma in Environmental Science</u>
Since 09/07	Doctorate at the GKSS Research Centre, Institute of Coastal Research in cooperation with the University of Hamburg, Thesis: Sources and sinks of reactive Nitrogen in the German Bight

---

**PUBLICATIONS**

---

Johannsen, A., Dähnke, K., Emeis, K. (2008) Isotopic composition of nitrate in five German rivers discharging into the North Sea. *Organic Geochemistry* 39: 1678–1689.

Pätsch, J., Serna, A., Dähnke, K., Schlarbaum, T., Johannsen, A., Emeis, K. (2010) Nitrogen cycling in the German Bight (SE North Sea) – Clues from modelling stable nitrogen isotopes. *Continental Shelf Research* 30: 203–213.

Dähnke, K., Emeis, K., Johannsen, A., Nagel, B. (2010) Stable isotope composition and turnover of nitrate in the German Bight. *Marine Ecology Progress Series* 408: 7–18.

Deek, A., Emeis, K., Struck, U. (2010) Seasonal variations in nitrate isotope composition of three rivers draining into the North Sea, *Biogeosciences Discussions* 7: 6051–6088.

Deek, A., Emeis, K., van Beusekom, J.: Denitrification in coastal sediments of the German Wadden Sea, resubmitted to *Biogeochemistry*.

Deek, A., Emeis, K., van Beusekom, J., Meyer, S., Voss, M.: Denitrification in sediments of the Elbe Estuary and adjacent coastal zones, in preparation.